TOMORROW TODAY

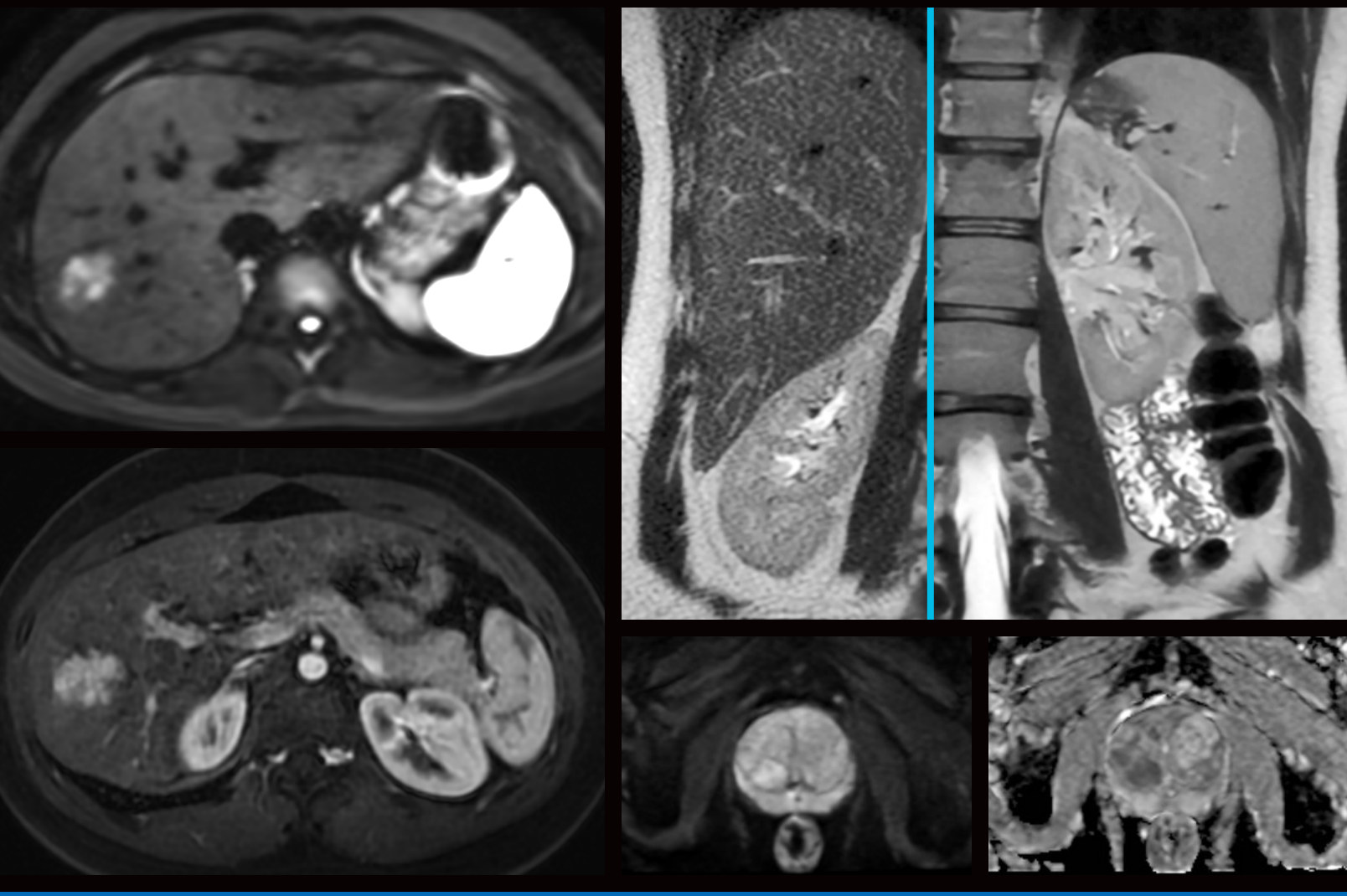

BodyWorks

A collection of articles from SIGNA™ Pulse of MR

2021 Edition

gehealthcare.com/mr

UNMISSABLE

A TRUE MRI STORY

Narrated by Gillian Anderson

WOW, JUST SIMPLY WOW

WHERE DIAGNOSTIC CONFIDENCE IS KEY, ONE IMAGING TECHNOLOGY STANDS ALONE

GE invites you to take a seat for the virtual screening of "**UNMISSABLE**", narrated by Gillian Anderson, a movie that pushes the boundaries of what's possible in MRI scanning.

Showcasing AIR™ Recon DL, a newly developed MRI technology with a learning capability that 'goes deep', the movie will challenge what you thought could be achieved in medical imaging.

So, don't get left behind with the conventional!

DON'T MISS THE UNMISSABLE

View now by scanning the QR Code with your phone camera or QR Code scanner

Prostate

Liver

Body

Gallery

Whole Body

Hiromitsu Onishi, MD, PhD
Osaka University Hospital
Osaka, Japan

Leveling up image quality for confidence in cancer care

Osaka University Hospital, located in the north of Osaka prefecture, Japan, is one of the country's premier facilities for advanced multidisciplinary treatment of cancer and malignant tumors. A large percentage of the hospital's MR exams are performed to diagnose cancer and plan treatment. This need for detailed MR imaging inspired the facility to install SIGNA™Works AIR™ IQ Edition, including AIR™ Recon DL, in November 2020.

"As a university hospital, we have more complex cases requiring more detailed information for an accurate diagnosis. In routine examinations, we think the quality of the examination is important," says Hiromitsu Onishi, MD, PhD, Associate Professor at Osaka University Hospital.

Image reconstruction is at the heart of every MR scan, and reducing noise is critical to achieving high diagnostic quality images. AIR™ Recon DL is an innovative reconstruction technology from GE Healthcare based on deep learning that offers a fundamental shift in the balance between image quality and scan time. It results in TrueFidelity™ MR images that elevate the science of image reconstruction for clinical excellence without conventional compromises. It uses a neural network trained on tens of thousands of images to recognize patterns characteristic of noise and low resolution to reconstruct the ideal clinical image.

Improved SNR in abdominal imaging

Dr. Onishi reports the software upgrade is having a significant impact on the facility's abdominal imaging, particularly in liver studies. The facility uses AIR™ Recon DL in liver and abdominal exams with Snapshot SSFSE imaging and T2 fast spin echo (FSE) imaging, for improved SNR.

"Since this version of SSFSE can use SnapShot SSFSE, the contrast of water (longer T2 tissue) is better than conventional SSFSE. In the case of cystic lesions of the pancreas like IPMN (Intraductal Papillary Mucinous Neoplasm), I think it's useful because even small lesions are clearly delineated," says Dr. Onishi.

He adds that SnapShot SSFSE shortens the scan time compared to conventional SSFSE with respiratory triggering, as he is able to acquire multiple slices in each respiratory cycle. The entire liver can be covered in just a single acquisition, in under a one-minute scan time.

He notes that in abdominal T2-weighted imaging, FSE delivers better image quality in patients who can breathe steadily, but tends to degrade image quality in other patients. SnapShot SSFSE, however, is useful in these patients who have an unstable breathing cycle. In addition, SSFSE has a lower SNR than FSE and therefore can benefit from the increased SNR that can be achieved with AIR™ Recon DL. In liver imaging, the number of excitations (NEX) of FSE T2-weighted images was reduced from two to one, shortening the acquisition time.

At Osaka University, they combine SnapShot SSFSE with AIR™ Recon DL to improve exam time as well as better depict small cystic lesions such as intraductal papillary mucinous neoplasms, which are tumors that grow within the pancreatic ducts. "There's no reason not to use AIR™ Recon DL for SnapShot SSFSE," Dr. Onishi adds. "In the pelvis, the combination of SnapShot SSFSE and AIR™ Recon DL is useful when a wide area needs to be scanned quickly."

Higher resolution scans

The facility is also using AIR™ Recon DL in prostate imaging, where T2-weighted images are an important sequence (Figure 1). Clinicians have updated their protocols because of the technology's impact in reconstructing higher resolution and better SNR images. FSE T2-weighted images in prostate exams were changed to a higher spatial resolution by reducing the FOV and slice thickness.

Dr. Onishi says AIR™ Recon DL improves the depiction of anatomy and lesions, leading to higher diagnostic confidence.

"In the prostate, AIR™ Recon DL can increase the spatial resolution of the T2-weighted images, which makes it easier to see capsular invasion and cysts within nodules."

Dr. Hiromitsu Onishi

In addition, clinicians at Osaka University Hospital can more easily set up imaging protocols that comply with Prostate Imaging Reporting & Data System (PI-RADS®) guidelines.

"Until now, it was difficult to comply with PI-RADS® because SNR was too low. As a benefit of AIR™ Recon DL, the combination of improved image quality and reduced imaging time, by reducing the NEX and increasing the spatial resolution, is excellent. We are using LAVA Flex for T1-weighted imaging of the prostate, and we hope that AIR™ Recon DL can be applied to 3D sequences soon," says Dr. Onishi.

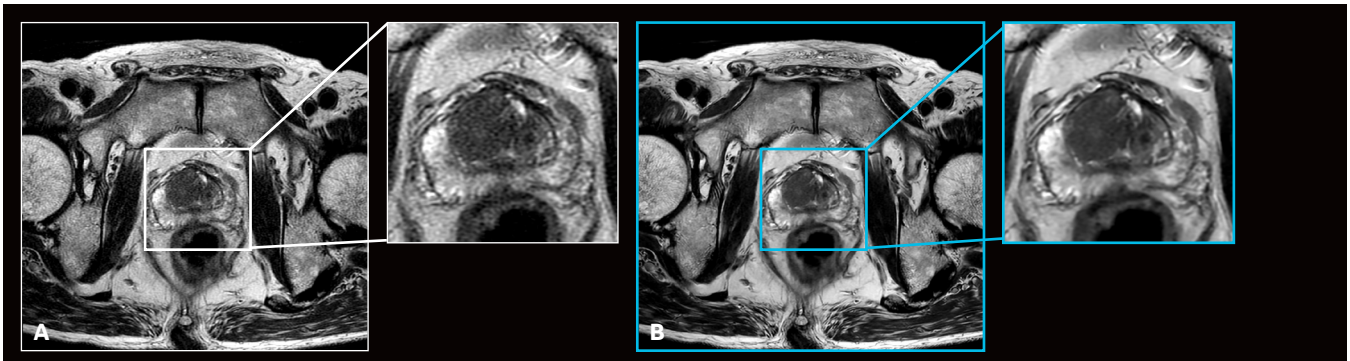

Figure 1. Comparison of T2w image in prostate exams, 0.4 x 0.7 x 3.0 mm, (A) with conventional reconstruction and (B) with AIR™ Recon DL.

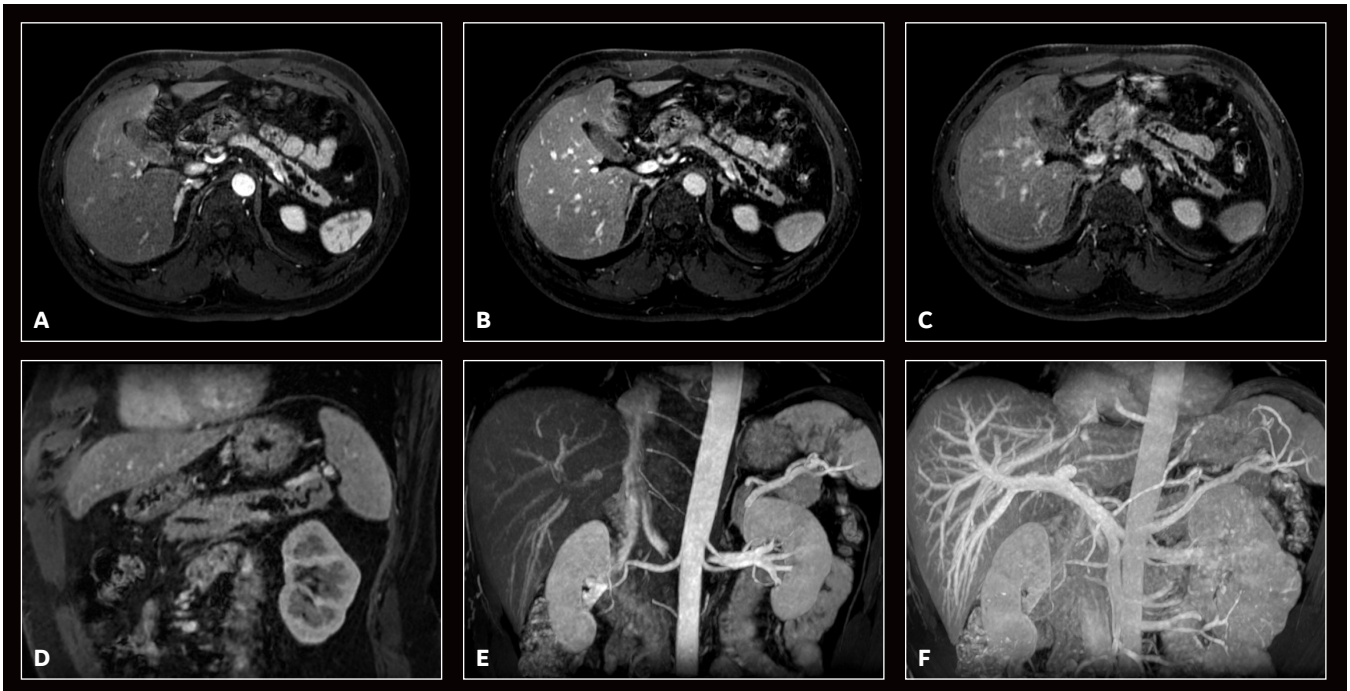

Figure 2. Dynamic LAVA with HyperSense in pancreas exam, 1.2 x 1.2 x 1.2 mm/0.6 sp. (A) dynamic 1st phase, (B) dynamic 2nd phase, (C) dynamic 3rd phase, (D) oblique coronal reformat, (E) MIP image in arterial phase, and (F) MIP image in portal-venous phase.

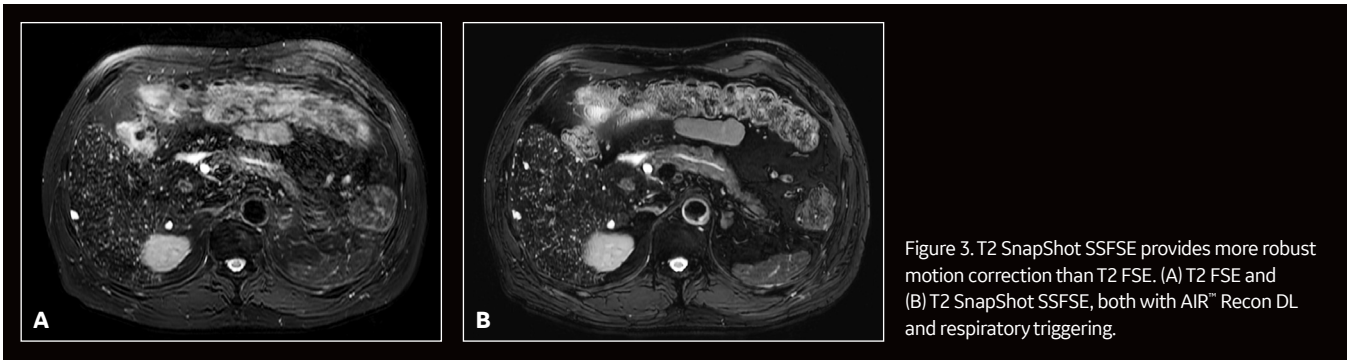

Figure 3. T2 SnapShot SSFSE provides more robust motion correction than T2 FSE. (A) T2 FSE and (B) T2 SnapShot SSFSE, both with AIR™ Recon DL and respiratory triggering.

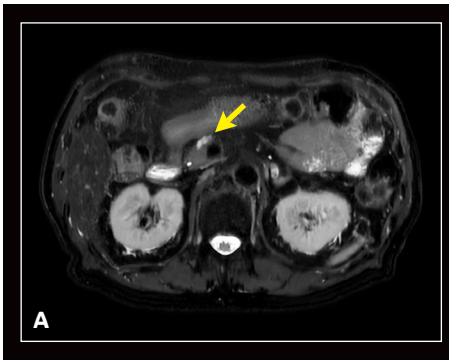

Figure 4. The combination of SnapShot SSFSE and AIR™ Recon DL enable more clear visualization of the IPMN (yellow arrow).

Improved abdominal sequences

As part of their software upgrade, the facility also implemented HyperSense from GE, an acceleration technique based on sparse data compressibility allowing scan time reduction while maintaining SNR efficiency. Osaka University Hospital uses HyperSense in nearly all of its pelvic MR studies to capture high-resolution images in less time. Currently, the hospital is performing dynamic imaging of the pelvis using DISCO with HyperSense.

"I think HyperSense can contribute to higher resolution for 3D LAVA in a reasonable time. I think it improves the quality of diagnosis. If it's used to shorten the scan time, the motion artifact from bowel movement can be reduced."

Dr. Hiromitsu Onishi

HyperSense is used for exams that require detailed information, such as the pancreas and biliary system (Figure 2). For dynamic pancreas imaging, HyperSense helps to increase the spatial resolution and shorten the scanning time. Shortening the scanning time in the pancreas is useful because the organ is positionally susceptible to the movement of the stomach and intestinal tract.

Thin slice imaging is facilitated by HyperSense in the hepatobiliary phase of the liver as well as in the prostate, uterus and rectum scans.

The hospital is using HyperSense to acquire thinner slice images. "We're scanning with thin slice thickness in body MR imaging thanks to HyperSense, which can be observed with reformatting. I think that reformatted MR images from thin slice imaging can be used clinically," says Dr. Onishi.

The facility also implemented the new non-Cartesian, accelerated acquisition DISCO Star sequence. "I think that DISCO Star should be used in patients who need a liver EOB study and cannot hold their breath," says Dr. Onishi.

Clinicians at Osaka University Hospital have embraced the use of deep-learning reconstruction in both MR and CT imaging. Although the noise reduction in CT imaging is impressive, Dr. Onishi feels MR imaging will benefit more because MR images have better contrast resolution than CT images. Plus, the added benefit of MR scan time reductions with AIR™ Recon DL may increase the utilization of MR in cases where the better contrast resolution aids patient evaluation and diagnosis.

"If in the future, AIR™ Recon DL and other advancements in MR can achieve sub-millimeter slice thickness within a breath-hold like CT, then we may see a change in how MR is used for patient diagnosis," Dr. Onishi adds.

Nicola Schieda, MD, FRCPC
The Ottawa Hospital
Ottawa, Canada

Fast MR prostate protocol in less than 15 minutes

By Nicola Schieda, MD, FRCPC, Associate Professor of Radiology and Director of Abdominal and Pelvic MRI and Prostate Imaging, The Ottawa Hospital, Ottawa, Canada

The introduction of the Prostate Imaging Reporting and Data System (PI-RADS®) for prostate MR in 2012 has led to more standardized acquisition, interpretation and reporting of prostate MR. The revised PI-RADS® Version 2 and Version 2.1 have improved upon the original PI-RADS® and, based on multiparametric (mp) MR imaging findings, enable assessment of the level of suspicion that an MR abnormality represents a clinically significant cancer.[1]

After starting our MR prostate program in 2012 where we performed approximately 85 studies per year, our volume has grown exponentially to over 2,000 exams per year. Our initial protocol was approximately 40 minutes and was abbreviated to our main protocol which was approximately 30 minutes and included: localizers, coronal T2-weighted SSFSE, three planes of T2-weighted FRFSE, axial T1-weighted in-plane (IP) and out-of-plane (OP), conventional DWI including acquired high b-value (NEX 10), DCE (5 minutes) and large field-of-view (FOV) T1-weighted LAVA Flex post-contrast sequences.

Discovery™ MR750w

PARAMETERS	*Coronal T2w*	*Axial T2w*	*MAGiC DWI*	*DCE*
TR (ms):	7100	5200	3000	min
TE (ms):	128	128	74	min
FOV (cm):	20	20	22	35
Slice thickness (mm):	3	3	4	2
Frequency:	320	320	80	128
Phase:	256	256	128	128
NEX:	2	2	1, 2, 4	1
Scan time (min):	2:20	2:20	2:12	0:09 / phase
Options/other (b-value, no-phase wrap, etc.)	N/A	N/A	b-values: 0, 500, 1000	
BW (kHz):	41	41	250	62
ETL:	20	20	N/A	N/A

In autumn of 2018, we switched to a pseudo-fast protocol using conventional DWI by eliminating sequences (namely multiplanar T2-weighted FRFSE and elimination of large FOV imaging). This reduced scan time to under 20 minutes.

To further improve scan times, in March 2019 we introduced MAGiC DWI, which included calculated (rather than acquired) high b-value DWI. For approximately one month, patients were evaluated with both conventional and synthetic DWI, and our observations were similar image quality and artifacts on ADC map images, but with improved contrast on the synthetic high b-value DWI compared to the conventional acquisition with tumor-to-background contrast improvements.

In April 2019, we fully converted patients who were undergoing prostate MR for pre-biopsy assessment, active surveillance or with previous negative biopsy but persistent concern for possible cancer to a fast mpMR protocol using MAGiC DWI. We have performed over 250 fast mpMR exams so far.

The fast MR reduced scan time from the conventional sequence by more than half. We can scan patients door-to-door in under 15 minutes. We book four patients per hour. The doubling of efficiency enabled us to manage precious resource allocation, which is limited in Canada, and provide access

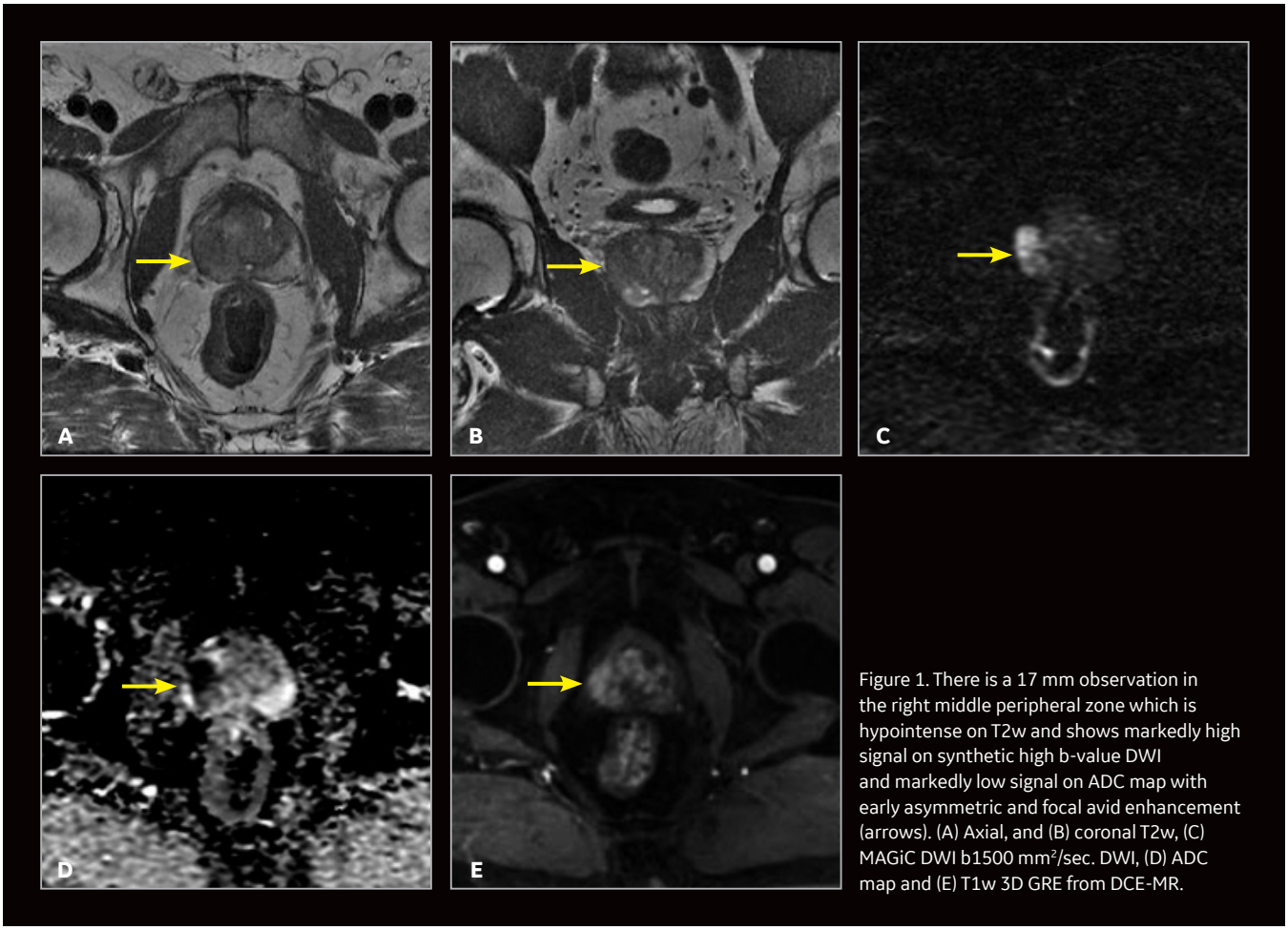

Figure 1. There is a 17 mm observation in the right middle peripheral zone which is hypointense on T2w and shows markedly high signal on synthetic high b-value DWI and markedly low signal on ADC map with early asymmetric and focal avid enhancement (arrows). (A) Axial, and (B) coronal T2w, (C) MAGiC DWI b1500 mm^2/sec. DWI, (D) ADC map and (E) T1w 3D GRE from DCE-MR.

for increased utilization of prostate MR (volume doubled from 2016 to 2019) without an increase in operational hours or blocking access to MR for other patients.

Further reductions in scan time could be achieved if using an abbreviated biparametric (bp) MR rather than an mpMR exam. The main difference between bpMR and mpMR is the use of gadolinium-based contrast agents (GBCA) and dynamic contrast-enhanced (DCE) imaging in the later protocol.

The use of GBCA for DCE in prostate MR is a controversial topic due to concerns of gadolinium retention, higher associated costs and longer scan times. In general, there has been increased scrutiny regarding the liberal use of GBCA for many MR exams, leading to interest in bpMR.

A meta-analysis of 33 studies found that the pooled specificity between mpMR and bpMR were not significantly different.[2] However, bpMR had a statistically significant lower sensitivity (80 percent compared to 85 percent) that the authors suggest may be attributed to the ability to detect subtle lesions with DCE-MR, even though DCE has a limited role in the diagnosis of prostate cancer.[2]

A recent study comparing mpMR, bpMR and a "fast" (monoplanar) bpMR in 626 biopsy-naïve men reported the same sensitivity (95 percent) for all protocols and a specificity of 65 percent for the "fast" bpMR and 69 percent for both the bpMR and mpMR.[3] Inter-reader agreement was 90 percent for the fast bpMR and 93 percent for the bpMR.[3] The authors reported that both bpMR protocols had an equal detection rate of high-grade prostate cancer equivalent to mpMR, and the "fast" bpMR had a high negative predictive value of 97 percent. However, there are added benefits of the "fast" bpMR, such as the ability to increase prostate MR capacity at a lower cost and the avoidance of potential risks associated with GBCA administration.[3]

We presently do not perform bpMR at our institution and all patients undergo a comprehensive mpMR exam that is fully compliant with PI-RADS® v2.1 guidelines, including two planes of T2-weighted imaging, axial DWI and axial DCE. In our own experience, we estimate DCE is required in the following situations: approximately 10 percent of cases where DWI may be compromised by artifact (e.g., from rectal gas, hip prosthesis); in PI-RADS® v2.1 assessment category 3 lesions in the peripheral zone; and in patients who have undergone therapy (e.g., radical prostatectomy, radiotherapy) and there is concern for local recurrence. We are actively considering the use of bpMR with the strategy of calling patients back when DCE-MR is required; however,

we continue to perform mpMR in all patients. For patients referred for local staging of a known significant prostate cancer, we perform a comprehensive staging mpMR, which is acquired in under 30 minutes but includes all three planes of T2-weighted imaging and large FOV sequences of the whole pelvis to assess for lymphadenopathy and the pelvic marrow.

Patient history

A 64-year-old male with Prostate Serum Antigen (PSA) 12.3 ng/mL undergoing fast prostate MR for targeting pre-biopsy.

Results

A low T2-weighted lesion in the peripheral zone with marked restricted diffusion and avid early asymmetric enhancement was noted. The observation was characterized as a PI-RADS® v2.1 category 5 (clinically significant cancer is very likely to be present). Subsequent transrectal ultrasound-MR fusion biopsy confirmed Gleason 4+3=7 prostate cancer.

Technique

Our first attempt at fast MR included one plane of T2-weighted imaging (the axial plane). Our experience, which is in line with PI-RADS® v2.1 recommendations, is that a proportion of transition zone nodules may appear partially or incompletely circumscribed, partially or incompletely encapsulated, or show blurred or indistinct margins due to volume averaging effects when using only axial T2-weighted images. PI-RADS® v2.1 suggests at least one additional plane of T2-weighted imaging in addition to the axial plane, and we have found that this strategy improves our characterization of transition zone nodules. The use of a T2-weighted 3D sequence (i.e., Cube) is another strategy and, when used with a novel time saving technique that combines parallel imaging and compressed sensing (i.e., HyperSense), could be a real alternative to a conventional T2-weighted 2D sequence with expected marked reduction in scan time and artifact.

Discussion

In our experience using the fast mpMR technique, we found no difference in the detection of cancers overall but subjectively improved contrast-to-noise on synthetic high b-value DWI, improving reader confidence for detection of prostate cancers. There was also no change in biopsy rates or accuracy; however, we did experience improved reader confidence when evaluating potential tumor to background on the synthetic high b-value images.

More importantly, we doubled our capacity to accommodate a significant increase in requests for prostate MR with no change in operational hours or funding, or an increase in wait times. Patients are very satisfied with the shorter exams.

The accuracy of the fast mpMR protocol is not better than the standard mpMR protocol; however, it is not inferior in terms of cancer detection rates, and that is important. Based on the results from the PRECISION trial[4], we could infer that in the 30 percent of men who have a negative mpMR and are undergoing imaging for elevated PSA or abnormal DRE, biopsy could be avoided in the future if further validation of this practice becomes available, thus saving costs and potential morbidity for the patient.

At The Ottawa Hospital, we are evaluating switching to a bpMR protocol for most patients and recalling the subset of patients who require DCE-MR if we believe that may help to improve the exam quality (e.g., artifact compromising DWI, PI-RADS® 3 peripheral zone observation). More vigilant protocolling of cases, i.e., identifying patients with metallic implants in the pelvis and those with suspected local recurrence of tumor after therapy, would further delineate which patients would require GBCA at the time of their first exam.

Based on our experience in prostate MR, we are considering implementing MAGiC DWI into all of our pelvic MR protocols, especially those for rectal and cervical cancer assessment.

Other institutions that evaluate synthetic DWI sequences such as MAGiC DWI may also discover what I have found: more is not better. Patient tolerance for MR exams decreases over time and the shorter the exam, the better success in reducing patient-induced motion artifacts. The results from our adoption of the synthetic DWI, combined with our own reductions in sequences, incorporate engineering advances with practical experience to improve exam quality, shorten exam times, increase patient tolerance and enhance access/capacity while maintaining diagnostic accuracy.

References

1. Purysko AS, Rosenkrantz AB, Barentsz JO, Weinreb JC, Macura KJ. PI-RADS Version 2: A Pictorial Update. Radiographics. 2016 Sep-Oct;36(5):1354-72.
2. Niu XK, Chen XH, Chen ZF, Chen L, Li J Peng T. Diagnostic Performance of Biparametric MRI for Detection of Prostate Cancer: A Systematic Review and Meta-Analysis. AJR Am J Roentgenol. 2018 Aug;211(2):369-378.
3. van der Leest M, Israël B, Cornel EB, et al. High Diagnostic Performance of Short Magnetic Resonance Imaging Protocols for Prostate Cancer Detection in Biopsy-naïve Men: The Next Step in Magnetic Resonance Imaging Accessibility. Eur Urol. 2019 Jun 2. pii: S0302-2838(19)30436-1.
4. Kasivisvanathan V, Rannikko AS, Borghi M, et al. MRI-targeted or standard biopsy for prostate-cancer diagnosis. N Engl J Med 2018;378:1767e77.

Isogai Takeshi, RT(R)
The Second Kawasaki Saiwai Clinic
Kawasaki, Japan

Minayoshi Shinsuke, RT(R)
The Second Kawasaki Saiwai Clinic
Kawasaki, Japan

Non-contrast prostate and vascular imaging

By Isogai Takeshi, RT(R), and Minayoshi Shinsuke, RT(R), The Second Kawasaki Saiwai Clinic, Kawasaki, Japan

Concerns regarding the use of gadolinium-based contrast agents in MR imaging, particularly in patients with renal or kidney disease, have led to an increase in the use of non-contrast MR sequences in Japan. There is also growing awareness that many procedures involving needles such as biopsy and sedation can have potentially dangerous side effects to patients, add additional costs to procedures and extend patient recovery times. At The Second Kawasaki Saiwai Clinic, we have embraced the use of GE Healthcare's Needle-Free Suite of sequences for many common MR imaging exams. We believe that avoiding the use of contrast can improve patient comfort, simplify workflow and reduce cost.

Although contrast-enhanced MR has been the current standard for non-invasive detection of prostate tumors, several studies suggest that non-contrast biparametric MR with T2-weighted and diffusion-weighted imaging (DWI) may be sufficient for diagnosis and also satisfy the requirements of PI-RADS® v2.1.[1] For non-contrast prostate exams at The Second Kawasaki Saiwai Clinic (Kanagawa, Japan), the use of PROPELLER and DWI are important for the detection of cancerous tumors (see Cases 1-3).

PROPELLER reduces effects of patient voluntary and physiologic motion without sedation, and reduces susceptibility artifacts. Since The Second Kawasaki Saiwai Clinic uses PROPELLER MB to minimize motion artifacts they do not need to use glucagon or a paralytic drug to suppress bowel motion. DWI provides high SNR diffusion images with short acquisition times and multiple b-values to provide measurement of apparent diffusion coefficient (ADC) map with reduced effect of perfusion.

In addition to prostate imaging, we also find that non-contrast MR is very useful for the follow-up of stent grafts to detect endoleak (see Case 4). Historically, CT imaging is used to follow-up patients after performing a stent graft treatment. However, because stent grafts are composed of artificial blood vessels (grafts) and metal frameworks (stainless steel, nitinol), the quality of the CT exam is often affected by metal artifacts. MR imaging is typically less impacted by metal artifacts and is therefore often utilized for these cases.

Case 1

Patient history

A 79-year-old patient referred for MR exam for suspected prostate cancer.

MR findings

PI-RADS® score 4 with a lesion slightly smaller than 7 mm in the transition zone detected on DWI with ADC map.

SIGNA™ Creator — Cases 1-3

PARAMETERS

	Axial T2w PROPELLER	*Sagittal T2w PROPELLER*	*Axial T1w PROPELLER*	*Coronal T1w PROPELLER*	*Coronal T2w FatSat PROPELLER*	*Coronal STIR PROPELLER*	*DWI*
TR (ms):	4440	4000	400	600	4500	3500	5000
TE (ms):	120	120	15.4	15	129	81.5	86
FOV (cm):	20 x 20	22 x 22	20 x 20	24 x 24	24 x 24	24 x 24	35 x 28
Slice thickness (mm):	4	5	4	5	5	5	4
Frequency:	352	352	288	288	352	192	96
Phase:	352	352	288	288	352	192	128
NEX:	3	3	2.5	2.5	3	5	16
Scan time (min.):	3:38	3:16	2:58	2:09	3:25	3:44	4:10
b-value:							b1400

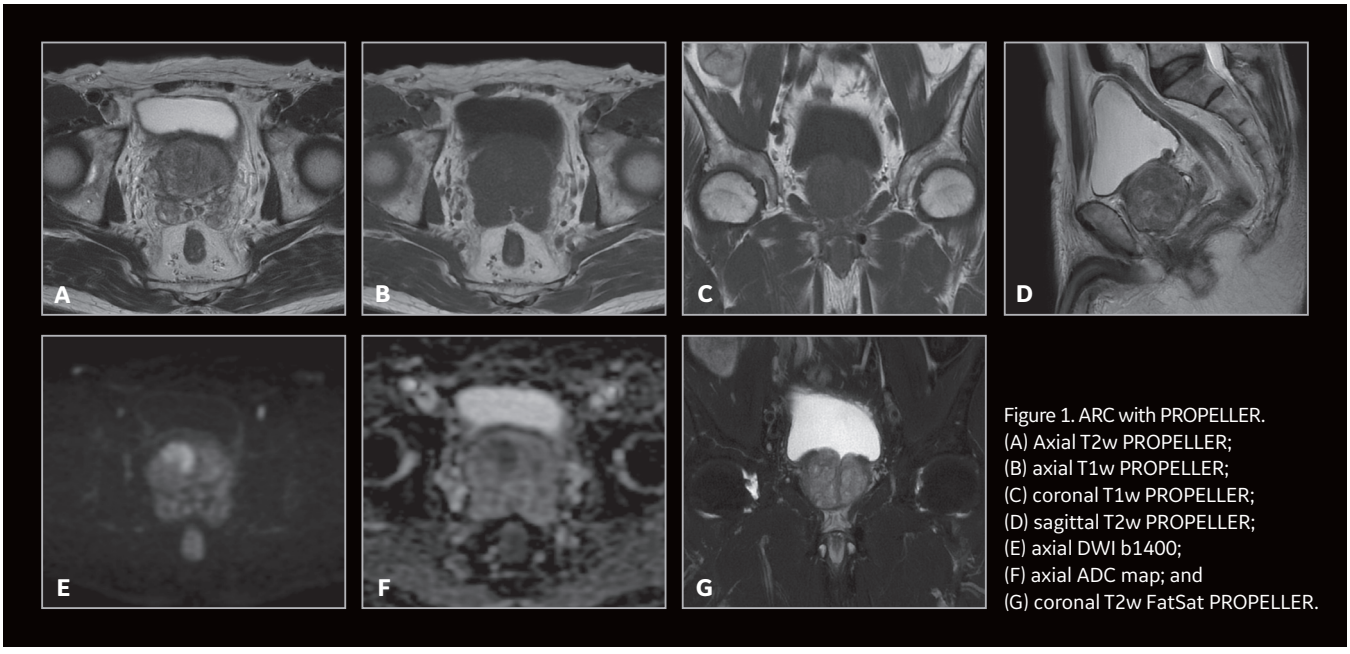

Figure 1. ARC with PROPELLER.
(A) Axial T2w PROPELLER;
(B) axial T1w PROPELLER;
(C) coronal T1w PROPELLER;
(D) sagittal T2w PROPELLER;
(E) axial DWI b1400;
(F) axial ADC map; and
(G) coronal T2w FatSat PROPELLER.

Case 2

Patient history

A 77-year-old man with persistent, high PSA and history of benign prostatic hyperplasia. Patient previously underwent surgery on his left femoral head and has an artificial joint.

MR findings

Prostate cancer, enlargement of prostatic intraepithelial neoplasia.

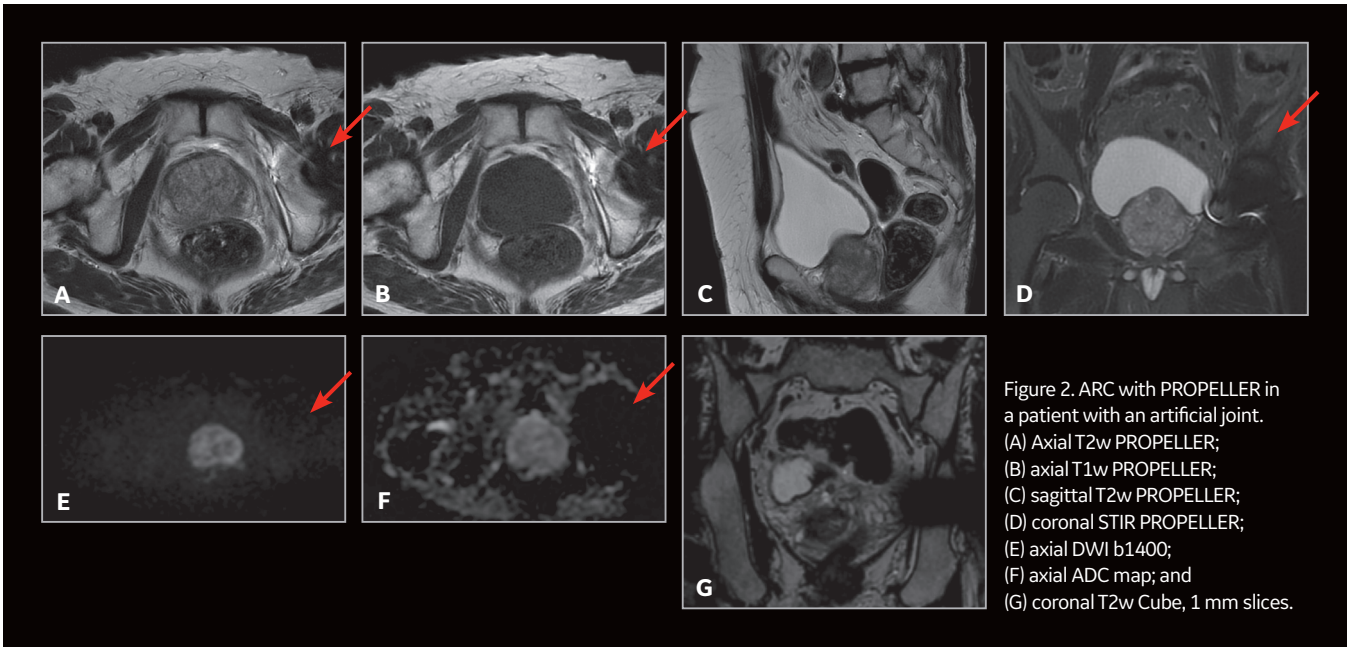

Figure 2. ARC with PROPELLER in a patient with an artificial joint.
(A) Axial T2w PROPELLER;
(B) axial T1w PROPELLER;
(C) sagittal T2w PROPELLER;
(D) coronal STIR PROPELLER;
(E) axial DWI b1400;
(F) axial ADC map; and
(G) coronal T2w Cube, 1 mm slices.

Case 3

Patient history

A 71-year-old man with persistent, high PSA and history of benign prostatic hyperplasia.

MR findings

Prostate cancer with PI-RADS® score 4.

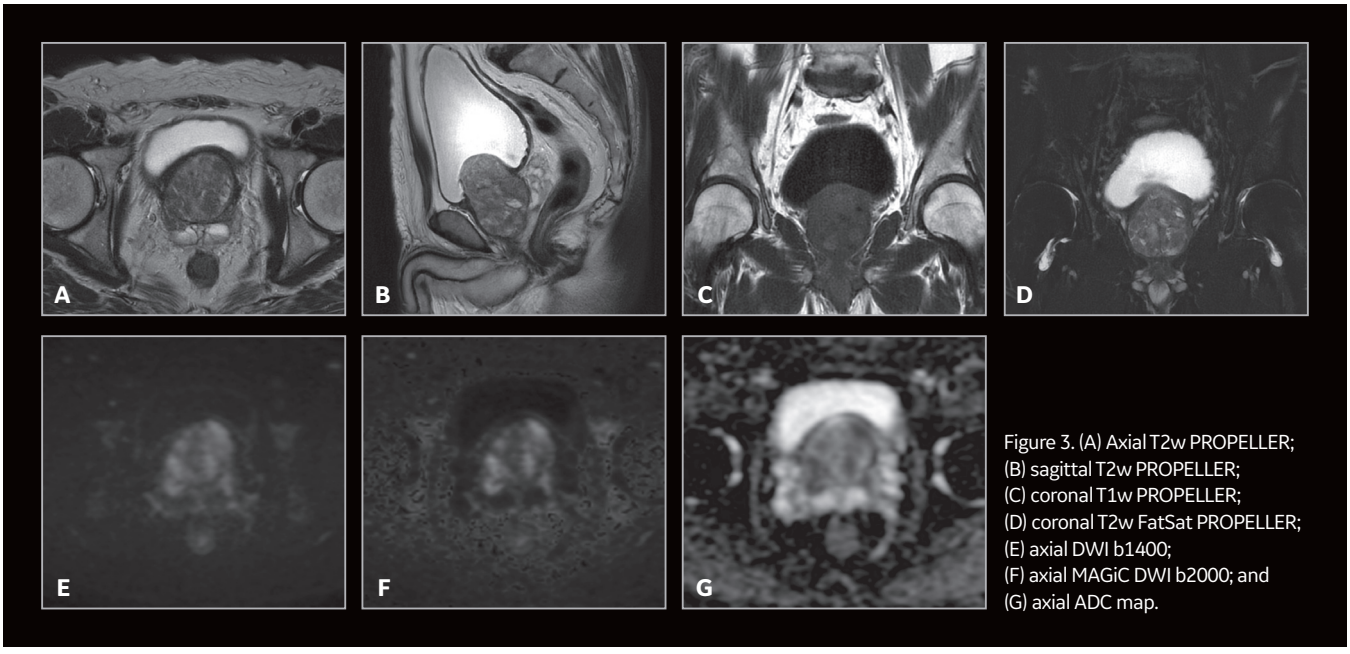

Figure 3. (A) Axial T2w PROPELLER;
(B) sagittal T2w PROPELLER;
(C) coronal T1w PROPELLER;
(D) coronal T2w FatSat PROPELLER;
(E) axial DWI b1400;
(F) axial MAGiC DWI b2000; and
(G) axial ADC map.

Case 4

Patient history

A 84-year-old man referred for MR exam for follow-up one month after an endovascular aneurysm repair. Metal artifacts obscured the anatomy on CT, necessitating the use of MR for suspected endoleak.

MR findings

Type III leak from stent graft in leg detected using non-contrast-enhanced blood vessel imaging. (S)

Reference

1. The American College of Radiology. Prostate Imaging Reporting & Data System (PI-RADS). Available at: https://www.acr.org/Clinical-Resources/Reporting-and-Data-Systems/PI-RADS. Accessed on Oct. 12, 2019.

SIGNA™ Creator — Case 4

PARAMETERS

	Coronal 2D FIESTA FatSat	*Axial 2D FIESTA FatSat*	*Coronal 2D FIESTA Cine*	*Axial 2D FIESTA Cine*
TR (ms):	4.8	4.4	3.97	3.97
TE (ms):	2.2	2	1.77	1.77
FOV (cm):	38 x 38	38 x 38	38 x 38	38 x 38
Slice thickness (mm):	6	6	8	8
Frequency:	316	256	224	224
Phase:	320	256	256	256
NEX:	1	1	1	1
Scan time (min.):	15 sec.	16 sec.	2:12	5:44

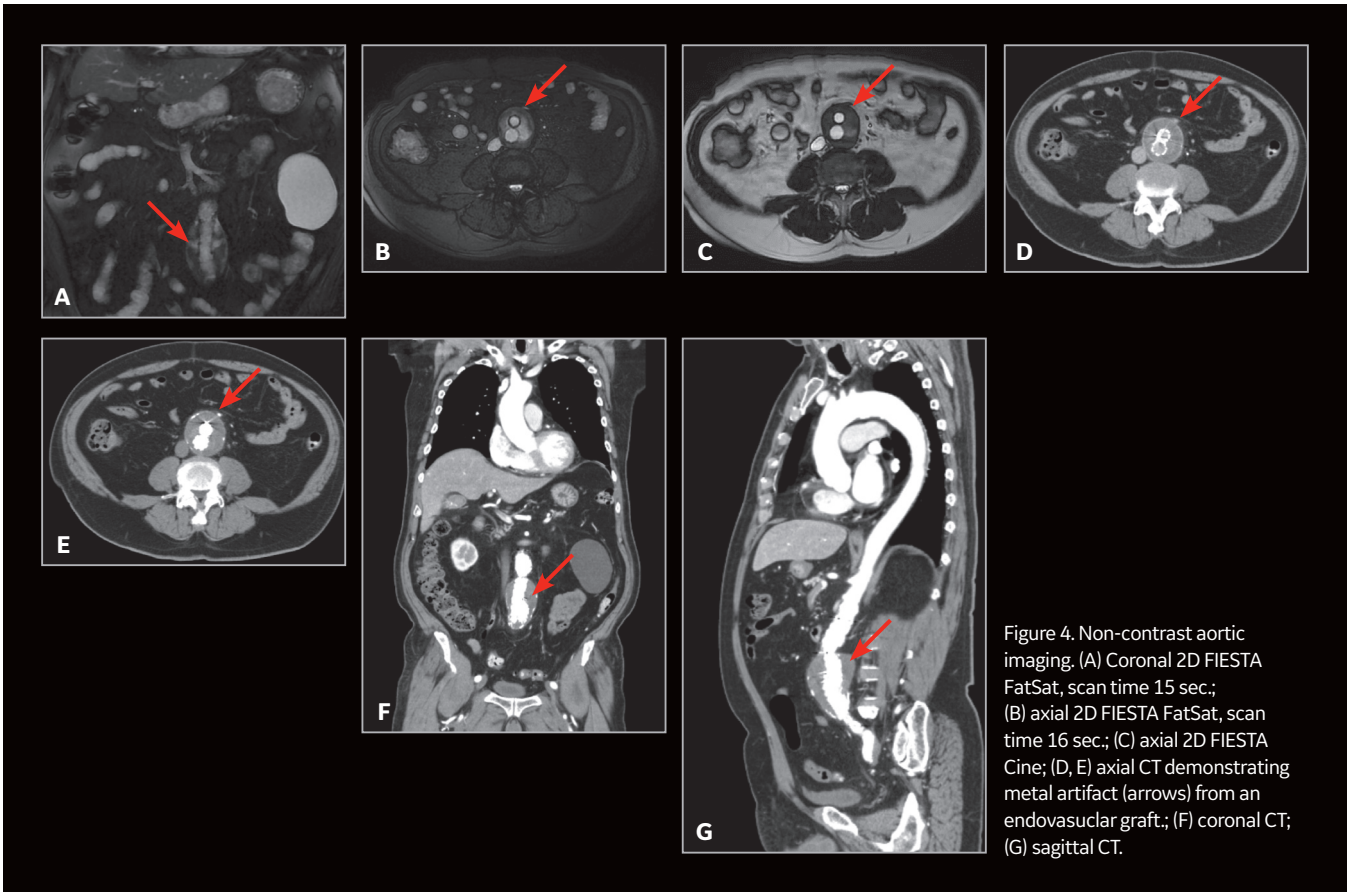

Figure 4. Non-contrast aortic imaging. (A) Coronal 2D FIESTA FatSat, scan time 15 sec.; (B) axial 2D FIESTA FatSat, scan time 16 sec.; (C) axial 2D FIESTA Cine; (D, E) axial CT demonstrating metal artifact (arrows) from an endovasuclar graft.; (F) coronal CT; (G) sagittal CT.

Bariş Bakir, MD, PhD
Istanbul University School of Medicine
Istanbul, Turkey

Lebriz Uslu Beşli, MD
Istanbul University-Cerrahpasa, Cerrahpaşa School of Medicine
Istanbul, Turkey

Sertaç Asa, MD
Istanbul University-Cerrahpasa, Cerrahpaşa School of Medicine
Istanbul, Turkey

Concurrent multiparametric MR with PET/MR for prostate cancer

By Bariş Bakir, MD, PhD, Professor of Radiology at Istanbul University School of Medicine, and Lebriz Uslu Beşli, MD, and Sertaç Asa, MD, Istanbul University-Cerrahpaşa, Cerrahpaşa School of Medicine, Nuclear Medicine Department, Istanbul, Turkey

In the past 10 years, there have been groundbreaking developments in the field of prostate cancer. Among these, developments in PET and MR radiopharmaceuticals specific to receptors stand out. Multiparametric MR (mpMR) helps in the detection and localization of prostate cancer, as well as biopsy guidance. Although mpMR is an effective imaging method, the false negative rates of up to 20 percent may create challenges.

The ability of Gallium-68 (^{68}Ga) prostate-specific membrane antigen (PSMA)[‡] PET imaging, offering up to 90 percent detection sensitivity, complements MR when mpMR falls short. Thus, PET/MR systems combining ^{68}Ga PSMA PET and mpMR provide a substantial increase in lesion detection rates[1,2]. It has been shown that ^{68}Ga PSMA PET/MR has a higher accuracy rate with respect to mpMR in primary lesion detection[3,4].

It is expected that mpMR performed concurrently with ^{68}Ga PSMA PET/MR may have more prominent significance in clinical practice. The following cases demonstrate, although not yet with histopathological confirmation, how PET and MR reinforce (cases 1 and 5) or complement (cases 2-4) each other.

SIGNA™ PET/MR - prostate protocol

	Axial T2 PROPELLER	*Sagittal T2 PROPELLER*	*Coronal T2 PROPELLER*	*FOCUS DWI*	*T1 DCE FSPGR*
FOV (cm):	20 x 20	20 x 20	20 x 20	28 x 11.2	25 x 21.3
Slice thickness (mm):	3	3.5	3	4	4
Frequency:	352	320	320	160	128
Phase:	352	320	320	164	100
Scan time (min.):	4:04	4:28	2:59	6:08	4:05
Options / other (b-value, no-phase wrap, etc.):				b50, b800, b1400	7 sec./phase

[‡]^{68}Ga PSMA is not approved by the US FDA and may not be available for clinical use in all markets.

Case 1

Consistent with both mpMR and ^{68}Ga PSMA PET scans, a prostatic lesion (red arrow) is observed at the left posteromedial peripheral zone with a suspicion of malignancy that could indicate prostate cancer.

A less significant PSMA uptake (blue arrow) with cancer suspicion that was observed in the ^{68}Ga PSMA PET images of the prostatic gland right peripheral zone were non-existent in the multi-parametric prostatic MR sequences.

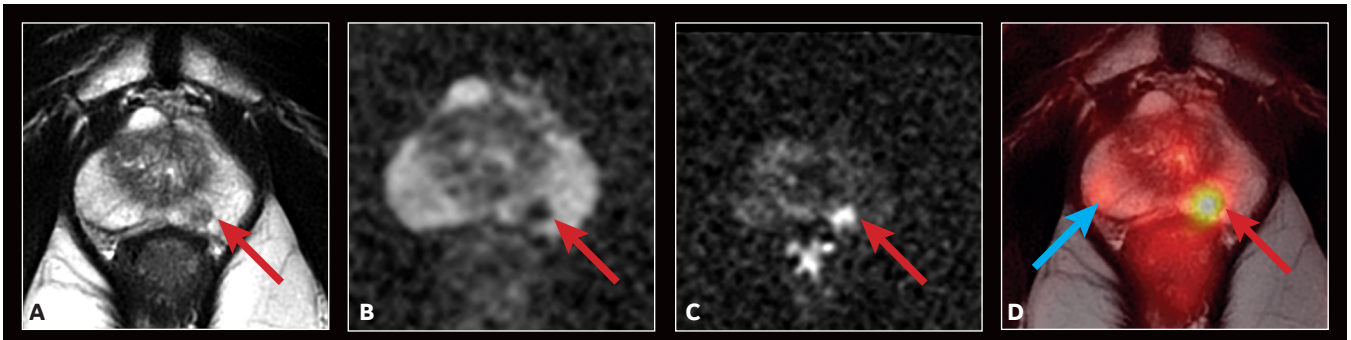

Figure 1. (A) Axial T2w, (B) ADC map, (C) high b-value DWI and (D) ^{68}Ga PSMA PET/MR fused image.

Case 2

The ^{68}Ga PSMA PET images of the left peripheral zone posteromedial show PSMA uptake with prostatic cancer suspicion. In the mpMR sequences, the same lesion is not clearly visible among the hemorrhage foci.

The patient's pathology results indicate a Gleason Score of 3+3 on two foci after transrectal ultrasound biopsy (TRUS) biopsy.

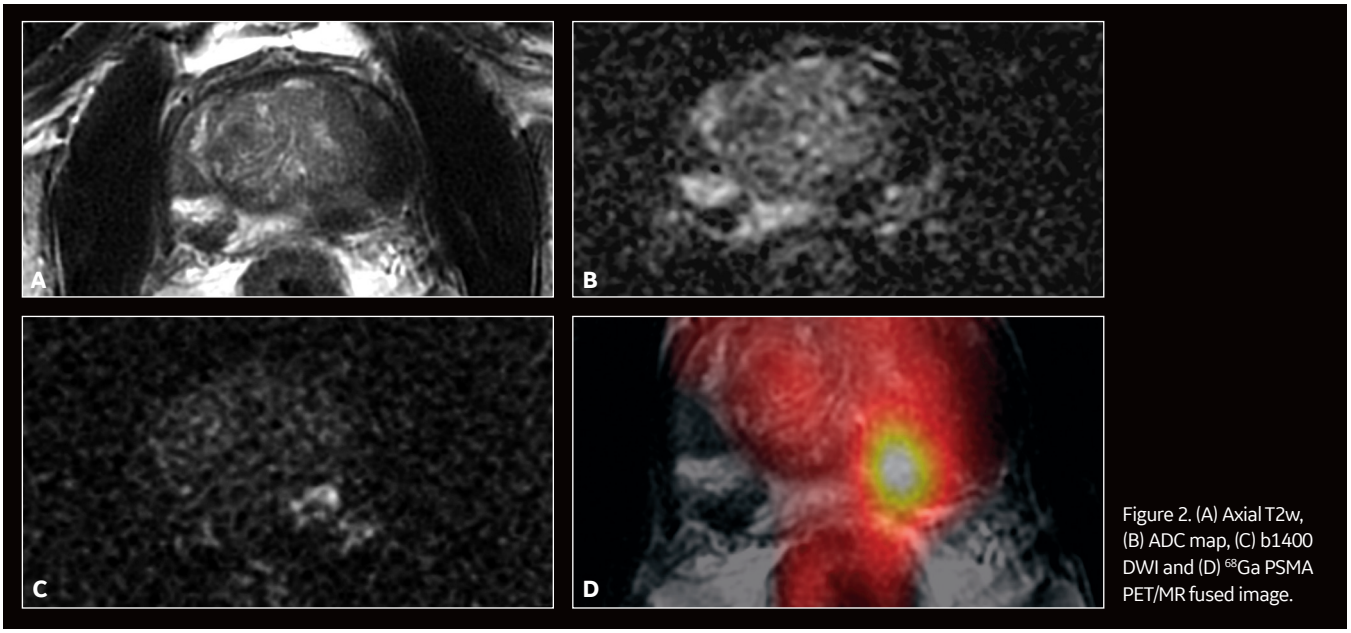

Figure 2. (A) Axial T2w, (B) ADC map, (C) b1400 DWI and (D) ^{68}Ga PSMA PET/MR fused image.

All mpMR images taken concurrently with ^{68}Ga PSMA PET/MR images are courtesy of Cerrahpaşa School of Medicine, Nuclear Medicine Department.

Case 3

The ^{68}Ga PSMA PET images of the left transition zone show PSMA uptake with prostatic cancer suspicion. The same lesion cannot be observed in the mpMR sequences.

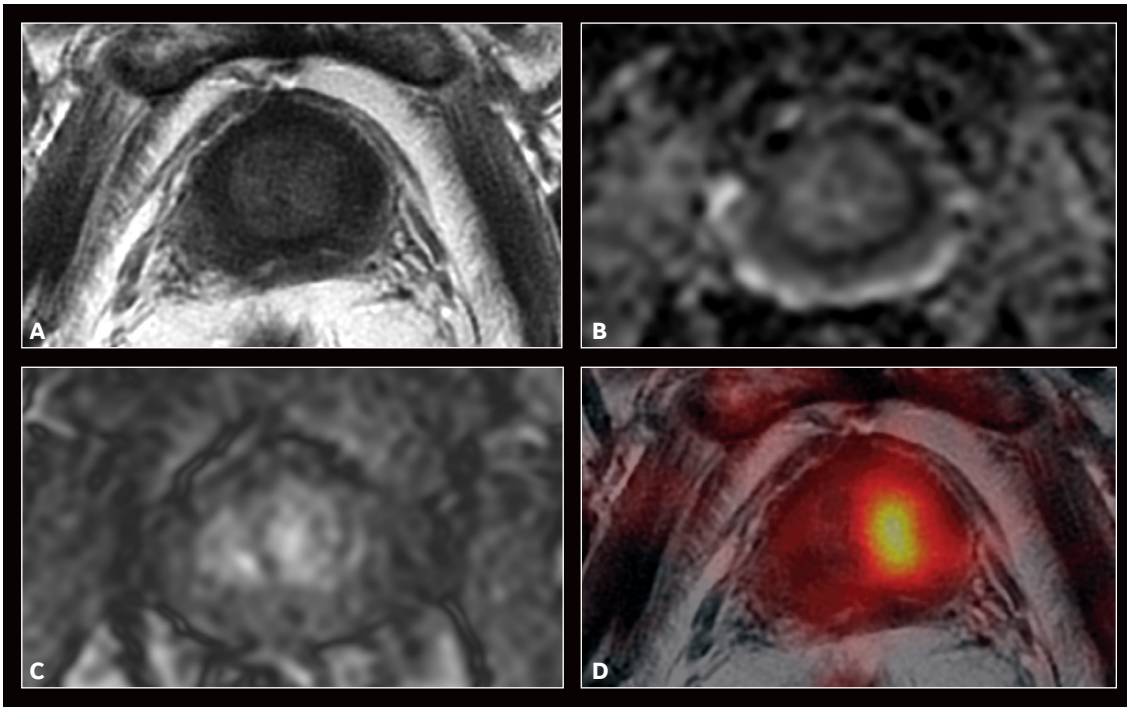

Figure 3. (A) Axial T2w, (B) ADC map, (C) post-contrast T1w image and (D) ^{68}Ga PSMA PET/MR fused image.

Case 4

In the sections that intercept the mid-gland level at the prostatic gland, the presence of two recurrent tumoral lesions in both posteromedial peripheral zones indicate growth in the follow-up mpMR assays, observed due to prostate cancer and after brachytherapy. Lesions in the diffusion-weighted MR image are observed as hyperintense. Distinct early arterial contrast uptake is observed at the post-contrast subtraction T1 images. Lesions are observed with a different color code at the perfusion k-trans mapping. At the ^{68}Ga PSMA PET/MR fused image, only the right lesion can be observed while the one on the left is non-existent.

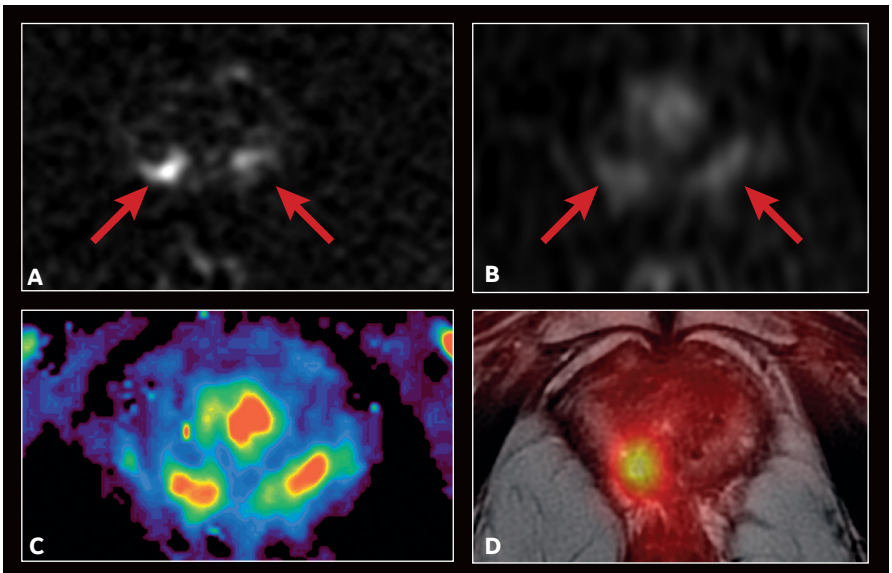

Figure 4. (A) DWI, (B) T1 post-contrast, (C) perfusion k-trans mapping and (D) ^{68}Ga PSMA PET/MR fused image.

Case 5

A 64-year-old patient with a Gleason Score 3+5 prostate cancer after radical prostatectomy operation was referred for PET/MR. The patient had metastatic pelvic lymph nodes and bone lesions, which showed complete or near-complete regression on the ^{68}Ga PSMA PET after hormone therapy. A 23 x 12 x 10 mm sized residual prostatic lesion on the left side of the bladder neck with diffusion restriction was observed on mpMR. The lesion also showed increased perfusion (not shown). The ^{68}Ga PSMA PET image exhibited no uptake on the residual mass, likely due to response to therapy similar to the other metastatic foci.

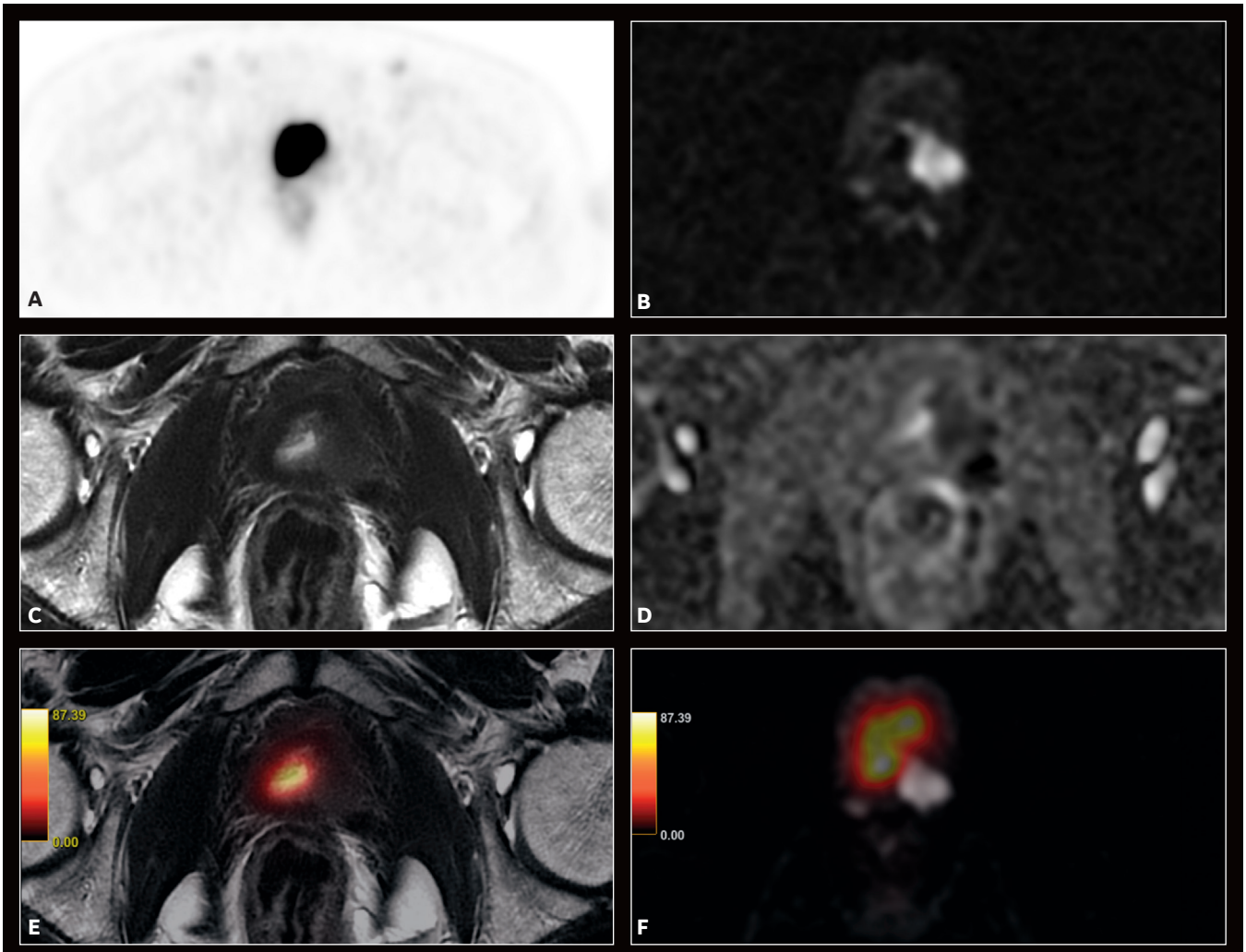

Figure 5. (A) ^{68}Ga PSMA PET, (B) b1400 DWI, (C) axial T2w, (D) ADC map and ^{68}Ga PSMA PET fused with (E) T2w and (F) DWI.

Case 6

A 69-year-old patient with Gleason Score 4+4 prostate cancer after TRUS biopsy. mpMR shows a PI-RADS® 5 lesion extending from the left transitional zone to the left peripheral zone of the prostate gland. ^{68}Ga PSMA uptake is observed only on left transitional zone, underestimating the tumor extension in the peripheral zone.

Histopathology results after radical prostatectomy operation revealed Gleason Score 4+3 prostate cancer extending from the transitional zone to the peripheral zone of the gland, which was in accordance with the mpMR images.

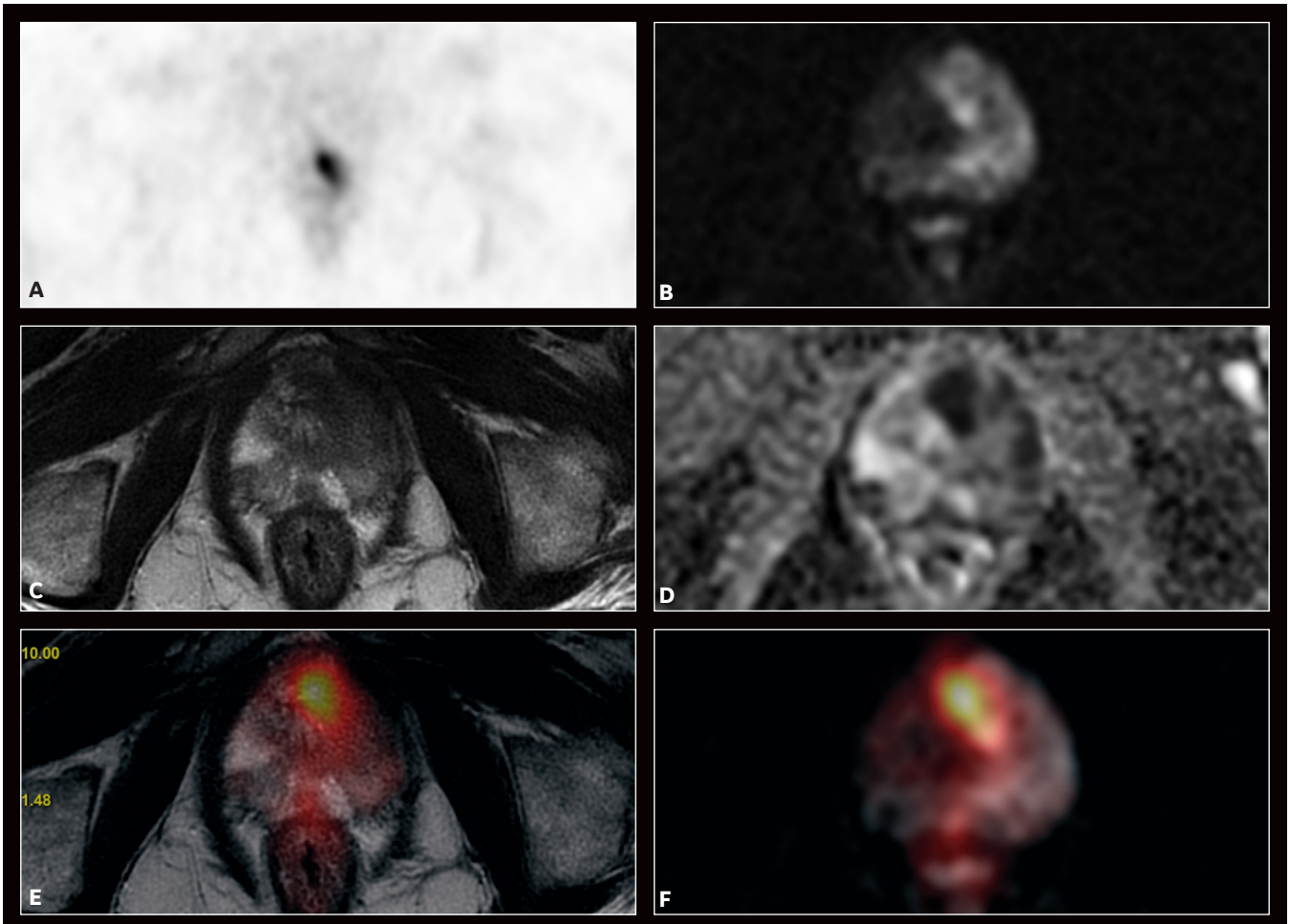

Figure 6. (A) ^{68}Ga PSMA PET, (B) b1400 DWI, (C) axial T2w, (D) ADC map and ^{68}Ga PSMA PET fused with (E) T2w and (F) DWI.

Discussion

^{68}Ga PSMA PET/MR imaging offers a significant advancement in the diagnosis and management of prostate cancer, including for the detection of primary lesions and designation of prognosis and staging. We anticipate the simultaneous ^{68}Ga PSMA PET and mpMR method will be an effective component of our diagnostic and treatment algorithms in the near future.

References

1. Kranzbühler B, Müller J, Becker AS, et al. Detection Rate and Localization of Prostate Cancer Recurrence Using ^{68}Ga-PSMA-11 PET/MRI in Patients with Low PSA Values ≤ 0.5 ng/mL. J Nucl Med. 2020;61(2):194–201.
2. Barbosa FG, Queiroz MA, Nunes RF, Marin JFG, Buchpiguel CA, Cerri GG. Clinical perspectives of PSMA PET/MRI for prostate cancer. Clinics (Sao Paulo). 2018;73(suppl 1):e586s. Published 2018 Sep 21.
3. Hicks RM, Simko JP, Westphalen AC, et al. Diagnostic Accuracy of ^{68}Ga-PSMA-11 PET/MRI Compared with Multiparametric MRI in the Detection of Prostate Cancer. Radiology. 2018;289(3):730–737.
4. Muehlematter UJ, Rupp NJ, Mueller J, Eberli D, Burger IA. ^{68}Ga-PSMA PET/MR-Positive, Histopathology-Proven Prostate Cancer in a Patient With Negative Multiparametric Prostate MRI. Clin Nucl Med. 2018;43(8):e282–e284.

Ercan Karaarslan, MD
Acıbadem Maslak Hospital
Istanbul, Turkey

Multi-parametric prostate MR imaging with structured reporting

by Ercan Karaarslan, MD, Professor of Radiology, Acıbadem Maslak Hospital, Istanbul, Turkey

The clinical demand for multi-parametric MR imaging continues to grow as it provides important information for patient management decisions. With prostate cancer, there is a range of biologic activity; in many patient cases, it is a slow-growing disease that does not lead to a prostate-cancer related death and in others it can be a very aggressive form. Considering that several treatment options have significant side effects such as rectal injury, incontinence and impotence, patient disease stratification and staging is imperative.

Technological advancements around oncologic imaging, in general, have enabled us to diagnose at an earlier stage, allowing us to more closely personalize patient treatment and, in many cases, utilize less invasive treatment methods. Our hospital also specializes in interventional radiology and prostate surgery with more than 1,000 patients receiving MR/Ultrasound fusion prostate biopsy or robotic surgery in the last few years.

In February 2020, a SIGNA™ Premier 3.0T was installed in our facility, providing new capabilities such as the AIR™ Anterior Array (AA) Coil and SIGNA™Works AIR™ Edition software featuring MUSE, FOCUS DWI, MAGiC DWI and DISCO. These capabilities provided a wing-to-wing solution for prostate imaging that improves image quality, the reporting process and patient comfort.

The patient experience is vastly improved, which has positively impacted compliance and, therefore, image quality. Patients have commented on the difference in comfort with the AIR™ AA Coil compared to conventional coils. They do not feel the same pressure on their body as with a conventional coil due to the lightweight nature of the AIR™ AA Coil. With SIGNA™ Premier, patients enter the bore feet-first so their head is near the edge of the magnet, reducing claustrophobia.

Patient history

An 85-year-old male with dysuria was referred by his urologist for prostate MR assessment.

Results

Patient has a right mid-prostatic peripheral zone with a score 5 dominant lesion and bilateral peripheral zone with score 4 and 5 lesions.

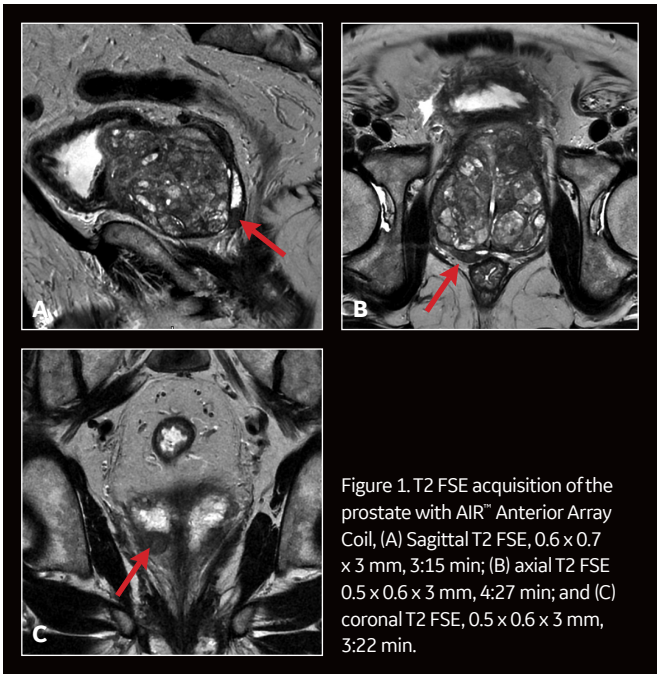

Figure 1. T2 FSE acquisition of the prostate with AIR™ Anterior Array Coil, (A) Sagittal T2 FSE, 0.6 x 0.7 x 3 mm, 3:15 min; (B) axial T2 FSE 0.5 x 0.6 x 3 mm, 4:27 min; and (C) coronal T2 FSE, 0.5 x 0.6 x 3 mm, 3:22 min.

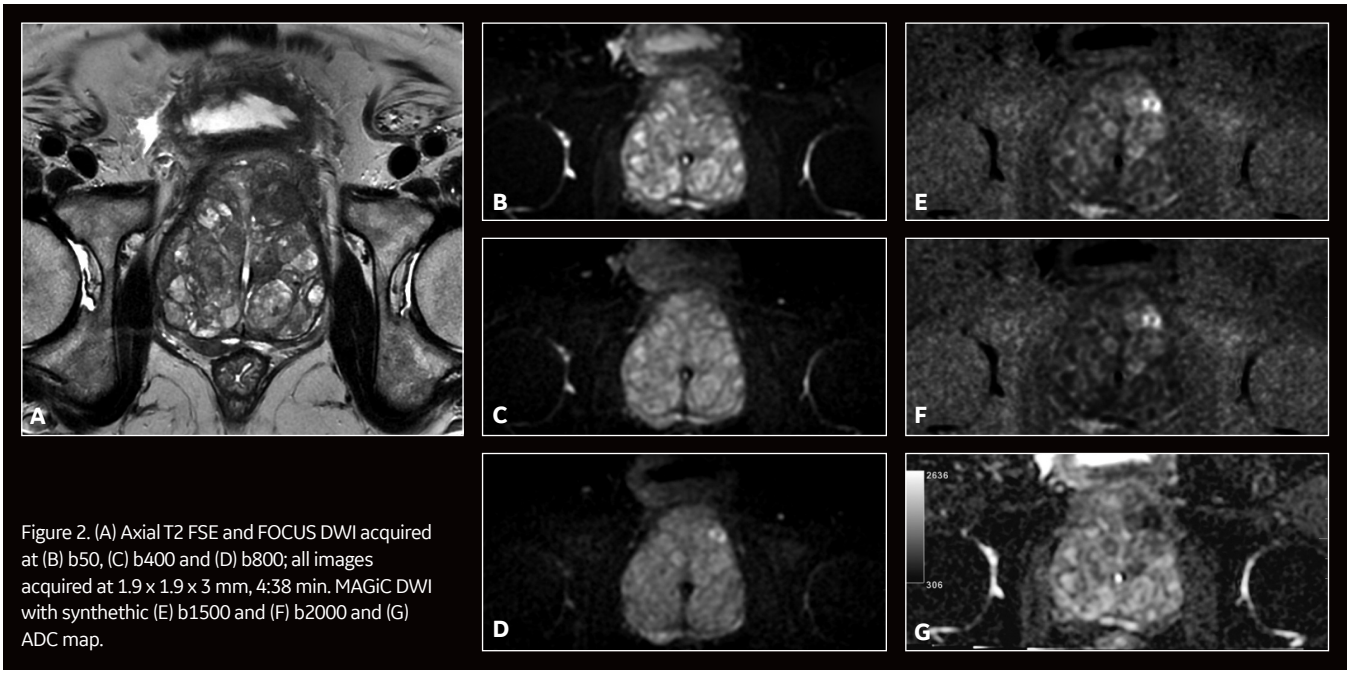

Figure 2. (A) Axial T2 FSE and FOCUS DWI acquired at (B) b50, (C) b400 and (D) b800; all images acquired at 1.9 x 1.9 x 3 mm, 4:38 min. MAGiC DWI with synthethic (E) b1500 and (F) b2000 and (G) ADC map.

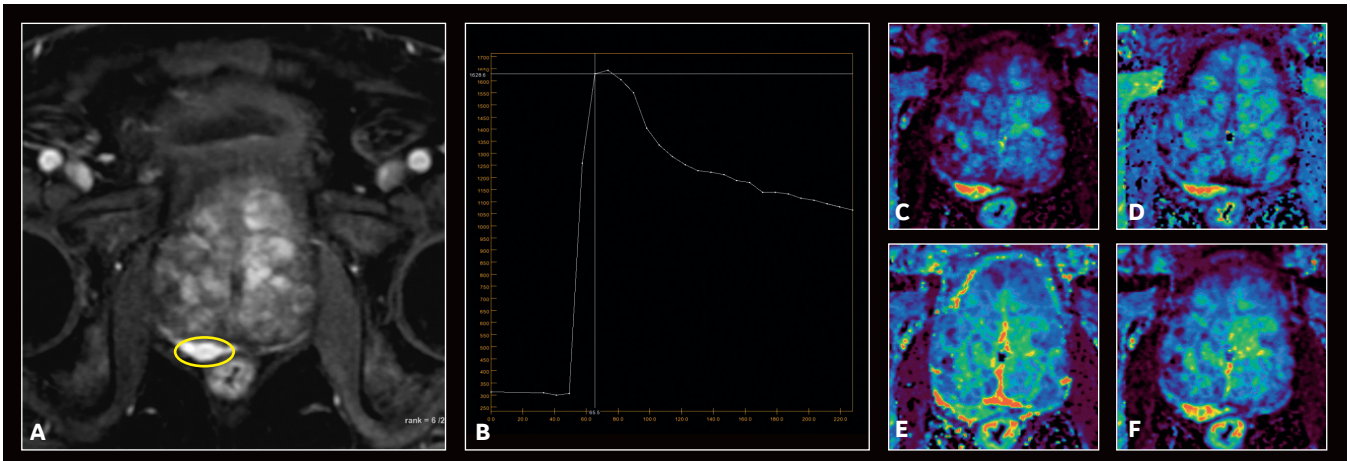

Figure 3. (A) DISCO acquisition with AIR™ AA Coil, 1.1 x 1.2 x 3 mm, temporal resolution 6.6 sec, total scan time 3:24 min., (B) dynamic enhancement curve generated by DISCO and (C) permeability maps created with GenIQ.

Discussion

The combination of FOCUS DWI with MAGiC DWI improves SNR and image quality for high b-value DWI information and also improves the resolution in small FOV DWI applications. MUSE is preferred for challenging patients with the presence of rectal gas, where the air-tissue interfaces increase susceptibility artifacts on DWI, making prostate peripheral zone assessment difficult. Compared to single-shot techniques, multi-shot MUSE is highly immune to susceptibility and the switching of frequency encoding direction to A-P (Phase read-out to R-L) also helps to minimize susceptibility artifacts in the peripheral zone.

Using DISCO for dynamic contrast enhancement (DCE) imaging delivers both high temporal and spatial resolution with FatSat. We further analyze this data using GenIQ for permeability analysis on our AW Server platform.

PROView 2.0 is designed to provide standardization of prostate reporting to allow for interdisciplinary agreement between the urologist and radiologist for patient follow-up. The PSA density and accuracy of prostate volume are important values in the follow-up of PI-RADS® category 3 patients who may be deferred for repeat biopsy[1,2]. Patients classified as PI-RADS® category 3 may have a low risk of clinically significant prostate cancer, and therefore may not require repeat biopsy. Our existing reporting method utilizes a standard ellipsoid measurement model (length x width x height x 0.52 mm) for prostate volume assessment. S

References

1. Washino S, Okochi T, Saito K, Konishi T, Hirai M, Kobayashi Y, Miyagawa T. Combination of prostate imaging reporting and data system (PI-RADS) score and prostate-specific antigen (PSA) density predicts biopsy outcome in prostate biopsy naïve patients. BJU Int. 2017 Feb;119(2):225-233. doi: 10.1111/bju.13465. Epub 2016 Apr 1. PMID: 26935594.

2. Truong M, Stevens E, Ward R, et al. Clinical utility of PSA density and PI-RADS for deferring biopsy for the detection of clinically significant prostate cancer. J Clin Oncol, February 20, 2020;8(suppl 6):298-298.

The PROView edge

PROView 2.0 is a review and reporting tool for prostate MR that applies the PI-RADS® v2.1 guidelines for the evaluation of prostate cancer. Its latest feature is designed to automate prostate segmentation through the power of deep learning and calculated volume measurements to deliver consistent quantification results, no matter who is processing the imaging data.

The system has a guided workflow for simple and standardized assessment that includes an intelligent display of multi-parametric prostate MR series along with a clinical history of the patient's PSA levels. It aligns with the PI-RADS® v2.1 reporting and integrates with standard dictation reporting systems. The report includes automated contouring and measurement of the prostate gland that, together with PSA level, help determine the PSA density (PSAD), which is relevant to the size of the prostate.

PROView also includes tools designed for lesion localization and for reporting on a PI-RADS® sector map, including:

- Lesion mapping to sectors and measurement for peripheral and transitional zones.
- Scoring of T2-weighted, DWI with integrated apparent diffusion coefficient (ADC) maps, and, when applicable, DCE acquisitions.

Reports are automatically generated along with all measurements and images, and these can be exported into HTML for seamless integration into external reporting solutions or saved through PDF and DICOM to PACS. PROView also allows physicians to select key images and manage them at any time during the review and embed in the report for referring physicians.

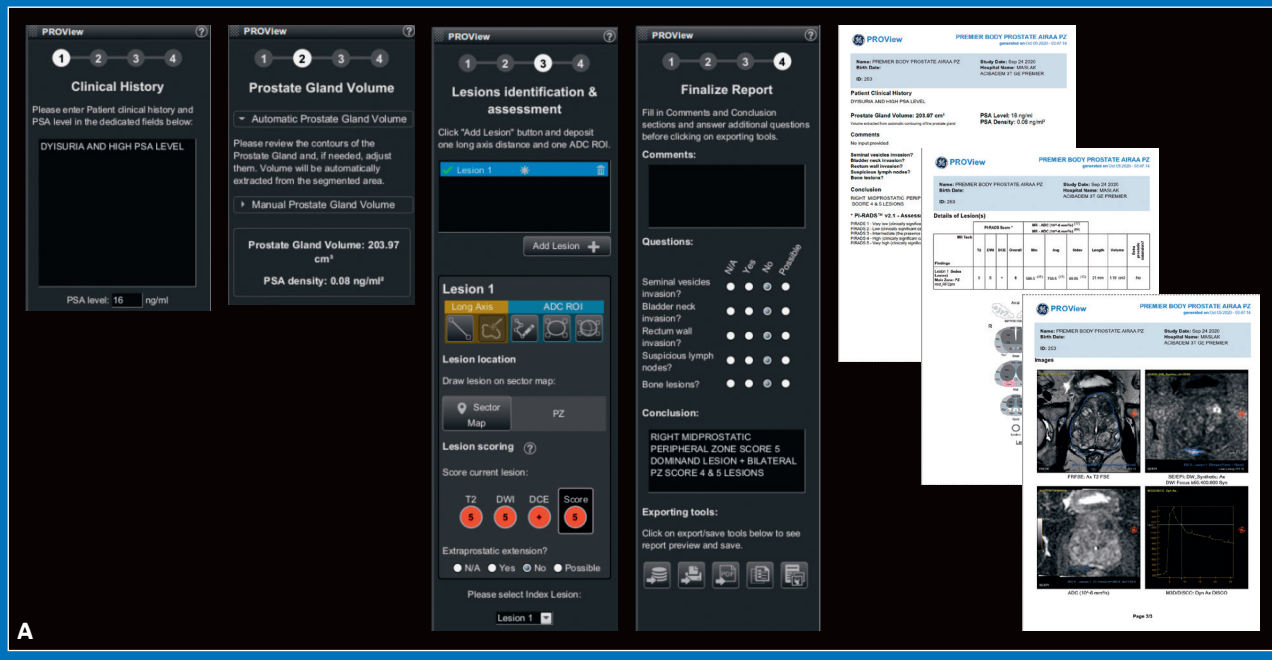

Figure 4. PROView 2.0 provides standardization of prostate reporting that aligns with the PI-RADS® v2.1 reporting and integrates with standard dictation reporting systems.

Catherine Kelly, PhD, MRes, Bsc (Hons)
Perspectum
Oxford, United Kingdom

Christina McSpedden
Touchstone Imaging
Franklin, TN

Quantitative analysis of multiparametric MR to detect early signs of liver disease

The economic burden of chronic liver disease in the US is estimated at $2.5 billion, with indirect costs up to $10.6 billion and hospitalization costs for patients with cirrhosis at $7.37 billion[1]. Globally, cirrhosis is the 11th most common cause of death, and liver cancer the 16th most common cause of death[2]. The rate of liver disease continues to grow, even as more treatments for liver disease become available. Identifying patients who can benefit from early intervention is needed to address this growing health issue.

Non-alcoholic fatty liver disease (NAFLD) is a disease that ranges from relatively harmless fatty liver to the more severe non-alcoholic steatohepatitis (NASH), where the accumulation of fat causes chronic inflammation and scar tissue (fibrosis). NAFLD is prevalent in approximately 25% of the world's population, with the highest prevalence in the Middle East and South America[3]. Advanced stages of the disease lead to cirrhosis and irreversible liver damage, causing cancer and liver failure.

"It is essential to detect NAFLD/NASH early, while treatment options such as lifestyle modification, bariatric surgery and drugs can actually work," says Catherine Kelly, PhD, MRes, Bsc (Hons), Chief Informatics Officer at Perspectum, a company developing digital technologies and quantitative assessments for the diagnosis and management of liver disease, diabetes and cancer. "It's therefore critical that clinicians have tools to diagnose, stratify and monitor patients with NAFLD."

Liver*MultiScan*® from Perspectum uses multiparametric MR to non-invasively quantify liver tissue to help clinicians evaluate liver diseases. It combines information from multiple parametric maps for a comprehensive analysis of liver tissue. Liver*MultiScan*® also provides quantitative measures that correlate with the histological features of NAFLD and NASH that are typically acquired from a biopsy.

According to Dr. Kelly, there has been a rapid expansion in the development of pharmacological agents to treat NASH, with the first novel therapies expected to come to market in the next few years. However, treating everyone with NAFLD would be an enormous economic burden on healthcare systems. Therefore, it is important to stratify patients so that those who are most at risk of developing serious NASH can get access to these drugs, before their condition becomes irreversible. Not all drugs will have the same effect on every patient, so monitoring response to therapy will be a critical component of patient management.

"It's all about getting the right patient on the right treatment for the right duration, using the most robust, precise non-invasive tools available."

Dr. Catherine Kelly

"Liver*MultiScan*® has been used as an endpoint in over 30 NAFLD/NASH trials and has shown utility in both diagnosing and monitoring therapy response."

Currently, patients with liver disease undergo blood tests, ultrasound and biopsy – often repeated – for both diagnosis and management. Liver biopsy is currently the only definitive method

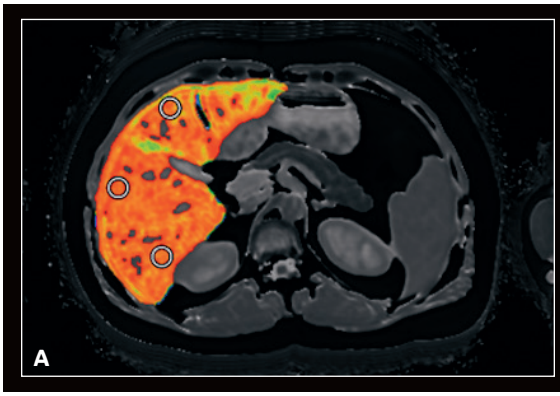

Figure 1. Using multiparametric MR, Liver*MultiScan*® generates maps that may indicate the presence of fibro-inflammation, as measured by the metric cT1.

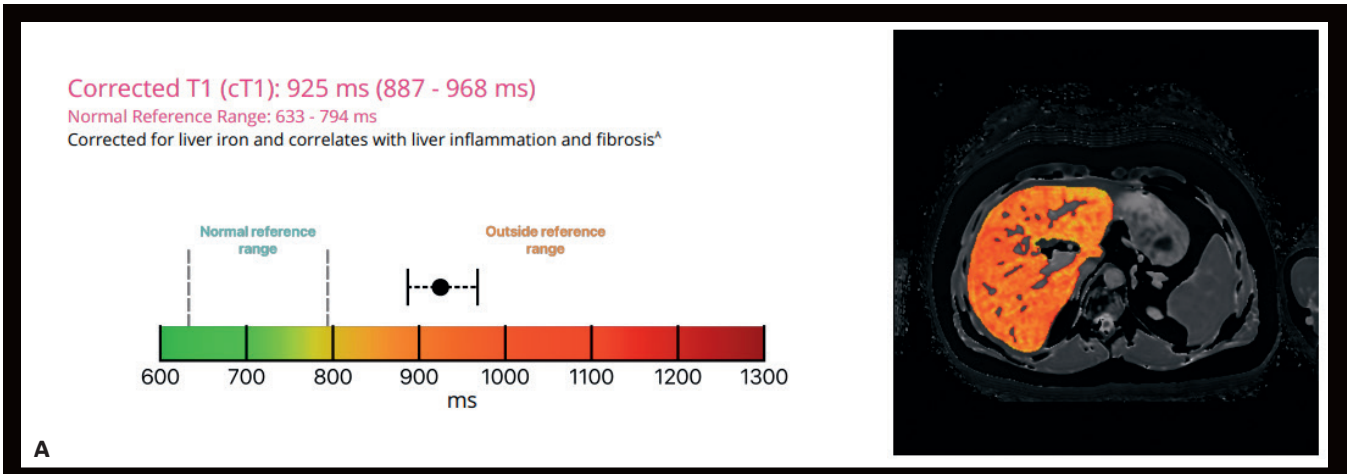

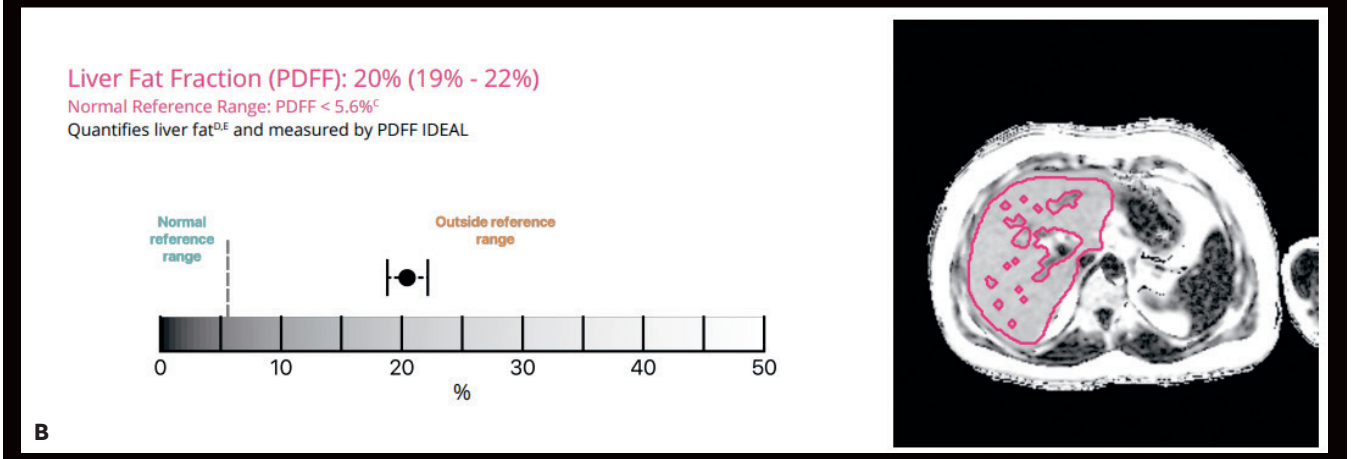

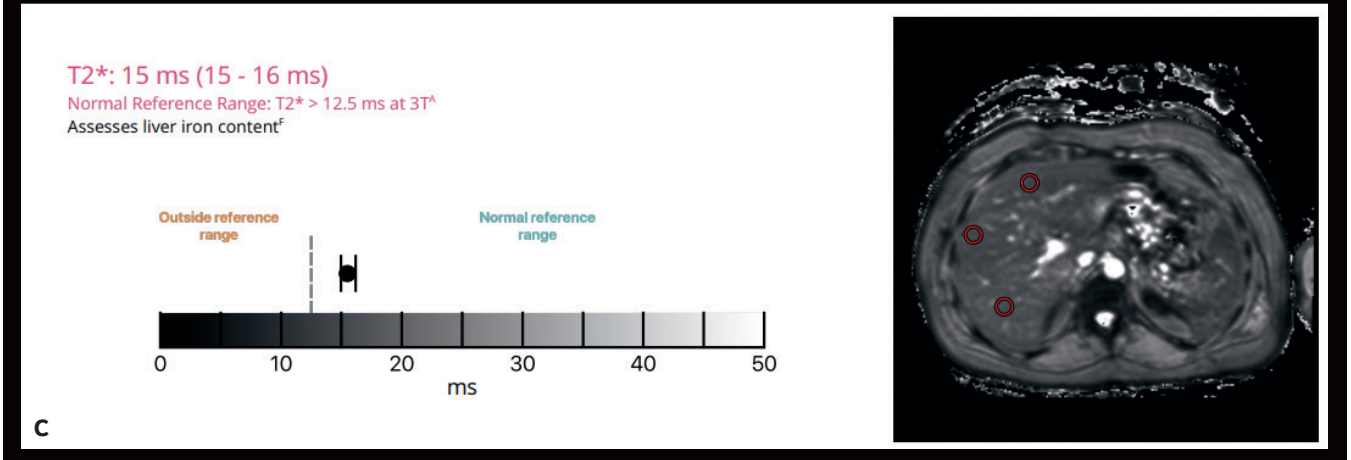

Figure 2. Liver*MultiScan*® report of a patient with NASH.

to diagnose NASH, yet it measures only 1/50,000th of the liver and is subject to inter-reader sampling variability. The procedure itself is costly and associated with complications that can be severe.

In a recent comparative study, Liver*MultiScan*® showed the highest agreement with biopsy in both NAFLD and NASH compared to other imaging techniques[4].

Early adopter

As one of the largest US radiology groups, US Radiology Specialists® is a partnership of subspecialized radiology groups and outpatient imaging center companies built around a commitment to best-in-class clinical excellence, operations, infrastructure and state-of-the-art technology. One of its imaging center partner companies, Touchstone Imaging, operates centers in six states and provides Liver*MultiScan*® in five of them. Its Central Austin and San Antonio locations in Texas are using the tool with an Optima™ MR450w 1.5T wide-bore system.

As an organization, Touchstone Imaging has participated in several research studies that included Liver*MultiScan*®. Approximately 500 patients have undergone exams with this tool across all of Touchstone Imaging's sites.

"Offering a comprehensive liver imaging/analysis solution that provides a quantitative report of a patient's liver health is an important differentiator for our organization," says Christina McSpedden, Regional Operations Manager for Touchstone Imaging. "Liver*MultiScan*® allows patients a more cost-effective evaluation and does not include the risks associated with a liver biopsy. It may help prevent patients from having to go through an invasive biopsy procedure and it can also be done without having to use IV contrast."

The reporting from Liver*MultiScan*® details the distribution of markers of fat, iron and inflammatory disease that can be used as a tool in the diagnosis of liver disease. The report is turned around quickly to providers, who appreciate the speed and accuracy of the report, she says.

"Liver*MultiScan*® has given our team access to previously inaccessible specialty physician groups that are looking for cost-effective options to help properly diagnose NASH patients."

Christina McSpedden

Touchstone Imaging also provides MR elastography and MR proton density fat fraction (PDFF) for a complete MR-based liver health assessment. Liver*MultiScan*® can help centers capture this new and growing clinical niche.

Implementing Liver*MultiScan*® doesn't require additional hardware and is compatible with both 1.5T and 3.0T systems running SIGNA™Works (DV26) or later. The acquisition protocol is loaded onto the scanner and phantom data is acquired for calibration. Images route to Perspectum's cloud-based service for analysis on the severity of liver disease by examining liver fat, iron and fibroinflammation and how these map across the organ. The completed Liver*MultiScan*® report from Perspectum can be sent directly into the patient's chart. Education and training are provided by Perspectum for the imaging center's staff.

Dr. Kelly adds that two new CPT codes (0648T and 0649T) from the American Medical Association for quantitative multiparametric MR covering Liver*MultiScan*® will become effective July 1, 2021[5].

There is increased demand for tools to diagnose, stratify and monitor liver disease, and GE Healthcare offers a complete array of solutions to address this growing need.

References

1. Desai AP, Mohan P, Nokes B, et al. Increasing Economic Burden in Hospitalized Patients With Cirrhosis: Analysis of a National Database. Clin Transl Gastroenterol. 2019;10(7):e00062. doi:10.14309/ctg.0000000000000062.
2. Asrani SK, Devarbhavi H, Eaton J, Kamath PS. Burden of liver diseases in the world. J Hepatol. 2019 Jan;70(1):151-171. doi: 10.1016/j.jhep.2018.09.014.
3. Younossi ZM, Koenig AB, Abdelatif D, Fazel Y, Henry L, Wymer M. Global epidemiology of nonalcoholic fatty liver disease-Meta-analytic assessment of prevalence, incidence, and outcomes. Hepatology. 2016 Jul;64(1):73-84.
4. Imajo K, Tetlow L, Dennis A, et al. Quantitative multiparametric magnetic resonance imaging can aid non-alcoholic steatohepatitis diagnosis in a Japanese cohort. World J Gastroenterol. 2021 Feb 21;27(7):609-623. doi: 10.3748/wjg.v27.i7.609.
5. Perspectum press release. Available at: https://perspectum.com/news.

Michael J. Kalutkiewicz
Resoundant, Inc.
Rochester, Minnesota

Richard L. Ehman, MD
Rochester, Minnesota

The growing need for a comprehensive, non-invasive liver health assessment

By Michael J. Kalutkiewicz and Richard L. Ehman, MD, President and CEO, Resoundant, Inc., Rochester, MN

There exists great need for a non-invasive diagnostic test that can help identify early stage liver disease, both fibrosis and steatosis, in a patient population that is prone to obesity and underlying metabolic disease (type 2 diabetes mellitus, obesity, hypertension, etc.). Recent innovations in rapid, low-cost MR imaging may be that answer.

Liver disease has rapidly emerged as a complex global health challenge, impacting advanced and developing countries alike. Worldwide, nearly one in four people are now known to have abnormal levels of lipid in their liver tissue, a condition known as non-alcoholic fatty liver disease (NAFLD).[1] NAFLD is defined as liver fat of greater than 5 percent with no history of excess alcohol consumption and is the precursor of a more advanced form of the disease called non-alcoholic steatohepatitis (NASH), which can lead to liver failure and death. In addition to NAFLD there are many other conditions that can eventually lead to end-stage liver disease such as chronic hepatitis B and C infections, which affect millions of people worldwide.

A recent study reports a five-fold increase in the incidence of NAFLD diagnosis from 1997 to 2014, based on data from the Rochester Epidemiology Project database.[2] This explosion in NAFLD and NASH has paralleled the rise in metabolic syndrome worldwide (e.g., type 2 diabetes) and is strongly linked to overnutrition and a sedentary lifestyle.

Part of the challenge is diagnosing NAFLD early, as patients often progress asymptomatically. Researchers are also seeking to better define observed differences in progression rates and directionality of disease advancement. All of this uncertainty makes it difficult to stage NAFLD, stratifying patients based on who might progress from the relatively benign and manageable NAFLD to the more worrisome NASH.

This matters not only in terms of healthier outcomes, but also systemic costs. The transition to NASH hallmarks the point at which modest lifestyle changes are less likely to be effective. There is hope that combination therapies will be able to halt or even reverse NASH progression, but the cost of such strategies is expected to be significant. Moreover, NASH patients remain at heightened risk of cirrhosis, liver decompensation and/or liver cancer — all of which are strongly linked to higher rates of mortality. Because of this, NAFLD and NASH are projected to be the leading cause of end-stage liver disease requiring liver transplantation as early as 2025.[3]

Figure 1. MRE*plus*+ is an automated liver analysis tool that creates ROIs for each liver metric (MRE and PDFF) based on the optimal data for each acquisition.

With the hopes of curtailing this trajectory, the European Union and the US have launched ambitious projects (e.g., LITMUS and NIMBLE) to identify reliable diagnostic approaches for evaluating suspected NAFLD and NASH patients. For decades, liver biopsy has been regarded as the only reliable diagnostic tool, providing a direct histologic assessment of steatosis and fibrosis. However, liver biopsy is invasive, costly and is affected by sampling error and subjectivity in histologic review, making this test a very imperfect gold standard.

Advances in imaging technology have offered alternatives to biopsy in assessing liver fat and fibrosis. Ultrasound-based elastography and attenuation measurements can be used to assess fibrosis and steatosis, respectively, but may be unreliable in NAFLD due to obesity, which is prevalent in over two-thirds of NAFLD patients.[4]

MR-based solution

MR is stepping up to fill this gap. Two advances in particular have gained consensus in the scientific and clinical community as new gold standards for liver assessment. MR elastography (MRE, MR Touch) for fibrosis staging and proton density fat fraction (PDFF, IDEAL IQ) for steatosis assessment are not only highly accurate, but also perform well in obese patients where ultrasound techniques are often difficult. These MR-based techniques can be combined in a short, efficient exam that has been called a “Hepatogram.”[5]

Both techniques are individually validated, widely available and recognized in leading gastroenterology and hepatology practice guidelines.[6,7] In the past, concerns about cost have hampered the adoption of powerful diagnostics based on MR imaging. But radiology as a medical specialty is embracing the public health challenge of NAFLD and NASH. Thanks to a new CPT code (76391), MRE and PDFF can be done as a rapid, low-cost standalone exam, perhaps marking an exciting trend toward adoption of a pragmatic MR exam that can be used in routine clinical practice for targeted applications.

To assist workflow, researchers have developed a comprehensive analysis tool for MRE and PDFF data that automatically quantifies these critical biomarkers. This tool, which will be made widely available from Resoundant as MRE*plus*+, instantly generates appropriate ROIs and measurements for MRE, PDFF and R2* images based on the optimal data from these acquisitions. The tool outputs these metrics and images in a format that can be used by the interpreting radiologist and provided to the referring physician and patient. The tool provides consistent and repeatable measurements, well-suited for longitudinal assessments of patients with NAFLD and for clinical trial support.

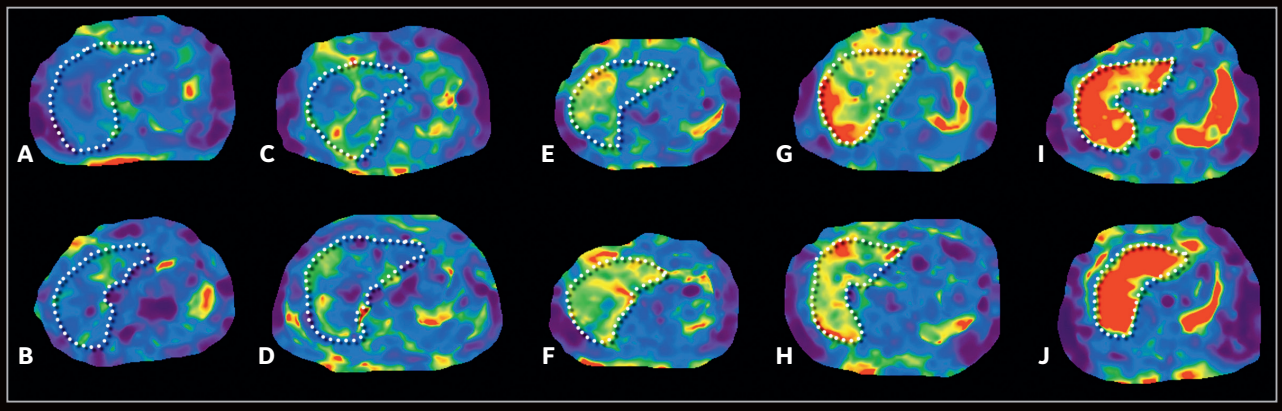

Figure 2. MR Touch helps the clinician identify variations in liver tissue stiffness. (A, B) Fibrosis 0 (F0); (C, D) F1; (E, F) F2; (G, H) F3; and (I, J) F4.

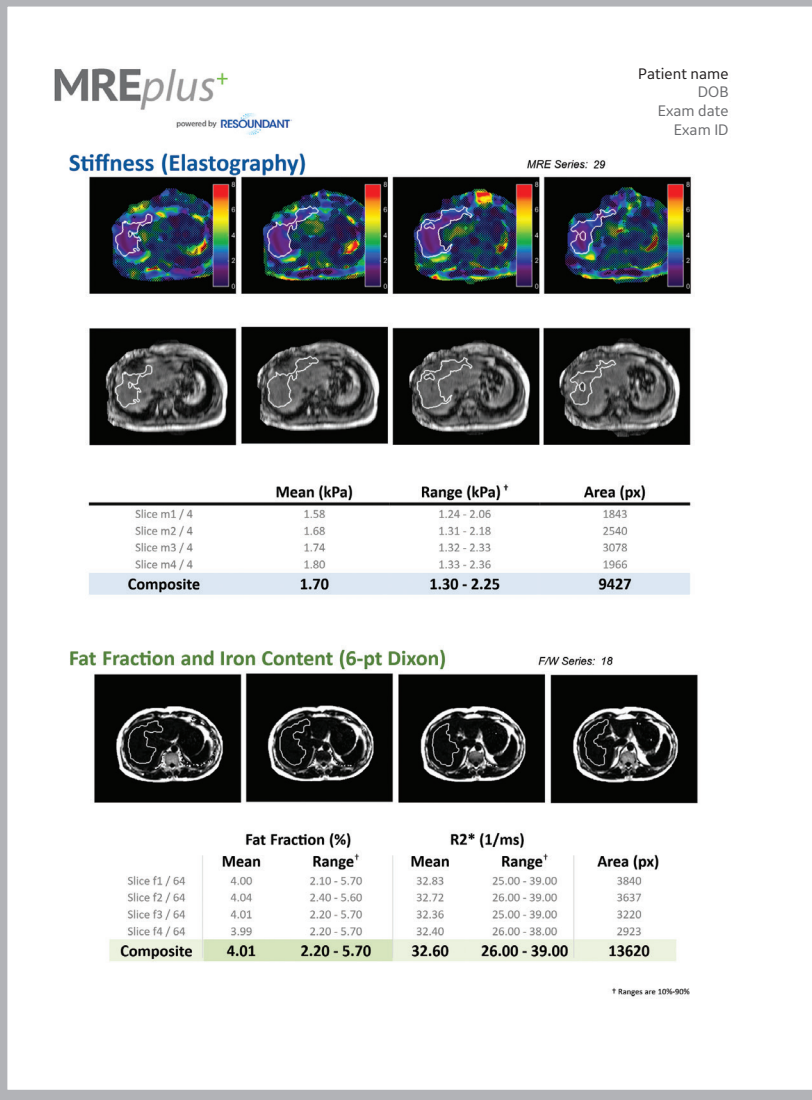

Figure 3. MRE*plus*+ provides an intuitive summary of the automated analysis with images showing ROIs and tabulated values for any combination of liver stiffness, proton density fat fraction and R2* data.

A new paradigm for MR

While the challenges presented by NAFLD and NASH are enormous, the addition of a rapid, low-cost MR exam is an example of how it is possible to democratize one of medicine's most powerful technologies — making it more accessible to the millions at risk for these conditions and transforming the way that clinicians and health systems approach the global problem of liver disease.

Disclosure: Dr. Ehman serves as President and CEO of Resoundant, Inc. The Mayo Clinic and Dr. Ehman have intellectual property rights and a financial interest in MRE technology.

References

1. Younossi ZM, Koenig AB, Abdelatif D, Fazel Y, Henry L, Wymer M. Global epidemiology of nonalcoholic fatty liver disease—Meta-analytic assessment of prevalence, incidence, and outcomes. Hepatology. 2016;64(1):73-84. doi:10.1002/hep.28431.
2. Allen Am, Therneau TM, Larson JJ, Coward A, Somers VK, Kamath PS. Nonalcoholic fatty liver disease incidence and impact on metabolic burden and death: A 20 year-community study. Hepatology. 2018 May;67(5):1726-1736.
3. Fan JG, Kim SU, Wong VW. New trends on obesity and NAFLD in Asia. J Hepatol. 2017 Oct;67(4):862-873.
4. Fazel Y, Koenig AB, Sayiner M, Goodman ZD, Younossi ZM. Epidemiology and natural history of non-alcoholic fatty liver disease. Metabolism. 2016;65:1017–1025.
5. Allen AM, Yin M, Venkatesh SK, et al. SAT-464-Novel multiparametric magnetic resonance elastography (MRE) protocol accurately predicts NAS score for NASH diagnosis. Journal of Hepatology. 2017;66:S659.
6. Lim JK, Flamm SL, Singh S, Falck-Ytter YT. American Gastroenterological Association Institute Guideline on the Role of Elastography in the Evaluation of Liver Fibrosis. Gastroenterology. 2017 May;152(6):1536–1543.
7. Chalasani N, Younossi Z, Lavine JE, et al. The diagnosis and management of nonalcoholic fatty liver disease: Practice guidance from the American Association for the Study of Liver Diseases. Hepatology. 2018 Jan;67(1):328-357.

Diego Hernando, PhD
University of Wisconsin Madison
Madison, Wisconsin

Scott Reeder, MD, PhD
University of Wisconsin Madison
Madison, Wisconsin

Quick and reproducible liver iron concentration measurements with MR

Liver disease is a growing global healthcare problem. IDEAL IQ was developed to provide reliable and repeatable fat fraction assessments of the liver. It may also be a useful measurement for liver iron concentration, another precursor for liver disease. Researchers led by Dr. Scott Reeder at the University of Wisconsin Madison are investigating the clinical utility of a modified IDEAL IQ MR sequence[‡] to provide the information clinicians need to address this important health issue.

In 2011, GE Healthcare introduced IDEAL IQ, a non-invasive, fat fraction assessment of the liver. Scott Reeder, MD, PhD, Professor, H.I. Romnes Faculty Fellow, Vice Chair of Research and Chief of MRI at the University of Wisconsin School of Medicine and Public Health in Madison, and his group helped develop IDEAL IQ and its predecessor, IDEAL, a 3-point Dixon technique that provides in-phase, out-of-phase, fat-only and water-only images. It was through this earlier work that Dr. Reeder and Diego Hernando, PhD, Assistant Professor and Director of Quantitative Body MRI at the University of Wisconsin School of Medicine and Public Health, saw the opportunity to utilize a method like IDEAL IQ to quantitatively measure liver iron concentration (LIC) using R2* with MR imaging[‡].

According to Dr. Reeder, cancer survivors, patients undergoing blood transfusions and people afflicted with thalassemia and sickle cell anemia are also at risk for high LIC. Further, iron overload is also the sine qua non feature of hemochromatosis, a genetic condition that leads to excessive absorption of iron from the gut. In addition to being a precursor for liver disease, too much iron in the body can also lead to iron overload cardiomyopathy, growth and other hormonal disturbances, and in extreme cases, even type 1 diabetes.

"Both iron and fat quantification are clinically relevant in these patient populations," Dr. Reeder explains. For example, adolescents who undergo treatment for leukemia will receive multiple blood transfusions, which leads to iron overload. They, and other cancer survivors, often gain weight during recovery and obesity is associated with the deposition of fat in the liver.

"A fat-corrected iron measurement is important for an accurate measurement of iron," explains Dr. Reeder. "It is also important to have an iron-corrected fat measurement for an accurate measurement of fat."

During the development of IDEAL IQ, Dr. Reeder and Dr. Hernando knew that they would need to measure and correct for R2* (=1/T2*) signal decay.

"IDEAL IQ gives us a fat-corrected R2* map, and while that was not the original intent it became very apparent we could use R2* to measure liver iron."

Dr. Scott Reeder

[‡]Technology in development that represents ongoing research and development efforts. These technologies are not products and may never become products. Not for sale. Not cleared or approved by the US FDA or any other global regulator for commercial availability.

Liver disease is a growing worldwide healthcare problem, with non-alcoholic fatty liver disease (NAFLD) affecting 25 percent of the world's population[1,2], of which 20 percent will develop the more aggressive form, nonalcoholic steatohepatitis (NASH)[1]. As NAFLD progresses, it leads to liver injury, inflammation, fibrosis, cirrhosis and ultimately liver failure. As a result, experts estimate that upwards of 3 million people in the US alone will have cirrhosis by 2030[3] leading to a significant increase in hepatocellular carcinoma and a growing need for liver transplantation. Hepatic steatosis, the earliest feature of NAFLD, is also associated with cardiovascular disease, the most important morbidity associated with NAFLD. There is also a strong relationship between steatosis, liver fat and the presence of metabolic syndrome. In patients with chronic liver disease including NAFLD, NASH, alcoholic liver disease and hepatitis C viral infection, higher iron levels may also be present.

The presence of fat in the tissue will confound the R2* measurement, explains Dr. Hernando, and therefore there is an inherent advantage in terms of accuracy and reproducibility to separate water and fat signals. Several patients who participated in research studies at the UW-Madison had both elevated fat and iron in the liver, further highlighting the need to quantify both, he adds.

The technique

When using IDEAL IQ to quantify fat, the acquisition separates water and fat signals by acquiring multiple echo times where the fat and water signals are acquired in different relative phases.

"In order to provide both fat and iron quantification from the same acquisition, you need to keep the flip angle small to avoid T1 bias," Dr. Hernando says. "If you are only quantifying R2*, you don't need to minimize T1 bias in the acquisition. For instance, one can use something closer to the Ernst angle and obtain higher SNR, although the resulting fat quantification would then have some bias."

In the presence of high iron concentration, the R2* relaxation rate of the MR signal becomes very large so the signal dissipates very quickly. Therefore, there is an advantage to acquiring shorter echo times in R2* acquisitions than would typically be used for measuring fat in patients with iron overload.

Dr. Hernando is researching the use of a modified IDEAL IQ acquisition for accurate and reproducible R2* quantification. Although IDEAL IQ is FDA cleared for measuring R2*, it may not work as well in patients with high LIC levels, such as cancer survivors and those suffering from thalassemia and sickle cell anemia. At UW-Madison, they were able to demonstrate on GE Healthcare 1.5T and 3.0T MR systems that a confounded-corrected R2* mapping method was reproducible across acquisition parameters.

Based on this initial research, Dr. Reeder and Dr. Hernando were awarded an NIH grant for a multi-center, multi-vendor study to evaluate an MR-based confounder-corrected R2* mapping reconstruction method[‡] as a quantitative imaging biomarker of LIC[4].

"Our goal was to develop and validate the next-generation fat-corrected R2* mapping techniques using a non-linear reconstruction method that improves the dynamic range of the R2* measurement across different platforms and field strengths," says Dr. Reeder. The study also compared the results against FerriScan®, an FDA-cleared measurement of LIC in milligrams of iron per dry gram of liver.

Although it is known that R2* and LIC are highly correlated, it was unknown whether R2* as a biomarker of iron concentration could be reproducible across different choices of acquisition parameters and systems, adds Dr. Hernando.

"We know that R2* in the presence of liver iron will be different at 3.0T than 1.5T because it increases with field strength," Dr. Hernando says. "Our overall goal was to develop R2* mapping methods that address the relevant confounding factors – the presence of fat, background magnetic field variations and noise at high iron levels – to attain a reliable measurement of R2* that is highly correlated with liver iron concentration and reproducible across acquisition parameters, resolution, echo times, imaging orientation and systems. Reproducibility is at the core of the technical validation of quantitative imaging biomarkers."

The study has since closed and results are still emerging during data analysis. However, it is clear to both Dr. Reeder and Dr. Hernando that the results demonstrate that by accounting for all the relevant factors, they have developed a reproducible measurement of R2* that uses shorter echo times, high SNR and a non-linear reconstruction method.

One remaining limitation, however, is the use of Cartesian sequences in these studies. Cartesian acquisitions inherently limit echo times – they can be very short but not ultrashort – and therefore in cases of extreme iron overload the method may still fail.

[‡]Technology in development that represents ongoing research and development efforts. These technologies are not products and may never become products. Not for sale. Not cleared or approved by the US FDA or any other global regulator for commercial availability.

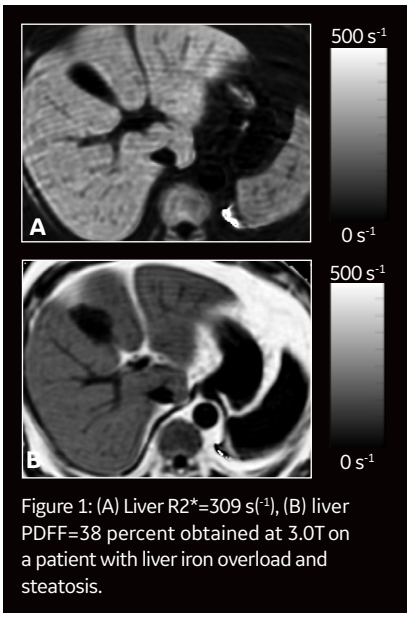

Figure 1: (A) Liver R2*=309 s(-1), (B) liver PDFF=38 percent obtained at 3.0T on a patient with liver iron overload and steatosis.

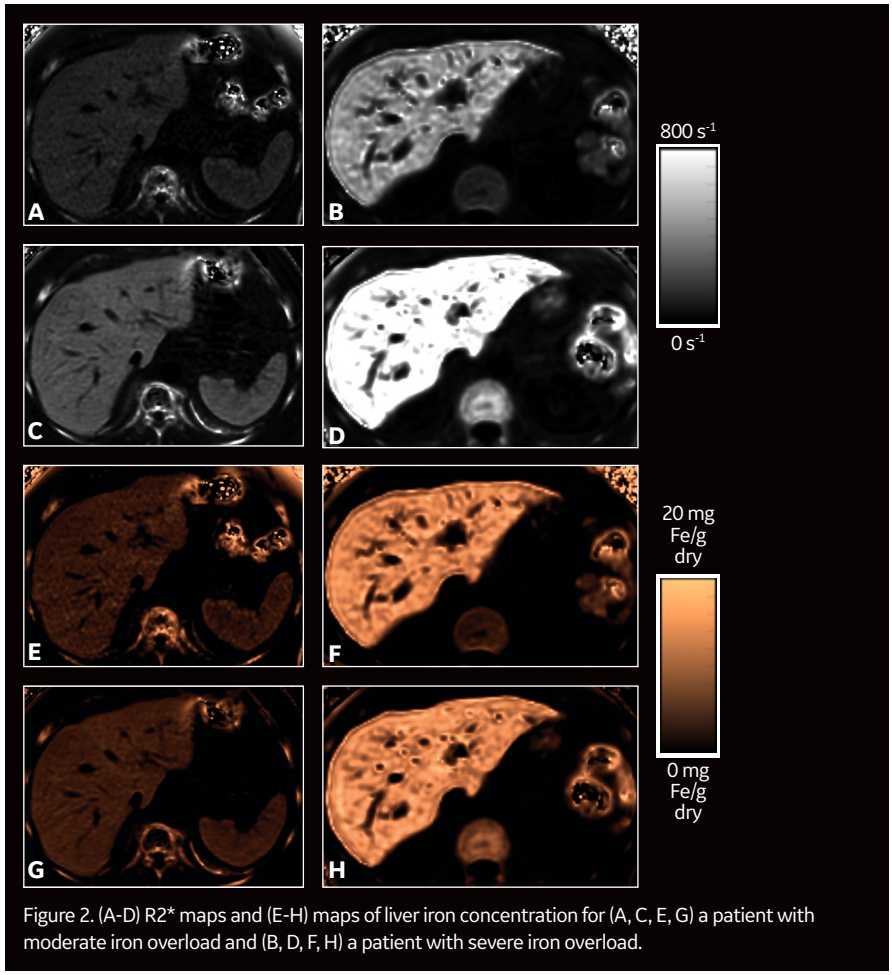

Figure 2. (A-D) R2* maps and (E-H) maps of liver iron concentration for (A, C, E, G) a patient with moderate iron overload and (B, D, F, H) a patient with severe iron overload.

"The natural extension of this in research is to move to ultra-short echo time radial and other non-Cartesian techniques that inherently allow us to acquire much shorter echo times," adds Dr. Hernando. "That may expand the dynamic range of R2* mapping in patients with massive iron overload.

However, the fact we could show the Cartesian techniques are reproducible across a wide range of iron overload is an exciting step forward."

What's next

In addition to demonstrating accuracy and reproducibility, Dr. Reeder is particularly enthused about the shorter acquisition time.

"Compared to older spin echo-based methods, this R2* method may provide an accurate measure of iron in the liver in a 10-20 second scan versus a 10-20 minute scan."

Dr. Scott Reeder

"That is important for workflow and the patient experience, especially in children where perhaps we can avoid sedation or anesthesia. It is also more precise than previous spin echo techniques, so we can generate better measurements in a lot less time."

This area of research has also led UW-Madison to develop a focused liver fat/iron quantification MR protocol. It is a three breath-hold protocol consisting of a localizer, IDEAL IQ and a single breath hold T2w SSFSE acquisition[5]. Patients spend a median time of 6 minutes on the table and Dr. Reeder says they have even scanned children as young as seven years old without sedation.

One other area of research interest that has surfaced from this work is the potential to measure magnetic susceptibility of tissue with IDEAL IQ.

"It turns out we can measure quantitative susceptibility mapping, or QSM†, from the same acquisitions that we use to measure R2*," says Dr. Hernando. "So, an extension of these projects is to develop, optimize and validate QSM for liver iron quantification. This is a fascinating topic with exciting research value at this earlier technical development stage."

References

1. American liver foundation. https://liverfoundation.org/for-patients/about-the-liver/diseases-of-the-liver/nonalcoholic-steatohepatitis-information-center/nash-definition-prevalence/.
2. Younossi Z, Tacke F, Arrese M, et al. Global Perspectives on Nonalcoholic Fatty Liver Disease and Nonalcoholic Steatohepatitis. Hepatology. 2019;69(6):2672–2682.
3. Shetty A, Syn WK. Health and Economic Burden of Nonalcoholic Fatty Liver Disease in the United States and Its Impact on Veterans. Fed Pract. 2019;36(1):14–19.
4. Confounder-Corrected Quantitative MRI Biomarkers of Hepatic Iron Content. Available at: https://clinicaltrials.gov/ct2/show/NCT02025543.
5. Pooler BD, Hernando D, Reeder SB. Clinical Implementation of a Focused MRI Protocol for Hepatic Fat and Iron Quantification [published online ahead of print, 2019 Mar 27]. AJR Am J Roentgenol. 2019;1–6.

†Technology in development that represents ongoing research and development efforts. These technologies are not products and may never become products. Not for sale. Not cleared or approved by the US FDA or any other global regulator for commercial availability.

Utaroh Motosugi, MD, PhD
Kofu Kyoritsu Hospital
Yamanashi, Japan

Addressing the challenges of SNR and respiratory motion in body MR

By Utaroh Motosugi, MD, PhD, Department of Radiology at Kofu Kyoritsu Hospital, Yamanashi, Japan

Lower SNR and respiratory motion have hindered the use of MR compared to CT in body imaging. However, MR has distinct advantages, namely higher contrast resolution, multiple contrasts and quantitative imaging. New technologies such as AIR™ Recon DL, HyperSense and DISCO Star help address these limitations for robust body MR imaging.

CT and MR are both often utilized for body imaging. Each provides distinct advantages over the other.

MR delivers inherently higher contrast resolution than CT, as well as provides multiple contrasts such as T1, T2, T2* and diffusion. Quantitative imaging is possible with MR, including ADC in diffusion imaging, measuring liver stiffness with MR elastography, and fat fraction and iron measurements using IDEAL IQ. Hepatobiliary MR contrast agents are available for functional analysis, e.g., phase imaging, and provide superior contrast for imaging liver metastases, enabling the visualization of small lesions that typically cannot be seen in CT images.

Advantages of CT imaging include higher spatial resolution, with a routine isovoxel of 0.5 mm. At best, MR provides 1.0 x 1.5 x 2.0 mm, primarily due to the limitation of SNR. Motion artifacts are less pronounced in CT as a result of shorter scan times; a whole liver scan can be performed in less than 5 seconds with CT compared to 10 seconds with MR.

Advancing the clinical utility of body MR requires addressing its two main limitations: SNR and respiratory motion.

SNR

Using traditional techniques, SNR can be improved by increasing the FOV; however, additional spatial resolution is required, which increases scan time. Increasing sampling time also improves SNR, yet it prolongs scan time which typically leads to more motion artifact.

A new approach to increasing SNR and resolution is the use of a deep-learning image reconstruction technique such as AIR™ Recon DL. AIR™ Recon DL uses a deep-learning network trained to reconstruct images with Intelligent True Resolution for artifact reduction and user-selectable SNR improvement,

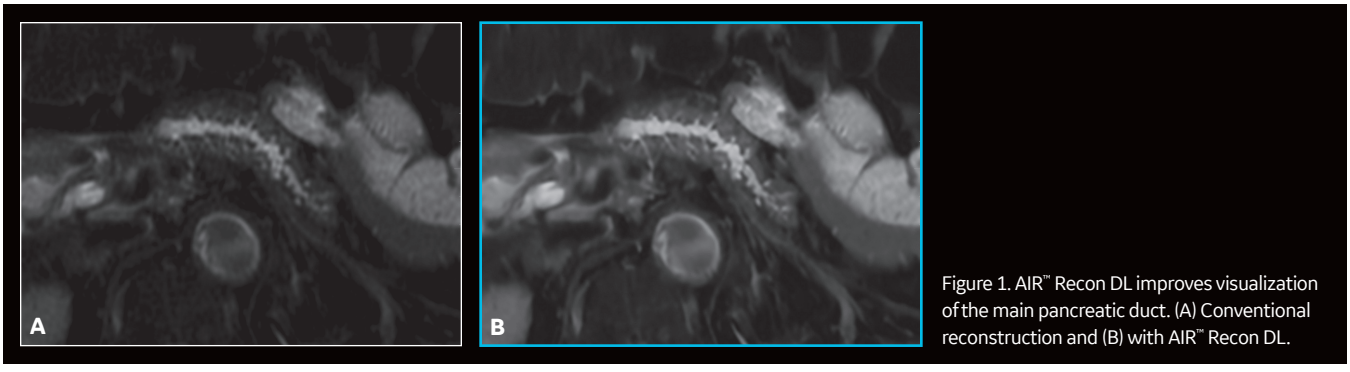

Figure 1. AIR™ Recon DL improves visualization of the main pancreatic duct. (A) Conventional reconstruction and (B) with AIR™ Recon DL.

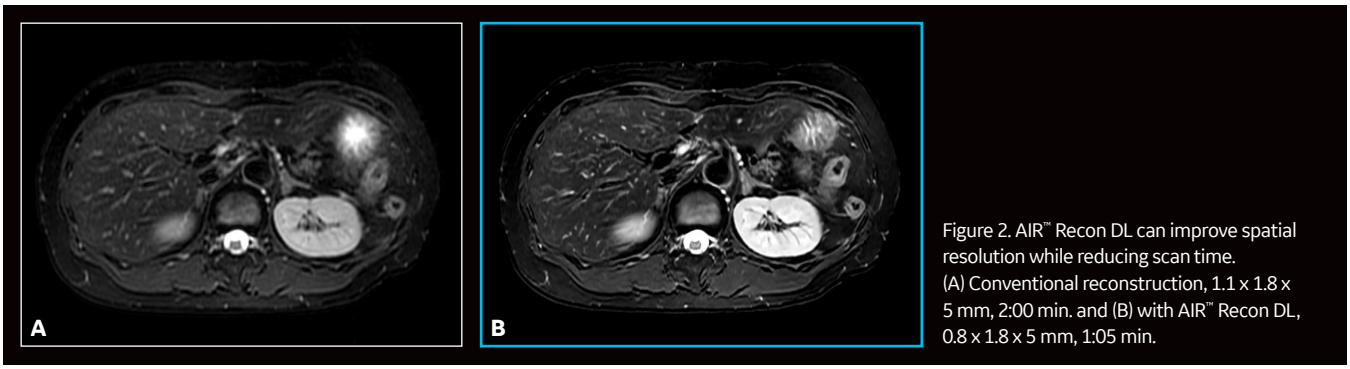

Figure 2. AIR™ Recon DL can improve spatial resolution while reducing scan time. (A) Conventional reconstruction, 1.1 x 1.8 x 5 mm, 2:00 min. and (B) with AIR™ Recon DL, 0.8 x 1.8 x 5 mm, 1:05 min.

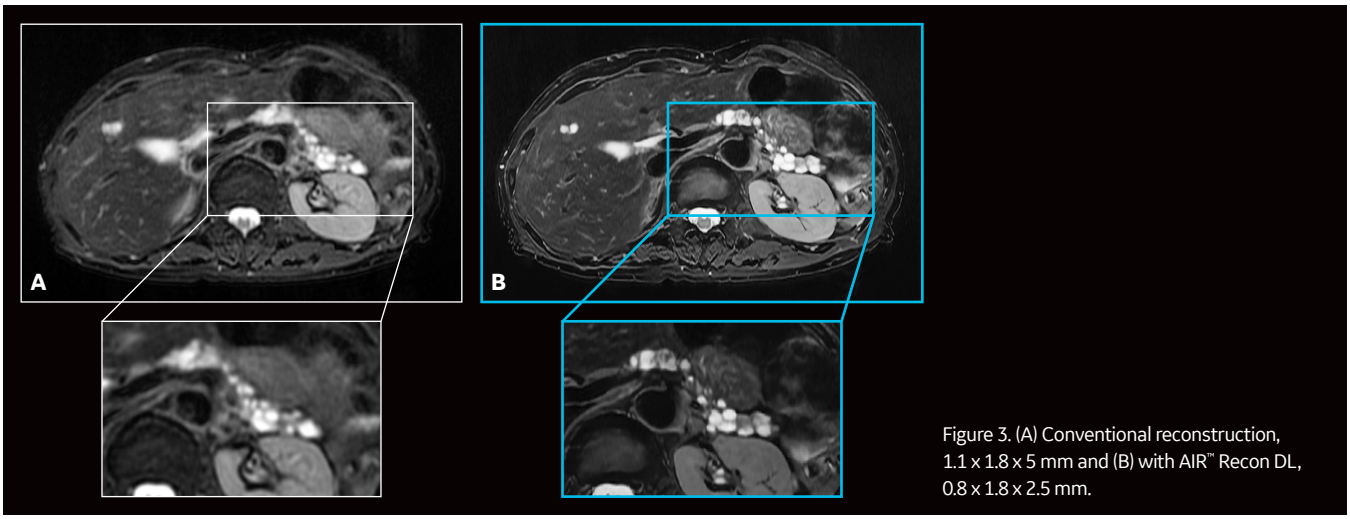

Figure 3. (A) Conventional reconstruction, 1.1 x 1.8 x 5 mm and (B) with AIR™ Recon DL, 0.8 x 1.8 x 2.5 mm.

without increasing scan time. It delivers high spatial resolution and enhanced sharpness of the object/anatomy, improving image clarity and visualization (Figure 1). With the SNR improvement, the user can reduce signal averaging or change other parameters to decrease scan time. In Figure 2, the image using conventional techniques was acquired in 2 minutes, compared to just 65 seconds for the AIR™ Recon DL image.

The typical spatial resolution in T2-weighted imaging of the body is around 10 mm^3 , or 1.1 x 1.8 x 5 mm. Using a higher spatial resolution of 3.6 mm^3, or 0.8 x 1.8 x 2.5 mm, results in poor SNR with conventional reconstruction techniques. With AIR™ Recon DL, the user can increase spatial resolution and increase SNR to more clearly visualize fine or small structures. Using a smaller voxel size with AIR™ Recon DL depicts more details and less noise than conventionally reconstructed images.

Respiratory motion

One solution to address respiratory motion in MR imaging is to decrease the acquisition time. HyperSense is a compressed sensing technique used to shorten scan time by reconstructing undersampled data, and it can be used with parallel imaging. It is effective for 3D imaging, particularly dynamic scanning in body MR, and provides scan time and breath-hold time reductions, as well as higher temporal and spatial resolution.

For example, a conventional arterial phase acquisition protocol with LAVA has one arterial phase. By adding HyperSense, we can get three arterial phases within one breath-hold. With three phases, we have a better chance to obtain one good image from the scan compared to relying on the one phase image. In the three phase acquisition using HyperSense with a single breath-hold, we can recognize details of the liver structures and have good SNR as well (Figure 4).

Another case of a metastatic pancreatic cancer from renal cell carcinoma demonstrates how adding more arterial phases using HyperSense can impact the diagnosis and treatment (Figure 5). The image contrast was best in the first phase, enabling detection of another metastasis in the tail of the pancreas.

DISCO is another option for acquiring a higher number of arterial phases and higher temporal resolution. In the conventional DISCO acquisition, six arterial phases can be acquired in one breath-hold with high temporal resolution. In cases where the patient cannot consistently hold their breath, leading to breathing artifacts in some of the phases, it is possible to make the diagnosis using the portions of the exam where the breath-hold was successful.

By adding HyperSense to DISCO, it is possible to shorten the scan time and breath-hold by 3 seconds and obtain an additional phase.

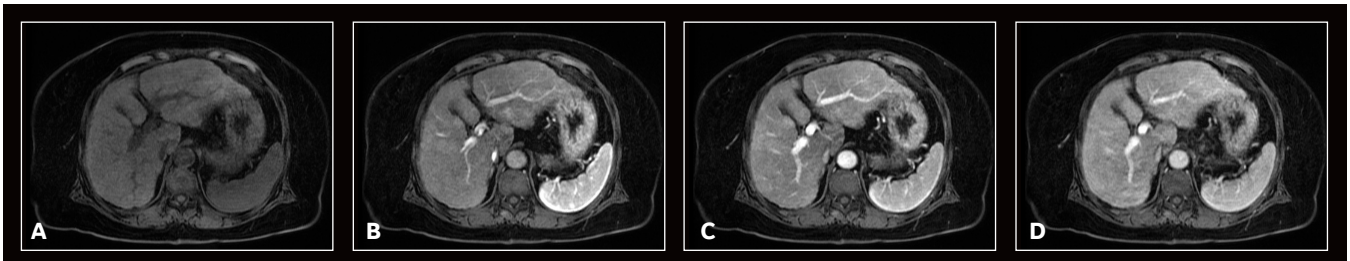

Figure 4. Using LAVA with HyperSense enables three phases in one breath-hold. (A) Mask, (B) 1st phase at 0 sec., (C) 2nd phase at 2.98 sec. and (D) 3rd phase at 5.97 sec.

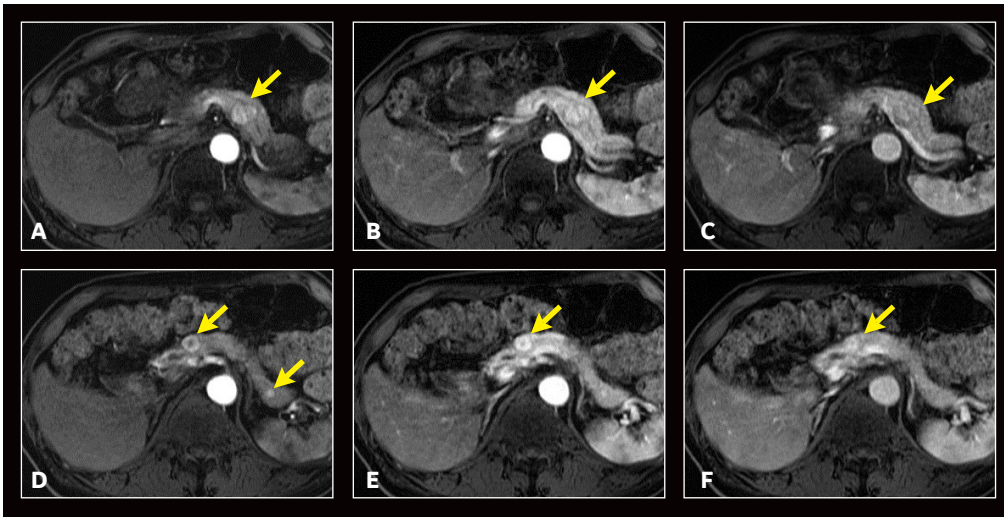

Figure 5. A 50-year-old man with a metastatic pancreas tumor from renal cell carcinoma. Using HyperSense to add more arterial phases enables detection of another metastasis in the tail of the pancreas (arrows).

As shown, there are multiple solutions depending on the patient and the clinical indication. If more than one phase is needed, LAVA HyperSense enables the acquisition of two or three phases in one breath-hold. If super high resolution is required, DISCO with HyperSense offers less-than-3-second temporal resolution in one breath-hold (Figure 6).

Having these tools available increases the potential to obtain artifact-free arterial phase imaging and decreases acquisition time. However, it is not perfect. Some patients may not be able to follow the breath-hold command at all, and a free-breathing protocol is necessary.

DISCO Star is a multiple acquisition of *k*-space center for a motion-insensitive image. DISCO Star has three advantages. One, we can perform a retrospective reconstruction with multiple phases. Two, since each spoke goes through that highly oversampled *k*-space center, it is robust to motion. Three, DISCO Star offers consistent dynamic timing as it is not dependent on the patient's breathing, which can vary, like Body Navigators. The data is then weighted according to the respiratory phase and the respiratory effect can be eliminated, which is called soft gating. Combining these two advantages results in dynamic free-breathing MR imaging with appropriately high resolution.

DISCO Star and HyperSense can also be combined. Figure 7 is an example of a continuous 90-second scan acquiring six phases with a temporal resolution around 12 seconds. The scan was performed without breath-holding. With this technique, we can obtain three arterial phases (first, second and third phase), two portal venous phases (fifth and sixth phase) and one additional phase between the arterial and venous phases (fourth phase). As shown in Figure 7, the hyper enhancement of hepatocellular carcinoma is captured at the second or third phase.

In summary, there are several methods available to address the challenges of SNR and respiratory motion in body MR imaging. AIR™ Recon DL can help increase SNR, HyperSense shortens the acquisition time to avoid respiratory motion and DISCO Star is a robust free-breathing protocol. S

To view the full webinar "Elevating MR body imaging with AIR™ Recon DL", visit: tinyurl.com/bodyimagingwithARDL

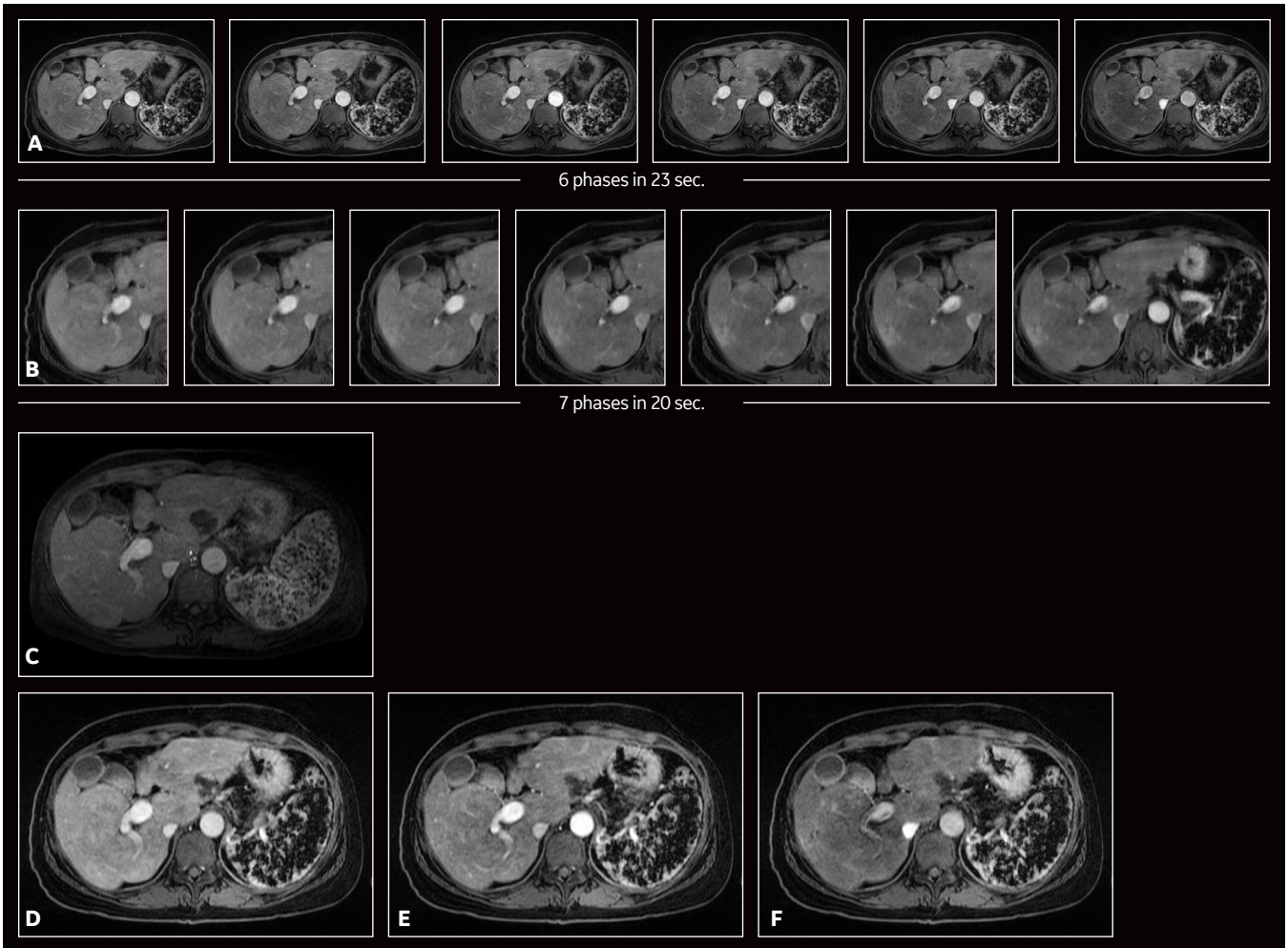

Figure 6. (A) Conventional DISCO acquisition, 320 x 192 in 23 sec.; (B) DISCO with HyperSense, 320 x 192 in 20 sec., offers less-than-3-second temporal resolution in one breath-hold and the acquisition of an additional phase in less time than the conventional acquisition. (C) Conventional LAVA, 320 x 160 in 20 sec.; (D-F) LAVA with HyperSense, 320 x 192, 24 sec., also enables additional phase acquisitons in less time than conventional LAVA.

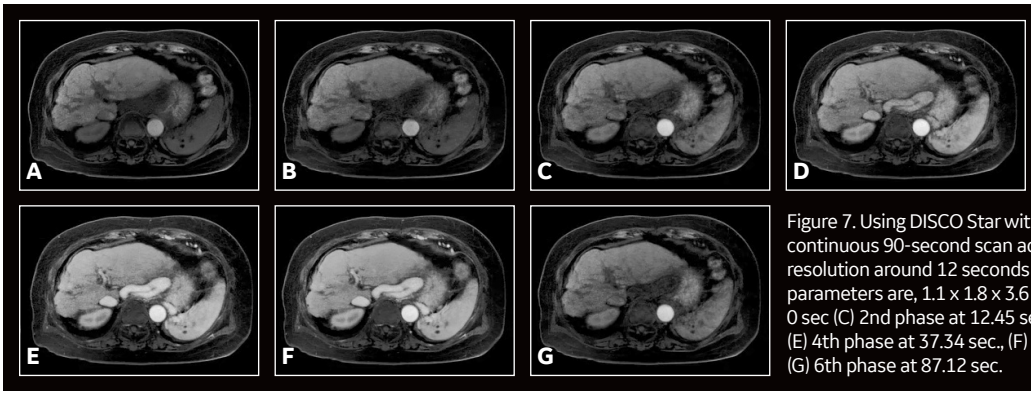

Figure 7. Using DISCO Star with HyperSense, we can perform a continuous 90-second scan acquiring six phases with a temporal resolution around 12 seconds without breath hold. Acquisition parameters are, 1.1 x 1.8 x 3.6 mm. (A) Mask, (B) 1st phase at 0 sec (C) 2nd phase at 12.45 sec., (D) 3rd phase at 24.89 sec., (E) 4th phase at 37.34 sec., (F) 5th phase at 49.78 sec. and (G) 6th phase at 87.12 sec.

Marc Zins, MD
Saint Joseph Hospital
Paris, France

Francois Legou, MD
Centre Cardiologique du Nord
Paris, France

In pursuit of fast and consistent free-breathing abdominal MR exams

Since its introduction in 2004, LAVA has become a staple in many abdominal MR exams due to its enhanced image contrast and uniform fat suppression. HyperSense was introduced in SIGNA™Works in 2016 and was shown to go faster and improve image quality with higher spatial resolution. GE has now extended HyperSense into additional body sequences, including LAVA, LAVA Flex and DISCO.

More recent iterations of the sequence include: Turbo LAVA, a rapid accelerated 3D T1 dynamic sequence offering homogeneous fat suppression with shorter scan times, and LAVA Flex, a dynamic 3D T1-weighted technique that generates four contrasts (fat, water, in phase and out of phase) in one rapid acquisition. LAVA, LAVA-Flex and DISCO offer different fat suppressed contrasts and can be used with Auto Navigator for a free-breathing acquisition or with patient breath-hold. While breath-holding remains the gold standard in abdominal imaging, free-breathing with Navigator provide a complete package of options for clinical use.

With the advent of compressed sensing and volumetric imaging, GE Healthcare is taking dynamic imaging – LAVA, LAVA Flex, DISCO – to the next level with the introduction of LAVA HyperSense T1 for sequences and DISCO Star.

Marc Zins, MD, Chairman of the Radiology Department at Saint Joseph Hospital, evaluated a prototype of LAVA HyperSense and Francois Legou, MD, radiologist at Centre Cardiologique du Nord (CCN), evaluated a prototype of DISCO Star at their respective facilities and shared their experience with SIGNA™ Pulse of MR.

LAVA HyperSense

At Saint Joseph Hospital, LAVA sequences are used in all liver and pancreas MR exams. According to Dr. Zins, the hospital will perform a pancreas MR exam for cystic lesion follow-up, to characterize a lesion incidentally detected on a CT exam, for assessment of chronic pancreatitis and for diagnosis and staging of pancreatic cancer. In the liver, an MR exam is generally performed for tumor staging or follow-up, liver cancer screening, post-ablation therapy or TACE assessment, and in cases where a lesion is incidentally found on a CT or ultrasound exam.

A prototype of LAVA HyperSense was installed on the Discovery™ MR750 at Saint Joseph Hospital in March 2018. Dr. Zins and his team tested different acceleration factors – using both ARC and HyperSense – and qualitatively evaluated image quality, including artifacts, blurring, lesion detection, reformat quality and the sharpness of organs and lesions. When used with other sequences, Saint Joseph Hospital typically uses a HyperSense factor of 1.3 to achieve a balance between higher spatial resolution and scan time.

The radiologists anticipate that their diagnostic confidence will improve due to the higher spatial resolution in the arterial phase sequences. In the example shown in Figure 1, the LAVA HyperSense prototype demonstrates improved in-plane resolution for the LAVA multi-arterial – three phases in one 25-second

breath hold – without changing the scan time. Also, the reduction in breath-hold times may enable fewer breathing artifacts or failed acquisitions due to patients who couldn't comply with breath holding.

"LAVA HyperSense could become the new standard reference technique on post-contrast 3D GRE T1 sequences to obtain a better balance between spatial and temporal resolution," Dr. Zins says. "In an arterial axial LAVA HyperSense post-contrast sequence, we can reduce the slice thickness for an isotropic acquisition. In the reformats we've performed with the prototype, we did not detect loss of detail or a decrease in image quality."

Dr. Zins explains the pancreas is a tortuous organ and, therefore, evaluating it in different planes and views is often desired for diagnosis. A faster LAVA sequence enabled by HyperSense could assist the radiologist in their diagnosis by allowing for higher spatial resolution by using thinner slices when evaluating the relationship between an enhancing lesion and a pancreatic duct.

As with any sequence utilizing compressed sensing (HyperSense), Dr Zins says choosing the right factor is crucial to avoid image blurring. It's only when the factor is too high that this issue occurs. "We have a high reproducibility of image quality with patients who can perform a good breath-hold."

In his evaluation, Dr. Zins was able to reduce breath-hold time by 25 percent using LAVA HyperSense compared to conventional LAVA.

With the shorter scan times from LAVA HyperSense, the clinical team could potentially utilize the time savings to obtain higher spatially resolved acquisitions. For example, in liver,

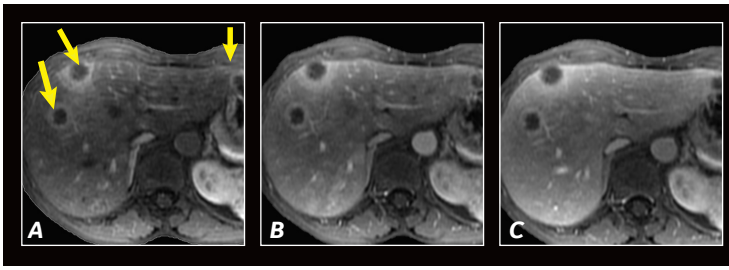

Figure 1. In initial evaluations of the LAVA HyperSense prototype, in-plane resolution increased compared to LAVA without HyperSense with the same breath-hold time to improve early enhancement visualization and facilitate lesion contrast enhancement analysis.
LAVA HyperSense (A) phase 1, (B) phase 2, and (C) phase 3, 1.5 x 1.5 x 3.6 mm, 25 sec., HyperSense factor of 1.3.

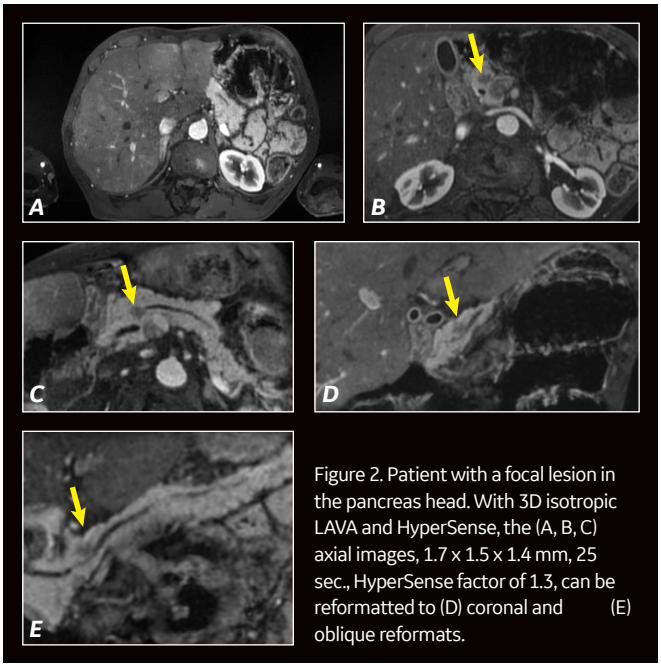

Figure 2. Patient with a focal lesion in the pancreas head. With 3D isotropic LAVA and HyperSense, the (A, B, C) axial images, 1.7 x 1.5 x 1.4 mm, 25 sec., HyperSense factor of 1.3, can be reformatted to (D) coronal and (E) oblique reformats.

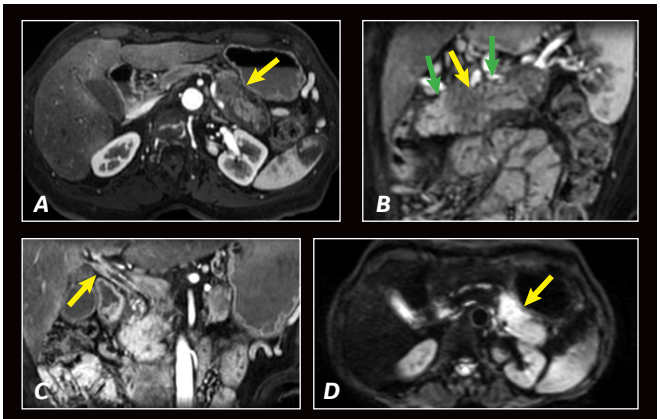

Figure 3. Patient with an auto immune pancreatitis, associated with cholangitis (stenosis, red arrow). A 3D isotropic volume was acquired in the same acquisition time as a 2D acquisition with LAVA HyperSense. (A) Acquisition plane, 1.7 x 1.5 x 1.4 mm, 30 sec., HyperSense factor of 1.3, (B, C) reformats and (D) axial DWI b800. With the coronal and oblique reformations of the LAVA Hypersense, the radiologist can review the normal portion (green arrow) of the pancreas around the lesion (yellow arrow).

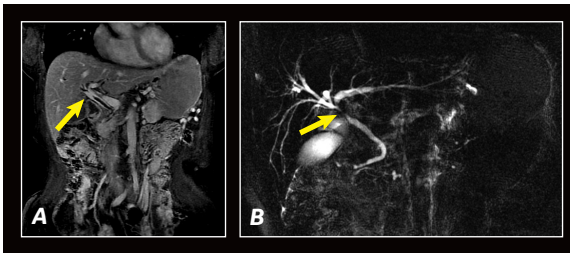

Figure 4. (A) Coronal LAVA HyperSense and (B) coronal SSFSE T2, 1.3 x 1.6 x 2.4 mm, 3:00 min.

biliary tract (gall bladder cancer and cholangiocarcinoma) and pancreas, it is important to capture excellent spatial resolution to look for tiny lesions with locoregional invasion.

"Before HyperSense, a highly resolved sequence required a long breath-hold duration, which was not feasible for patients and not acceptable in our clinical routine," Dr. Zins explains. "With a navigated dynamic 3D T1 sequence, it can be difficult to manage the timing of the arterial phase due to the patient's condition (poor cardiac output, for instance) making it challenging to characterize liver and pancreatic lesions."

DISCO Star

Each week, CCN performs approximately 30 abdominal MR exams on both the SIGNA™ Premier 3.0T and the SIGNA™ Artist 1.5T systems, with nearly two-thirds on the former. The primary indication is for liver and bile duct, small bowel and pancreas assessments. A dynamic 3D T1 sequence is the go-to acquisition for most of these exams.

In addition to imaging the pancreas for suspected cancer, MR is also used at CCN for a differential diagnosis of autoimmune pancreatitis. Liver MR exams are generally utilized to determine extension of colorectal cancer, bile duct pathologies and to characterize lesions detected on X-ray or ultrasound, including hepatocellular carcinoma (HCC).

Dr. Legou was excited to work with the DISCO Star prototype on SIGNA™ Artist because of the potential to provide a solution to respiratory motion in MR imaging of the liver and pancreas – some of the most demanding MR exams. Previously with the navigated sequence, the timing of the arterial phases may not always be consistent due to the patient's condition or ability to comply, making it difficult to characterize liver and pancreas lesions. From his initial evaluation of DISCO Star, Dr. Legou believes it can provide a consistent acquisition of the arterial phase during free breathing for good image quality without relying on patient cooperation or trackers or navigators.

"DISCO Star could help us detect and characterize many types of lesions in the liver where multiple differential diagnoses can be observed with very specific enhancement patterns," Dr. Legou explains. It is important to detect small lesions early in order to change the patient care pathway at the earliest possible disease stage.

"In my initial assessment of the DISCO Star prototype, the overall image quality was quite good in terms of spatial resolution, contrast and SNR, and I believe it will impact my diagnostic confidence thanks to the ability to precisely assess lesion perfusion."

Dr. Francois Legou

With DISCO Star, Dr. Legou was able to achieve consistent temporal resolution on a free-breathing, dynamic scan, around 10 seconds per phase, without compromising spatial resolution, which can be kept around 1.5 x 1.5 x 3.6 mm. It is important to find the best compromise between spatial and temporal resolution to avoid streaking artifacts.

He adds, "Based on our experience with the DISCO Star prototype, we anticipate it could allow for higher temporal resolution without sacrificing spatial resolution. Most important, this could be accomplished without patient breath hold."

The ability to deliver free-breathing abdominal exams is important due to the wide array of patient conditions, including those with sleep apnea or dyspnea, a condition where the patient does not inspire and expire at the

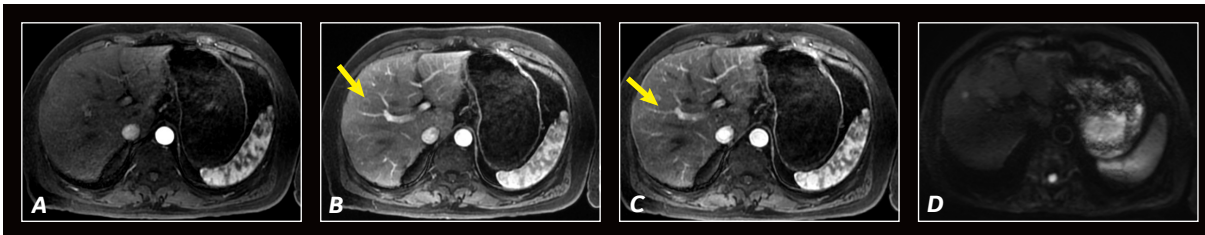

Figure 5. Patient with liver metastases. (A-D) DWI b400, 1.5 x 1.5 x 3.6 mm, 26 sec. for 3 arterial phases, HyperSense factor of 1.3.

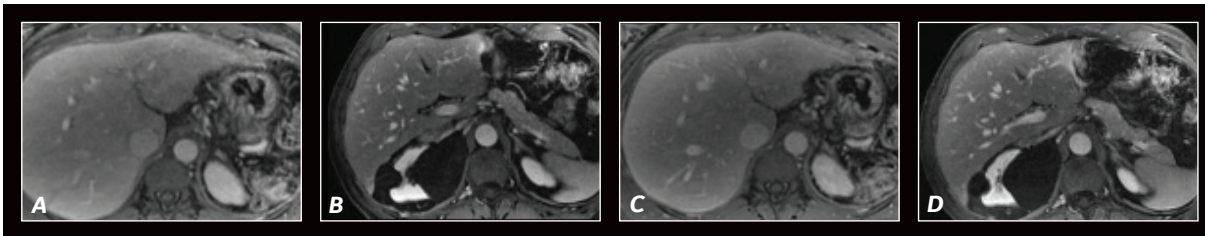

Figure 6. Multi-arterial phases improve early enhancement visualization and facilitate lesion contrast enhancement analysis. HyperSense is designed to reduce scan time without changing image quality. (A, B) LAVA without Hypersense in 25 sec. compared to (C, D) LAVA with HyperSense in 17 sec., a 25 percent reduction in breath-hold time. Acquisition voxel was 1.3 x 1.6 x 2.4 mm.

same level leading to motion artifacts, as well as in pediatric and elderly populations. Dr. Legou believes that DISCO Star could simplify the workflow and enable reproducible exams regardless of the technologist's expertise.

Dr. Legou says the need for an MR sequence that is robust to motion and adaptable to young and old patients is greatly needed. In addition to motion management due to respiration, abdominal MR imaging can be compromised by peristalsis and cardiac shading. Often, contrast media is required, adding the additional challenge of combining both high-temporal and high-spatial resolution in order to detect small lesions that can wash-in and wash-out very quickly.

"In my opinion, DISCO Star could help answer these challenges at the same time," he says.

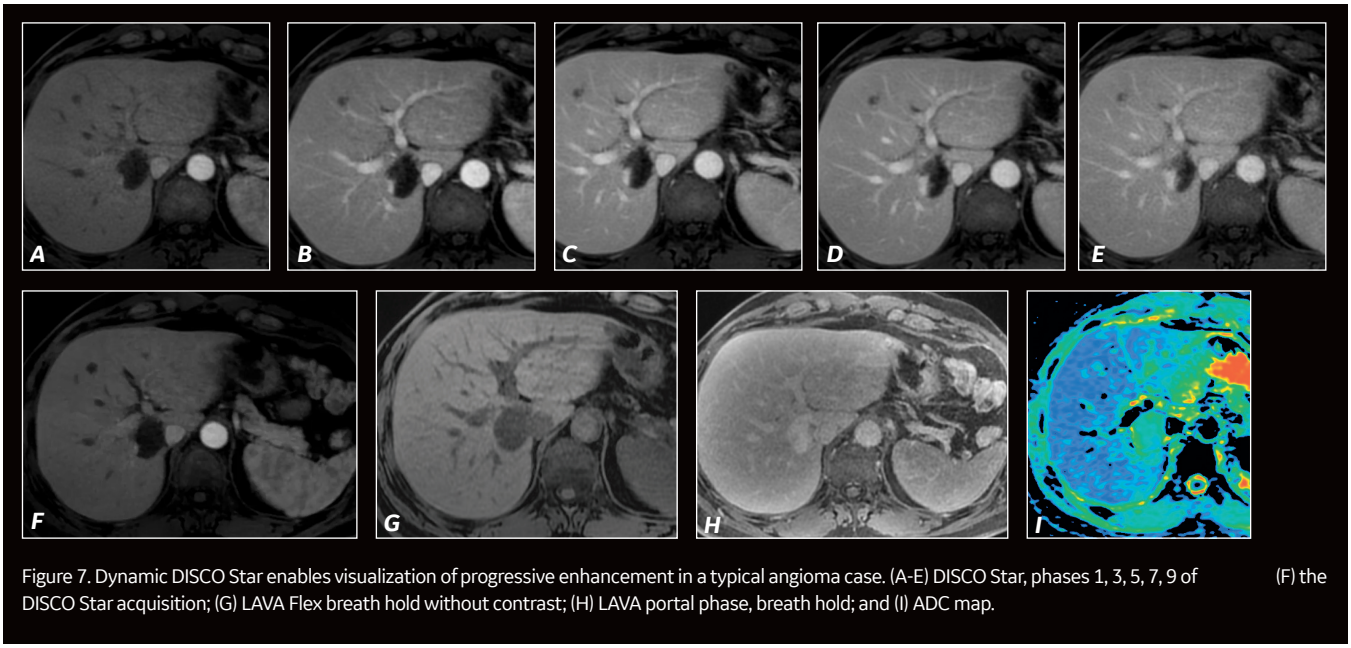

Figure 7. Dynamic DISCO Star enables visualization of progressive enhancement in a typical angioma case. (A-E) DISCO Star, phases 1, 3, 5, 7, 9 of (F) the DISCO Star acquisition; (G) LAVA Flex breath hold without contrast; (H) LAVA portal phase, breath hold; and (I) ADC map.

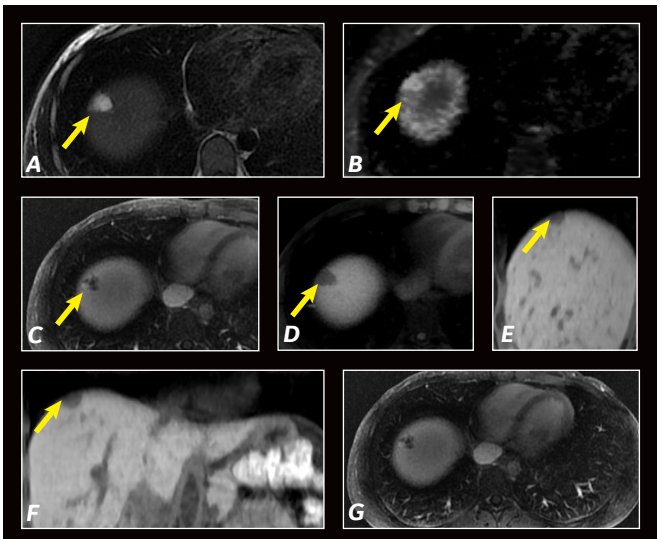

Figure 8. A 43-year-old man with liver hemangioma. (A) Axial T2 FatSat PROPELLER; (B) high ACD; (C) LAVA, late injected phase, 3 min.; (D) DISCO Star native axial plane; (E) DISCO Star sagittal reformat; and (F) DISCO Star coronal reformat. 1.5 x 1.6 x 2.8 mm, 10 temporal phases + Mask, 11.4 sec. phase temporal resolution, 3:22 min.

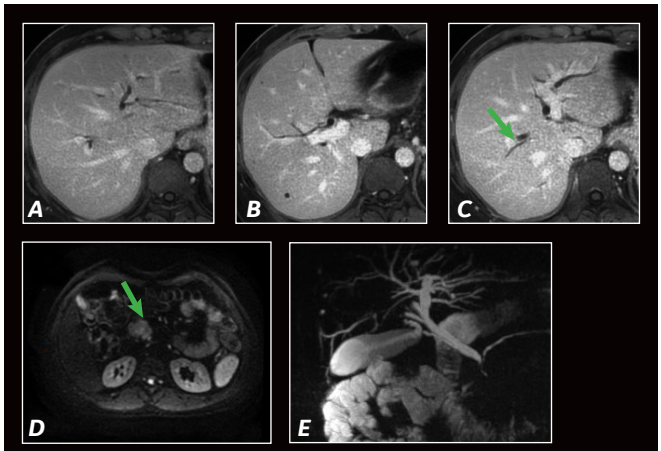

Figure 9. Excellent visualization of distal intrahepatic bile duct (C, arrow). 3D MRCP acquisition shows multiple stenoses of pancreas main duct. (A-C) DISCO Star, 1.5 x 1.6 x 2.8 mm, 10 temporal phases, 11.7 sec./phase, 3:19 min., (D) DWI b800 and (E) 3D MRCP.

Francois Legou, MD
Centre Cardiologique du Nord Hospital
Saint-Denis, France

A 10-minute complete abdominal MR exam

by Francois Legou, MD, Centre Cardiologique du Nord Hospital, Saint-Denis, France

Abdominal MR plays a major role in the detection and characterization of intra- and extra-hepatic lesions, making it possible in certain cases to postpone percutaneous biopsy, and also in the study of hepatic overload pathologies. It is one of the most complete techniques and a great semiological wealth in abdominal imaging.

Schematically, an abdominal MR exam is part of either a lesion detection process or a characterization process for a lesion visualized by another imaging method. MR imaging is often recommended as a second-line exam after an ultrasound or a CT scan, allowing a diagnosis to be refined with excellent precision. However, the French Society of Radiology (SFR) states that MR should be the first imaging method used for the characterization of hepatic lesions[1].

Depending on the clinical indication specific to each patient, an abdominal MR exam can sometimes be long and therefore uncomfortable for the patient. The challenge lies in the fact that the patient must be as cooperative as possible throughout the exam in order to obtain diagnostic image quality. Shortening exam time would be very important for improving this type of exam.

In September 2019, we installed a SIGNA™ Premier 3.0T system in our hospital along with the 30-channel AIR™ Anterior Array (AA) Coil. Nearly half of our weekly abdominal MR exams (average 30/week) are now performed on this system. The AIR™ AA Coil combined with the power of the SuperG gradient of SIGNA™ Premier allows us to configure abdominal exam protocols by accelerating sequence times, without any real compromise in image quality.

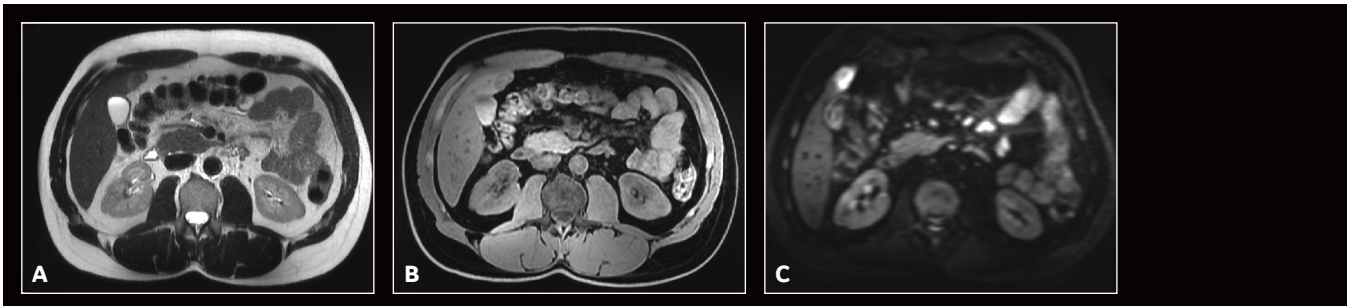

Figure 1. A 52-year-old male with metastatic colon cancer situated in right colic angle (hepatic angle). (A) Conventional SSFSE T2 sequence with a slice thickness of 3 mm and breath-hold was acquired in 25 sec. (possibility of two breath-holds). (B) LAVA Flex with breath-hold acquired in 19 sec. for in and out of phase, (C) MUSE multi-shots HR with respiratory trigger provide us with a good characterization of the lesion without compromise on image quality. These sequences were acquired before injection of gadolinium.

SIGNA™ Premier 3.0T

	Axial T2 SSFSE	*Axial T2 FatSat RTr PROPELLER*	*Axial LAVA Flex*	*Axial DWI MUSE (2 shots)*	*Axial DISCO FatSat (Multi-arterial and portal)*	*Axial LAVA FatSat 3 min. delay*
TR (ms):	456-513	2500-5455	4.2	4000-6667	3.1-3.2	3.1-3.2
TE (ms):	84.9-85.5	82.9-91.9	1.7	69-74	1.4	1.4
FOV (cm):	40 x 32	42 x 42	44 x 39.6	34 x 27.1	44 x 35.2	44 x 35.2
Slice thickness (mm):	4	5	3	5	2	2
Frequency:	400	368	340	100	280	272
Phase:	224	368	240	192	240	240
Acceleration factor:	Phase: 2 (ARC)	Phase: 2 (ARC)	Phase/slice: 2/1.2 (ARC)	Phase: 1 (ASSET)	Phase/slice: 2/1.5 (ARC)	Phase/slice: 2/1.2 (ARC)
NEX (kHz):	0.5	2	0	b50: 2 b800: 5	0.7	0.7
Scan time (min):	25-29 sec.	2:24-4:39	15-19 sec.	2:57-4:32	1:02 (17 sec.)	14-17 sec.
Options:	83.3 kHz	FatSat,RTr, NPW 1.3, 83.3 kHz	Zip2, 166.7 KHz	FatSat, RTr, Sat A/P, 250 kHz, ASSET	Zip2, FatSat Special TI 23, RT, 90.9 kHz, FA 12	Zip2, FatSat Special TI 23, RT, 83.3 kHz, FA 12

Technique

Each exam was performed on the SIGNA™ Premier with the AIR™ AA Coil, which can cover up to 60 cm in length. We establish an intravenous line before the start of the exam if the use of contrast is needed after the first sequence. There is no prior administration of anti-peristalsis.

We have been evaluating the use of fast protocols that allow us to reduce exam times to as short as 10 minutes while still obtaining six sequences for a complete exam to facilitate diagnosis. In general, the exam includes a series of breath-hold sequences – SSFSE T2, FSE T2 PROPELLER with FatSat coupled to the respiratory trigger, and LAVA Flex – followed by MUSE using b-values of 50 and 800 mm^2/sec with a respiratory trigger before injection. The dynamic sequence DISCO with FatSat allows us to obtain multi-arterial and portal phases while axial LAVA FatSat delivers a 3-minute delay late phase.

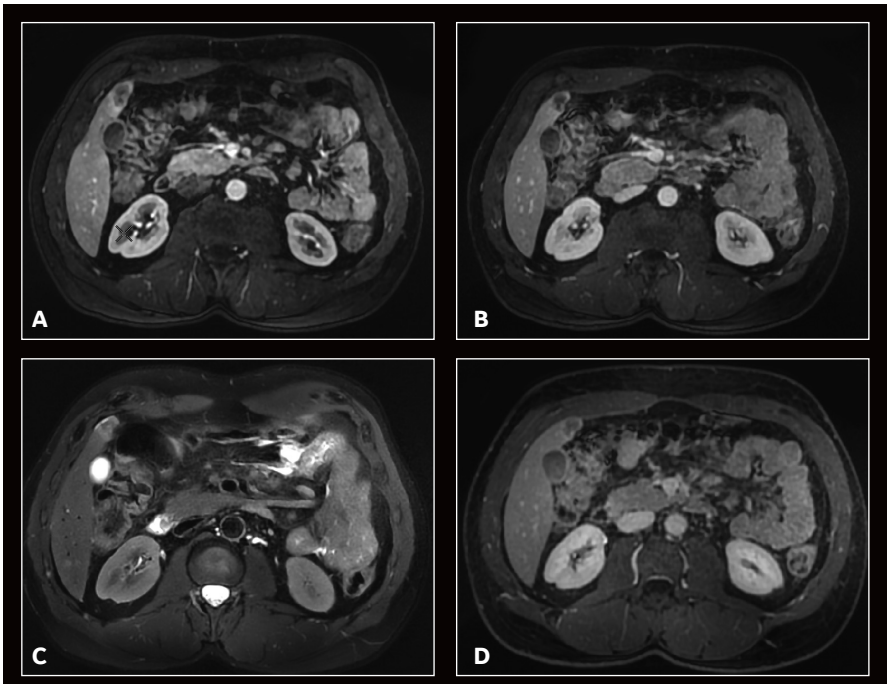

Figure 2. Dynamic 3D DISCO SPECIAL sequences with gadolinium are acquired for lesion characterization. This sequence has a temporal resolution of 8 sec. (A,B) Double multi-arterial two times followed by (C) a portal time and (D) a late time and 3 min. after injection of contrast.

Results

Prior to the implementation of our rapid abdominal scan protocol (see parameter table on previous page), each exam would take 20 to 25 minutes. Approximately 10 to 15 percent of these exams failed or resulted in poor diagnostic quality images.

Now, with the 10-minute abdominal scan, we are experiencing fewer failed/poor quality exams. As important, patient compliance improved due to the shorter exam time and the enhanced comfort with the AIR™ AA Coil. Further, the technological advancements of the AIR™ AA Coil – with a high channel count and reduced noise due to the coil elements being closer to the anatomy – allow for a clear increase in image quality. Radiographers report the coil is easier to handle and position on patients due to the coil's flexibility to conform to different sizes and shapes.

We look forward in the future to utilizing HyperSense, a compressed sensing technique that enables either a shorter late enhanced phase or higher spatial resolution. Two emerging sequences may further advance abdominal imaging: LAVA HyperSense is designed to enable either a shorter late enhanced phase or higher spatial resolution and DISCO Star, designed to provide the possibility to acquire dynamic acquisitions as a complete free-breathing radial acquisition. Applying image reconstruction techniques like AIR™ Recon or AIR™ Recon DL could further reduce acquisition time on SSFSE sequences and potentially in T2 FatSat and DWI sequences. Ⓢ

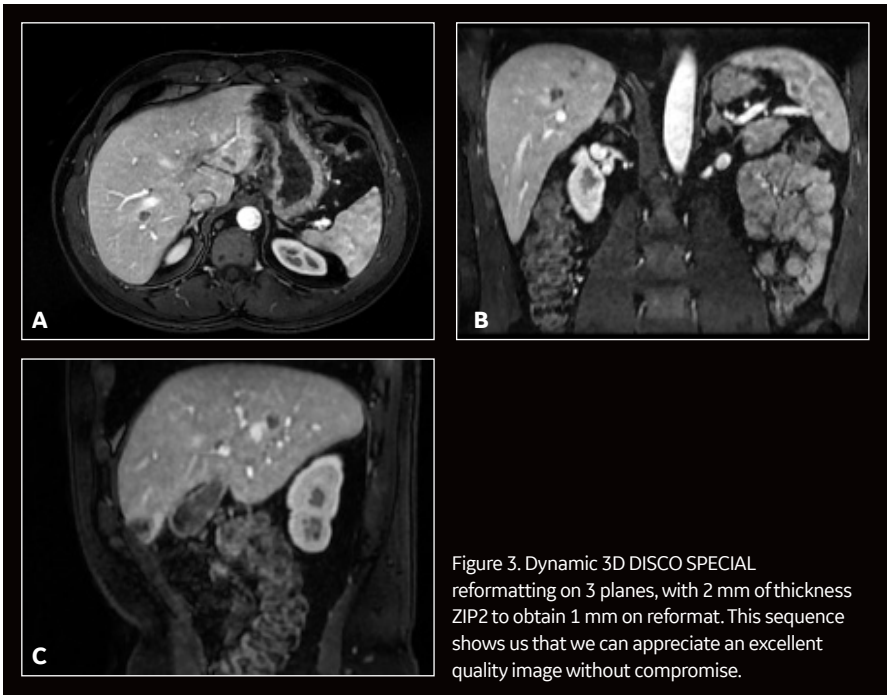

Figure 3. Dynamic 3D DISCO SPECIAL reformatting on 3 planes, with 2 mm of thickness ZIP2 to obtain 1 mm on reformat. This sequence shows us that we can appreciate an excellent quality image without compromise.

References

1. Baranas L, Luciani A. Imagerie des tumeurs bénignes du foie: actualisation 2014. Association Française de Formation Médicale Continue en Hépato-Gastro-Entérologie. Available at: https://www.fmcgastro.org/wp-content/uploads/file/pdf-2014/29_Luciani_1_630_v1.pdf.

Christian Kellenberger, MD

University Children's Hospital Zürich
Zürich, Switzerland

Pediatric free-breathing abdominal imaging

by Christian Kellenberger, MD, Radiologist-in-Chief, University Children's Hospital Zürich, Zürich, Switzerland

Abdominal MR imaging is challenging in young children because they often cannot hold their breath and may be unable to follow breathing instructions. Thus, having the ability to perform fast and completely free-breathing examinations is crucial to obtain high-quality images and ensure an accurate diagnosis.

After updating our software to SIGNA™Works on the Discovery™ MR750 3.0T and Discovery™ MR450 1.5T systems, we now have access to acceleration techniques such as HyperSense and HyperCube that are compatible with Auto Navigator and Respiratory Triggering (RTr) methods. These capabilities have helped to significantly reduce the acquisition time of 3D Cube sequences for abdominal imaging while increasing spatial resolution. We are routinely using Auto Navigator in our free-breathing protocols, as it allows for automatic diaphragm detection and tracker placement without user interaction, which simplifies the workflow.

Additionally, the latest generation of PROPELLER Multi-Blade (MB) allows us to achieve T1 and T1 FatSat FSE contrasts without respiratory motion artifacts. Without the use of respiratory gating or triggering, PROPELLER MB provides us with high-quality and artifact-free FSE T1-weighted images in free-breathing children, which is essential for the assessment of abdominal organs. Image quality is clearly improved and the acquisition is faster when compared to prior approaches for compensating respiratory motion, such as signal averaging by increasing the number of excitations or the use of respiratory compensation (RT) for T1-weighted SE.

Finally, the 3D DISCO sequence combined with Auto Navigator allows us to do free-breathing dynamic contrast enhanced (DCE) imaging without compromising spatial resolution and with a temporal resolution between 10-20 ms per phase, depending on the patient's respiration rate. It can be done in any plane and is compatible with Dixon techniques for robust fat saturation in every case.

Discovery™ MR750 3.0T

	T2 HyperCube STIR	*PROPELLER MB T2 FatSat RTr*	*Axial PROPELLER MB T1*	*PROPELLER MB T1 FatSat*	*Coronal DISCO Flex*
FOV (cm):	30	24	24	26	32
Slice thickness (mm):	3/1.5	5	5	5	3/1.5
Frequency:	320	300	292	292	260
Phase:	264	300	292	292	260
Scan time (min.):	4:24	4:39	4:17	4:34	3:31
Options/other (b-value, no-phase wrap, etc.):	ARC 2x1, HyperSense 1.2, Auto Navigator	RTr	Auto Navigator		Auto Navigator

Discovery™ MR450 1.5T

	T2 HyperCube STIR	*Axial PROPELLER MB T2 FatSat RTr*	*Axial PROPELLER MB T1*	*Axial PROPELLER MB T1 FatSat*	*Axial DWI RTr*	*Coronal DISCO Flex*
FOV (cm):	32	34	34	34	28	32
Slice thickness (mm):	3	5	5	5	5	3.4/1.7
Frequency:	384	340	332	332	128	288
Phase:	320	340	332	332	140	200
Scan time (min.):	2:05	3:32	3:09	3:29	3:11	3:49
Options/other (b-value, no-phase wrap, etc.):	ARC 2x1, HyperSense 1.2, Auto Navigator		Auto Navigator	Auto Navigator	b50, b1000, b1500, ADC	Auto Navigator

Case 1

Patient history

A three-year-old child with a pelvic cystic mass.

Technique

Performed a complete free-breathing exam on the Discovery™ MR750 using PROPELLER MB, T1 and RTr T2 FatSat, HyperCube, 3D DISCO and Auto Navigator (Figures 1-3).

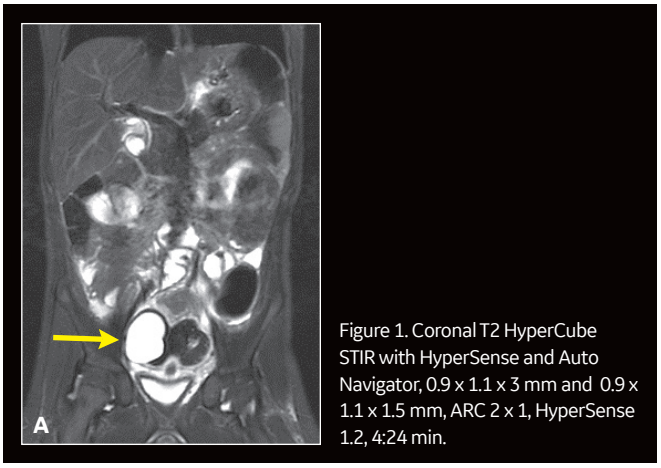

Figure 1. Coronal T2 HyperCube STIR with HyperSense and Auto Navigator, 0.9 x 1.1 x 3 mm and 0.9 x 1.1 x 1.5 mm, ARC 2 x 1, HyperSense 1.2, 4:24 min.

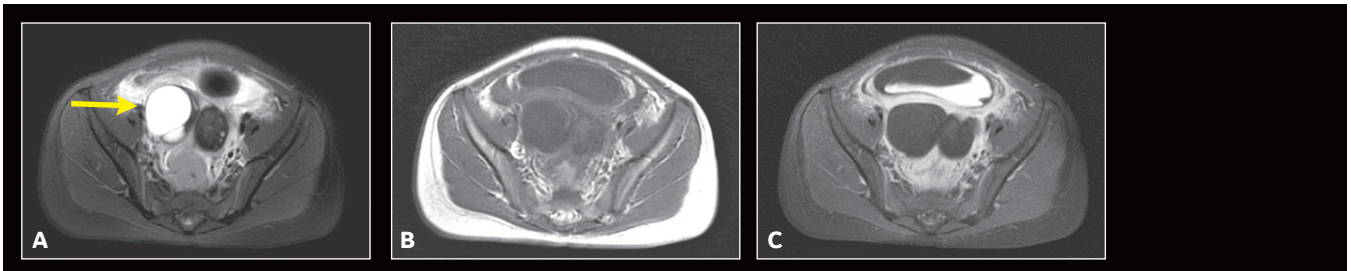

Figure 2. Axial PROPELLER MB with RTr T2 FatSat and free-breathing T1. (A) Axial PROPELLER T2 FatSat RTr FOV 24, 300 x 300, 4:39 min. (B) Axial PROPELLER T1 free breathing, 0.8 x 0.8 x 5 mm, 4:17 min. (C) Axial PROPELLER T1 FatSat post-contrast free breathing, 0.9 x 0.9 x 5 mm, 4:34 min.

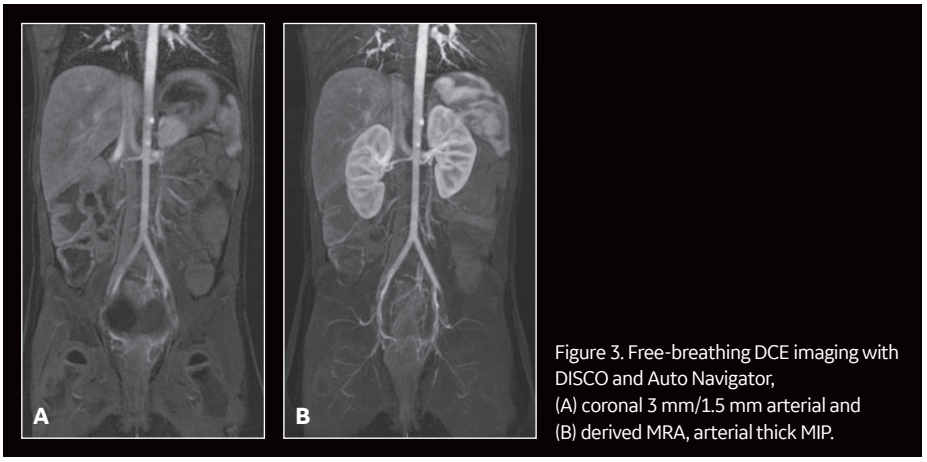

Figure 3. Free-breathing DCE imaging with DISCO and Auto Navigator,
(A) coronal 3 mm/1.5 mm arterial and
(B) derived MRA, arterial thick MIP.

Case 2

Patient history

A 16-year-old child with suspicion of angiomyolipoma or kidney cell carcinoma.

Technique

Performed a complete free-breathing exam on the Discovery™ MR450 using PROPELLER MB, T1 and RTr T2 FatSat, HyperCube STIR, 3D DISCO, DWI and Auto Navigator (Figures 4-6).

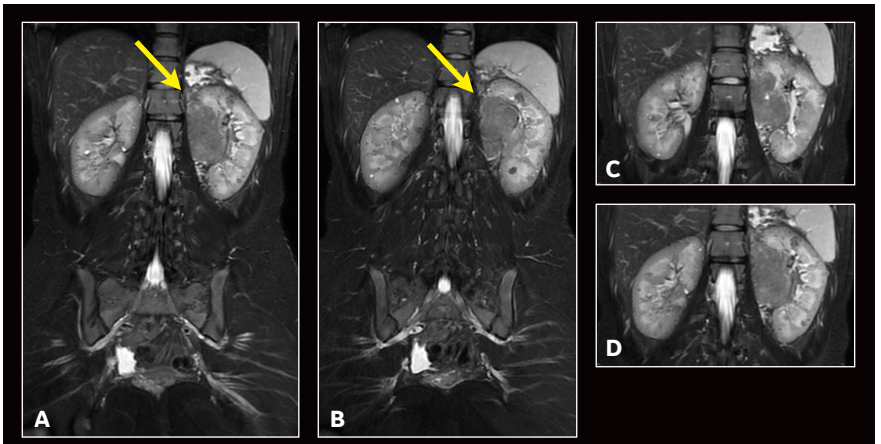

Figure 4. Free-breathing coronal HyperCube STIR with HyperSense and Auto Navigator, 0.8 x 1.0 x 3 mm, ARC 2x1, HyperSense 1.2, 2:05 min.

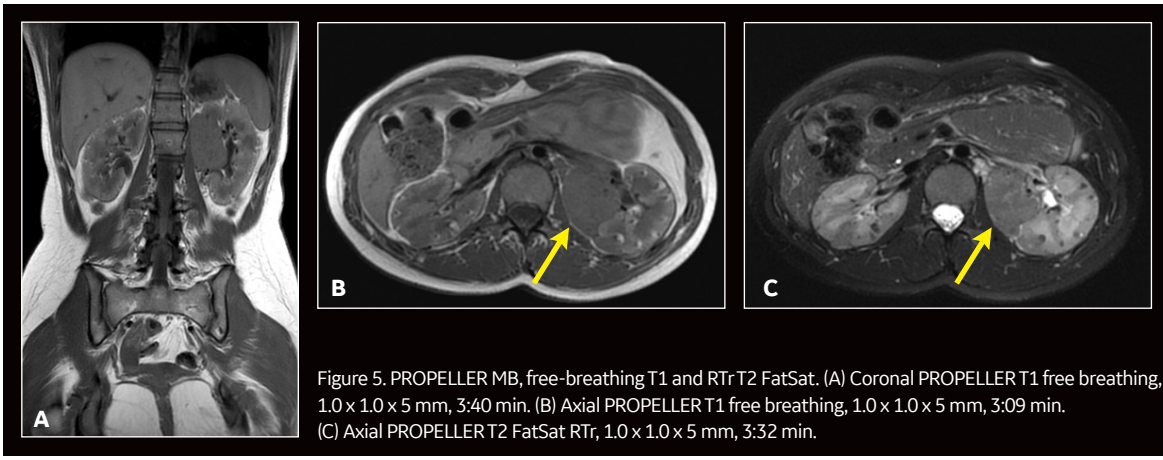

Figure 5. PROPELLER MB, free-breathing T1 and RTr T2 FatSat. (A) Coronal PROPELLER T1 free breathing, 1.0 x 1.0 x 5 mm, 3:40 min. (B) Axial PROPELLER T1 free breathing, 1.0 x 1.0 x 5 mm, 3:09 min. (C) Axial PROPELLER T2 FatSat RTr, 1.0 x 1.0 x 5 mm, 3:32 min.

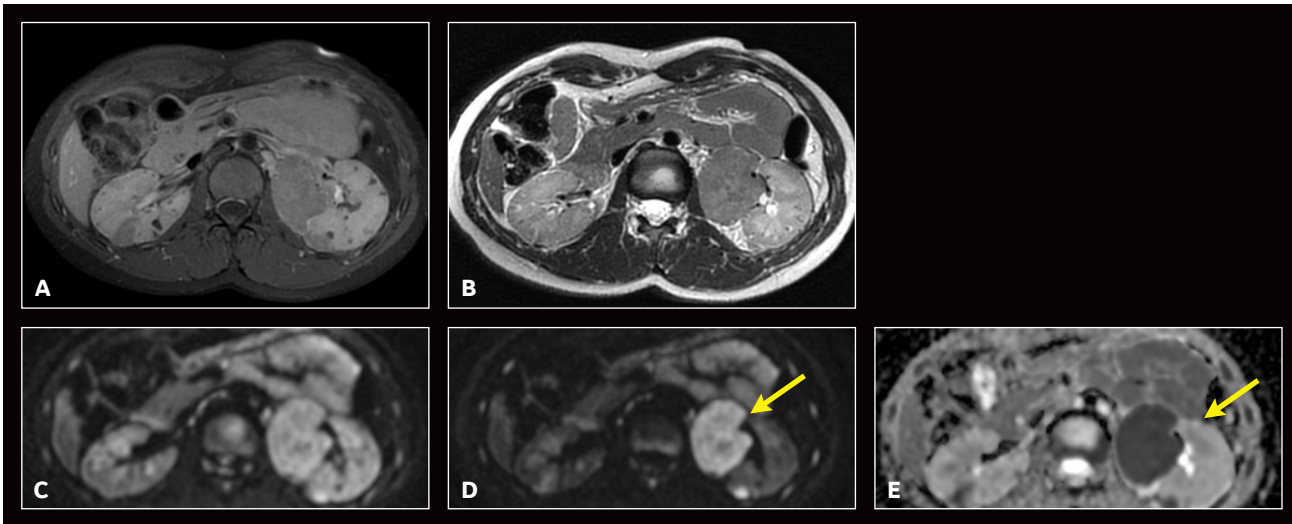

Figure 6. DWI and PROPELLER MB. (A) Axial PROPELLER T1 FatSat post-contrast free breathing, 1.0 x 1.0 x 5 mm, 3:29 min. (B) Axial PROPELLER T2 RTr, 1.0 x 1.0 x 3 mm, 3:46 min. (C-E) Axial DWI RTCF RTr, 2.1 x 2.0 x 5 mm, with (C) b50, (D) b1500 and (E) ADC.

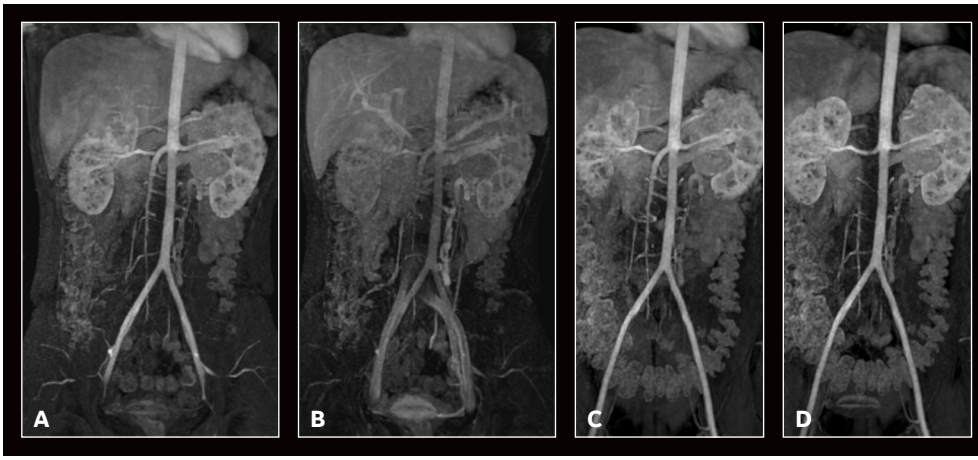

Figure 7. DCE free-breathing imaging with DISCO and Auto Navigator. (A-D) Coronal DISCO Flex and Auto Navigator 3.4 mm/1.7 mm, (A) arterial, (B) portal-venous and (C-D) derived MRA – arterial thick MIP.

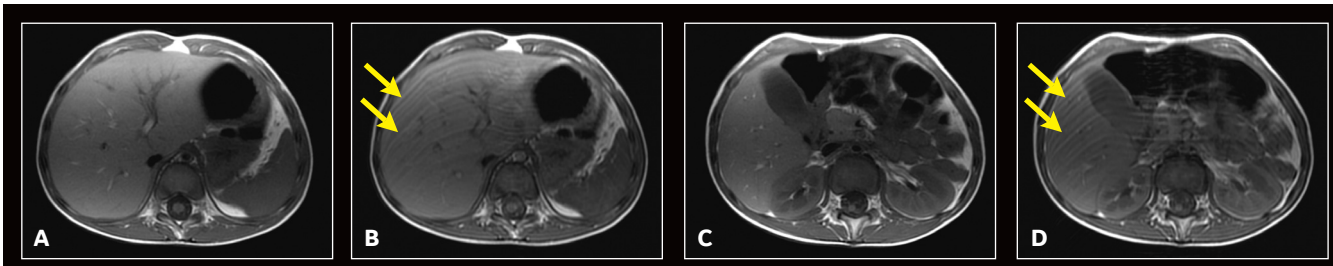

Figure 8. T1 PROPELLER MB vs. T1 SE respiratory compensation (RC). Note how PROPELLER MB T1 suppresses breathing motion artifacts compared to conventional T1 SE acquisition with remaining motion artifacts (yellow arrows). (A, C) Axial T1 PROPELLER MB free-breathing, 0.8 x 0.8 x 5 mm, 3:40 min., (B, D) Axial T1 SE RC free-breathing, 1.0 x 1.4 x 5 mm, 4:08 min.

Discussion

The latest sequence options from GE Healthcare are a real asset for achieving robust abdominal imaging in free-breathing children, adolescents and adults who are unable to hold their breath. In particular, PROPELLER MB T1 efficiently suppresses breathing motion artifacts compared to respiratory compensation techniques (Figure 8).

Marc Zins, MD
Saint-Joseph Hospital
Paris, France

3D MRCP with HyperSense: an evaluation of respiratory-triggered and breath-hold sequences

By Marc Zins, MD, Head of the Radiology Department, Saint-Joseph Hospital

Discovery™ MR750

PARAMETERS

	3D Coronal MRCP RT	*3D Coronal MRCP RT HS*	*3D Coronal MRCP BH HS*
TR (ms):	6000	3333	1878
TE (ms):	888	882	1055
FOV (cm):	34 x 27	34 x 27	36 x 28
Slice thickness (mm):	1	1	2.8
Frequency:	416	416	384
Phase:	352	352	300
HyperSense factor:	–	1.6	2.2
NEX:	0.5	0.5	0.5
Scan time (min):	6:32	2:19	0:24 (sec.)
Options:	Zip2, FatSat, RT, Sat A/P, 50 kHz	Zip2, FatSat, RT, 50 kHz	Zip2, FatSat, 62.5 kHz

Magnetic resonance cholangiopancreatography (MRCP) is a highly accurate, non-invasive diagnostic test used to assess the hepatobiliary and pancreatic systems. A challenge is that patient compliance is required for respiratory-triggered and breath-hold sequences to achieve diagnostic-quality images.

In October 2016, our institution implemented SIGNA™Works, GE Healthcare's productivity platform of pulse sequences across core imaging techniques. SIGNA™Works includes HyperSense, a compressed sensing acceleration technique based on sparse data sampling and iterative reconstruction that enables faster scan times or higher resolution.

To evaluate the impact of HyperSense in MRCP exams, we performed a series of comparisons using our existing protocol, a conventional respiratory-triggered Coronal 3D MRCP, a Coronal 3D MRCP respiratory-triggered with HyperSense and a Coronal 3D MRCP breath-hold with HyperSense.

Technique

Each exam was performed on the Discovery™ MR750 3.0T system with a 32-channel torso coil. The protocol included patient fasting of at least four hours, which reduced the amount of fluid in the stomach and digestive tract, distended the gallbladder and limited duodenal peristalsis. There was no prior administration of anti-peristalsis. The ingestion of pineapple juice just before the examination helped to act as a negative contrast agent, due to the paramagnetic properties of the manganese contained in the juice, thus limiting signal interference related to the digestive tract fluid onto the resultant images.

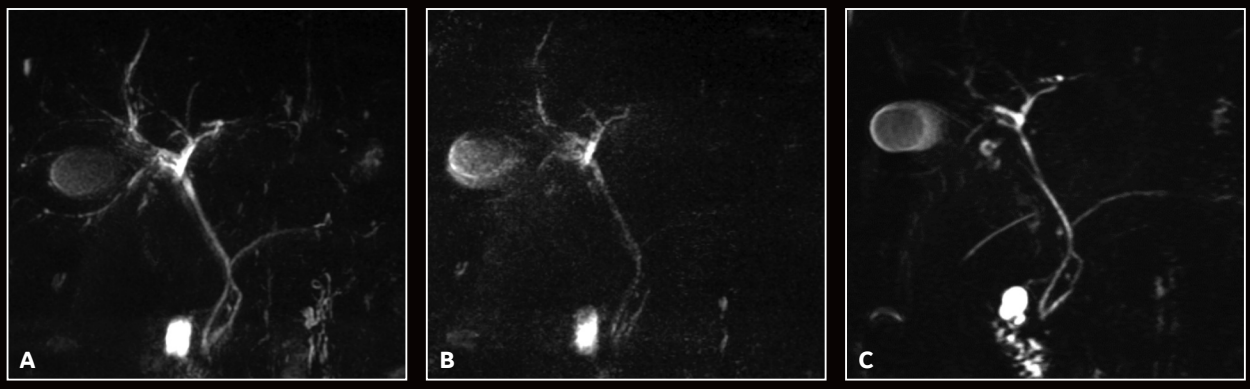

Figure 1. A 57-year-old female with unique IPMN of 12 mm situated in the head of the pancreas. (A) Conventional MRCP with respiratory-triggered sequence was acquired in 5:27 min.; (B) MRCP with respiratory-triggered and HyperSense acquired in 1:59 min.; and (C) MRCP breath-hold with HyperSense. The breath-hold sequence provides the same diagnostic information as the conventional sequence but in a far shorter scan time of 24 sec. and with fewer motion artifacts.

Figure 2. A 77-year-old female with a cystic lesion located in the pancreas body, in favor of an IPMN. (A) Conventional MRCP with respiratory-triggered sequence was acquired in 3:39 min.; (B) MRCP with respiratory-triggered and HyperSense was acquired in 2:19 min.; and (C) MRCP breath-hold with HyperSense was acquired in 21 sec. In this case, the patient could not hold their breath perfectly. The respiratory-triggered sequence with HyperSense was able to provide the same diagnostic information as the conventional sequence with a reduced scan time.

MR findings

First, we compared the respiratory-triggered conventional 3D MRCP against the respiratory-triggered HyperSense 3D MRCP sequence using a factor of 1.6. In almost all cases, we achieved similar image quality, however, with HyperSense we were able to reduce the sequence scan time by at least 34 percent. We were also able to reduce artifacts in the respiratory-triggered sequence with the addition of HyperSense due to the shortened exam time.

Next, we evaluated the respiratory-triggered HyperSense sequence against the HyperSense breath-hold sequence using the same factor of 2.2. While the spatial resolution was not the same between these two sequences, we found that the 3D MRCP breath-hold HyperSense sequence could often provide the information needed for a confident diagnosis. Plus, by using

Figure 3. A 53-year-old female with a 3 cm mass located in the pancreas head, which led to main and secondary pancreatic ducts dilation as well as intra- and extra-hepatic biliary ducts dilation. (A) Conventional MRCP with respiratory-triggered sequence was acquired in 6:32 min.; (B) MRCP with respiratory-triggered and HyperSense was acquired in 4:08 min.; and (C) MRCP breath-hold with HyperSense was acquired in 21 sec. All sequences provided the same diagnostic information.

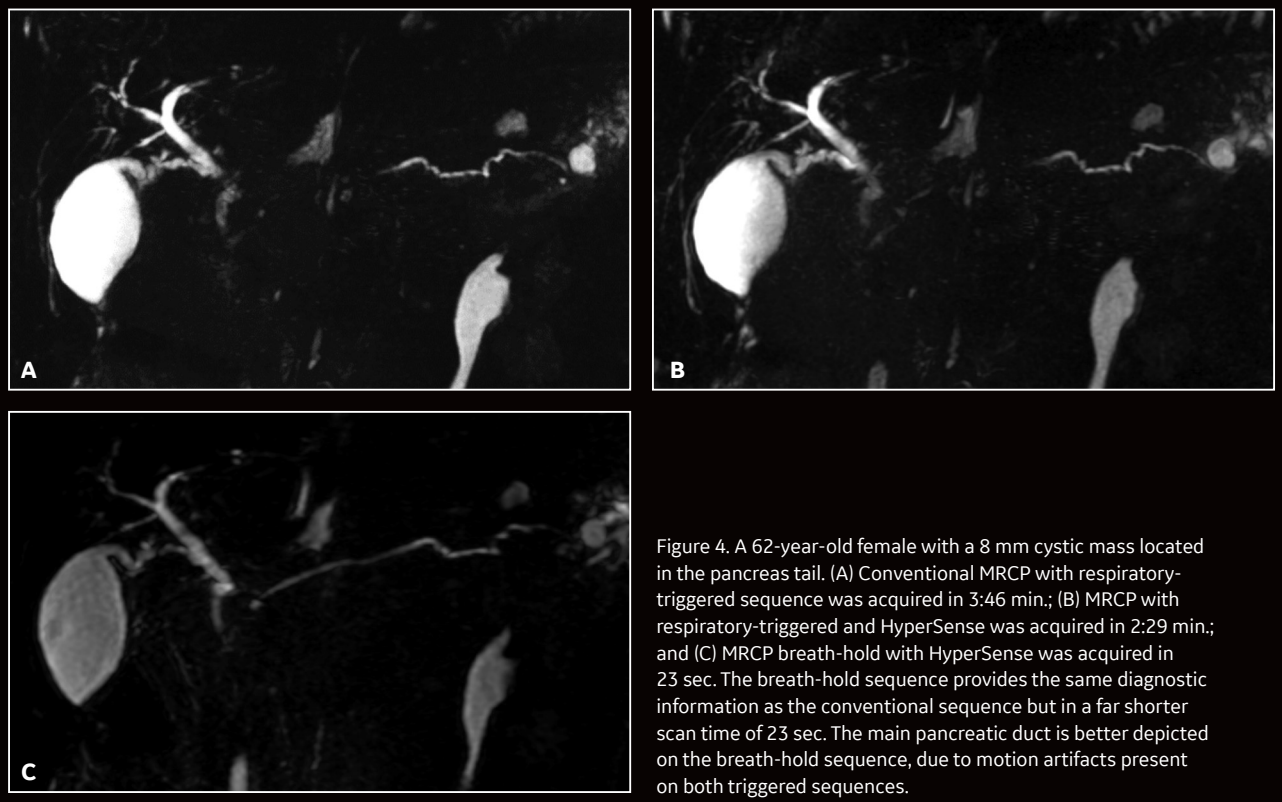

Figure 4. A 62-year-old female with a 8 mm cystic mass located in the pancreas tail. (A) Conventional MRCP with respiratory-triggered sequence was acquired in 3:46 min.; (B) MRCP with respiratory-triggered and HyperSense was acquired in 2:29 min.; and (C) MRCP breath-hold with HyperSense was acquired in 23 sec. The breath-hold sequence provides the same diagnostic information as the conventional sequence but in a far shorter scan time of 23 sec. The main pancreatic duct is better depicted on the breath-hold sequence, due to motion artifacts present on both triggered sequences.

HyperSense, the breath-hold sequence could be reduced to 24 seconds or less without respiratory-induced artifacts.

As a result of our evaluation, the Coronal 3D MRCP respiratory-triggered with HyperSense factor of 1.6 sequence has now replaced the conventional respiratory-triggered Coronal 3D MRCP sequence in our facility. Additionally, in patients who cannot tolerate the high-resolution, respiratory-triggered 3D MRCP with HyperSense scan, the Coronal 3D MRCP breath-hold HyperSense factor of 2.2 sequence is an excellent option that can result in a successful examination.

BodyWorks gallery:
AIR™ Recon DL

Cardiac

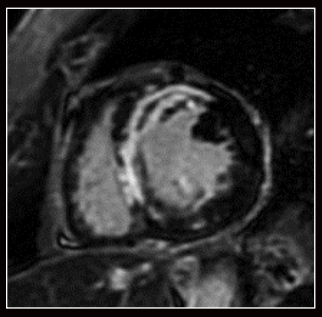

Conventional reconstruction

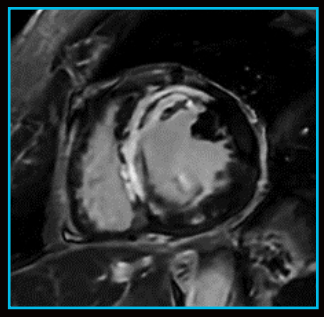

AIR™ Recon DL

Short Axis MDE
1.6 x 1.9 x 8.0 mm

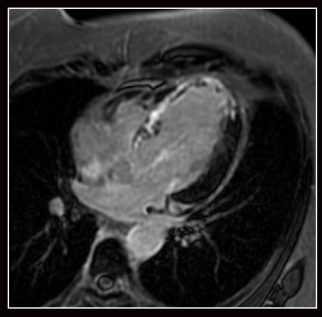

Conventional reconstruction

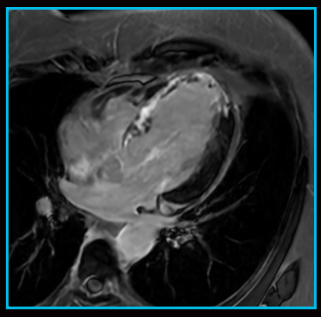

AIR™ Recon DL

4ch MDE
1.7 x 2.0 x 8.0 mm

Images acquired on SIGNA™ Pioneer 3.0T, courtesy of radiomed, Weisbaden, Germany.

Body

Male pelvis (prostate) using AIR™ Anterior Array Coil. PI-RADS®-compliant protocols can be achieved in much shorter acquisition times with AIR™ Recon DL.

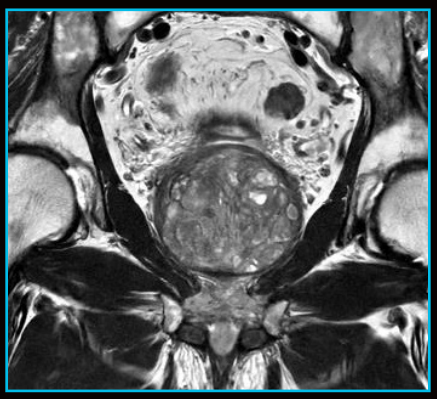

Axial T2 frFSE
0.4 x 0.7 x 3 mm, 37 slices
2:10 min.

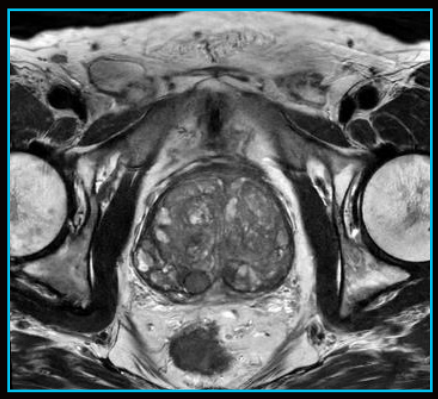

Coronal T2 frFSE
0.4 x 0.7 x 3 mm, 30 slices
1:31 min.

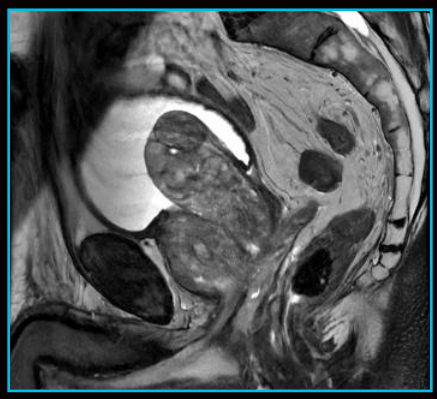

Sagittal T2 frFSE
0.4 x 0.7 x 3 mm, 24 slices
2:51 min.

Images acquired on SIGNA™ Pioneer 3.0T, courtesy of radiomed, Weisbaden, Germany.

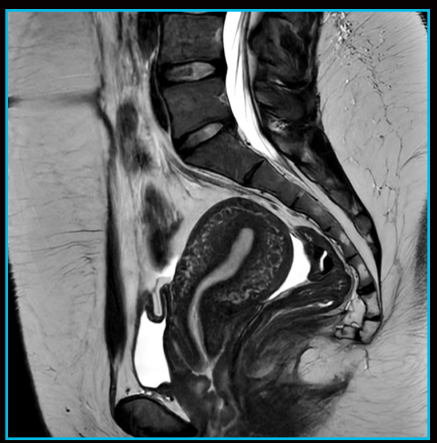

Sagittal T2 FSE
0.6 x 0.8 x 3 mm, 40 slices
2:00 min.

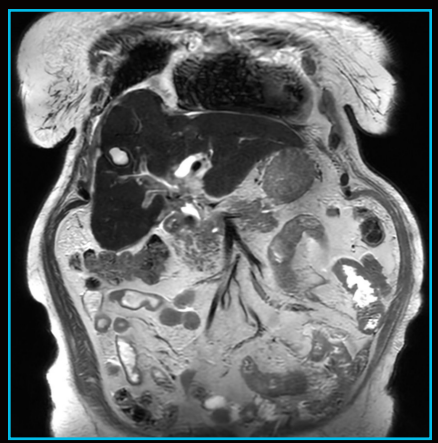

Coronal T2
1.1 x 1.7 x 4 mm, 42 slices
1:31 min.

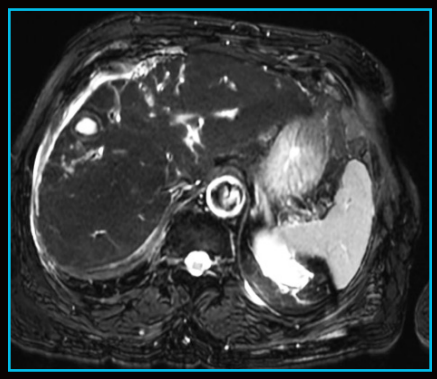

Axial TX FatSat
1.2 x 1.9 x 5 mm, 42 slices
1:39 min.

(Left) Image acquired on SIGNA™ Premier 3.0T, courtesy of Centre Cardiologique du Nord (CCN), Paris, France.
(Middle & right) Images acquired on SIGNA™ Premier 3.0T, courtesy of Acibadem Maslak Hospital, Istanbul, Turkey.

BodyWorks gallery:
Abdominal imaging (pancreas & MRCP)

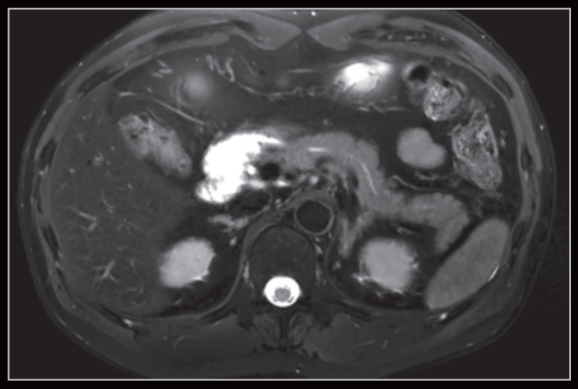

Axial T2 FatSat
PROPELLER MB
0.6 x 0.6 x 4 mm
ARC 4.0
4:24 min.

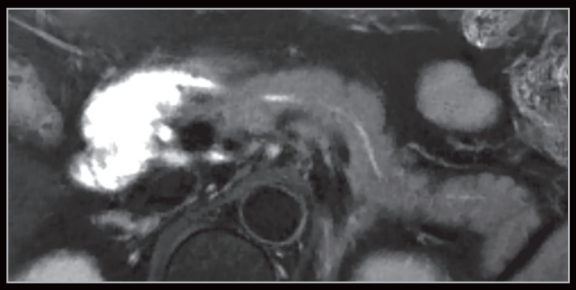

AIR™ Coils are comfortable for the patient and enable higher parallel imaging factors, which reduces patient exam times and drives productivity.

Images courtesy of Osaka University Hospital, Osaka, Japan

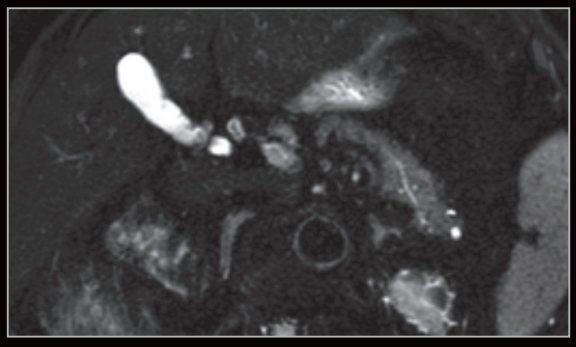

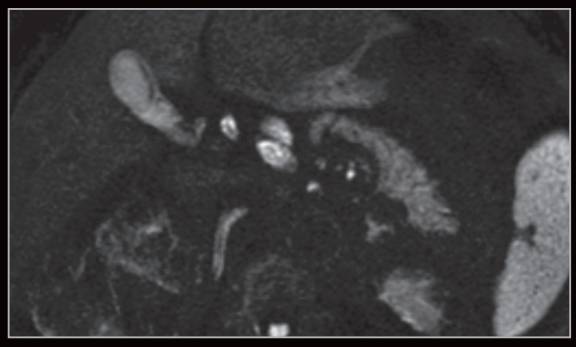

Improved DWI EPI imaging with multi-shot DWI and AIR™ AA Coils.

MUSE allows for reduced susceptibility artifacts, incorporates large matrices for submillimeter resolution and can be combined with distortion correction for additional artifact reduction. Combining MUSE with AIR™ Coils ensures a simply better patient experience and exceptional image quality.

Images courtesy of Emsey Hospital, Istanbul, Turkey

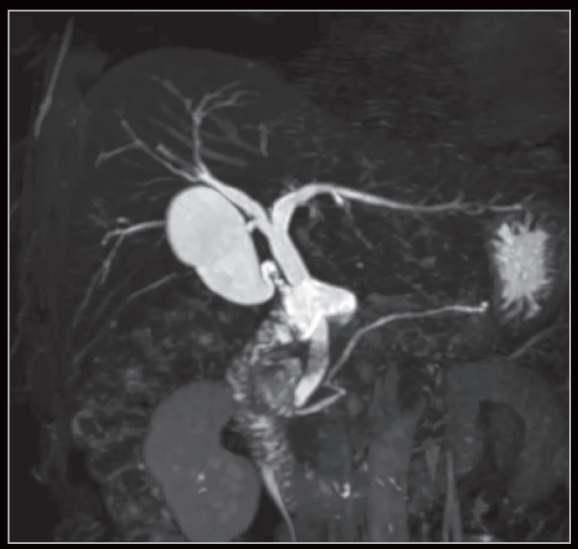

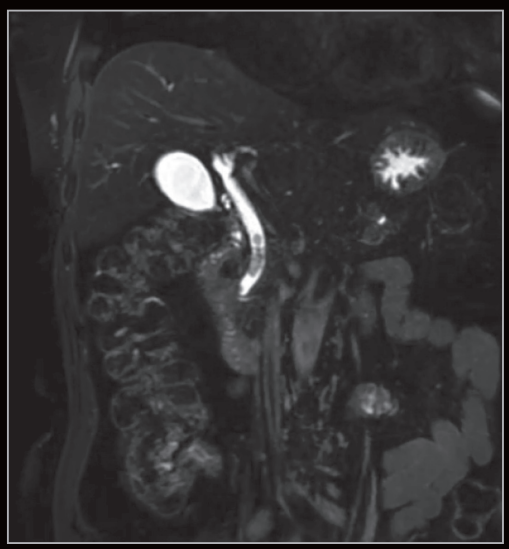

3D MRCP with HyperSense
1.2 x 1.2 x 1.6 mm
3:08 min.

Images courtesy of Haeundae Paik Hospital, Busan, Korea

BodyWorks gallery:
Pelvis imaging (male & female)

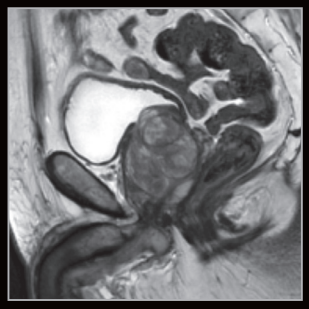

Sagittal T2 PROPELLER
0.7 x 0.7 x 3 mm
3:16 min.

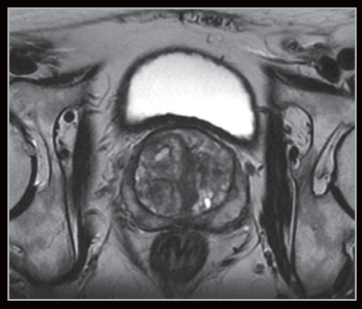

Axial T2 frFSE
0.6 x 0.8 x 3 mm
3:24 min.

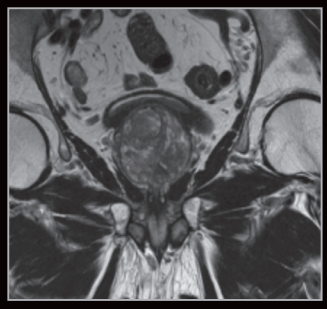

Coronal T2 frFSE
0.7 x 0.7 x 3 mm
3:50 min.

Images courtesy of radiomed, Mainz, Germany

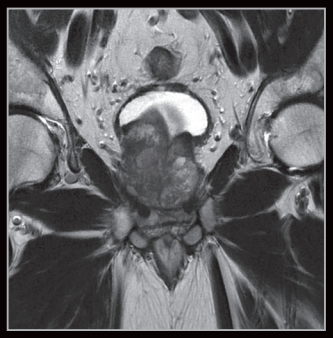

Without AIR™ Recon
4:35 min.

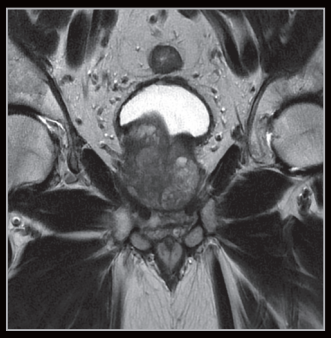

With AIR™ Recon
3:37 min.

AIR™ Recon allows reduction in scan times and can lessen out of field-of-view artifacts to improve image quality and workflow. Both coronal T2 PROPELLER scans were acquired with the same resolution, however, the left image was acquired in 4:35 min. while the image on the right was acquired in only 3:37 min. using AIR™ Recon.

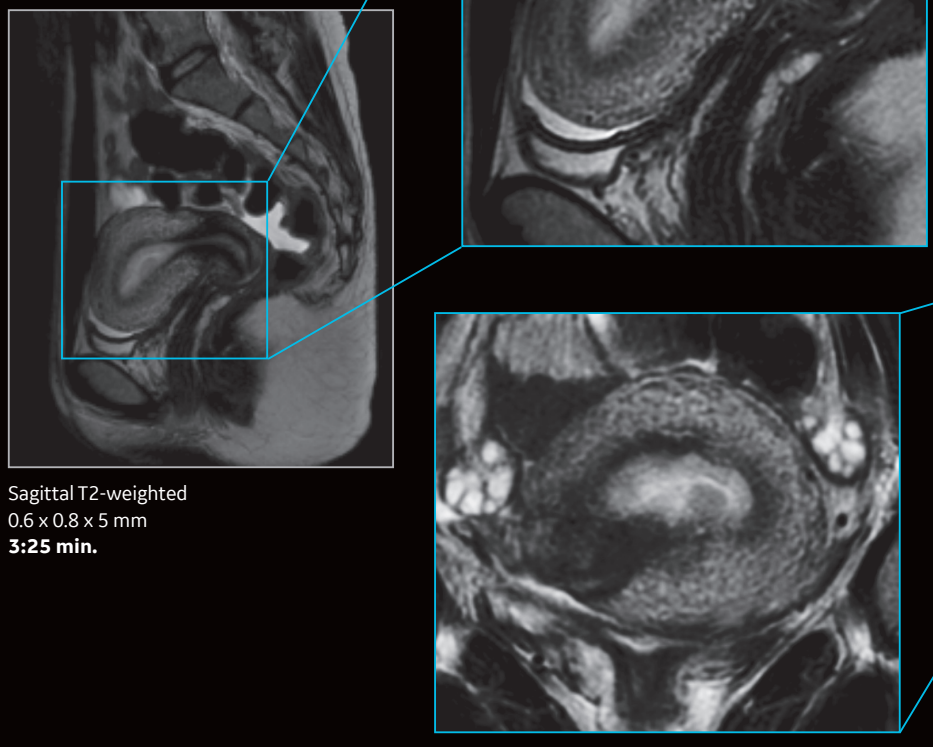

Sagittal T2-weighted
0.6 x 0.8 x 5 mm
3:25 min.

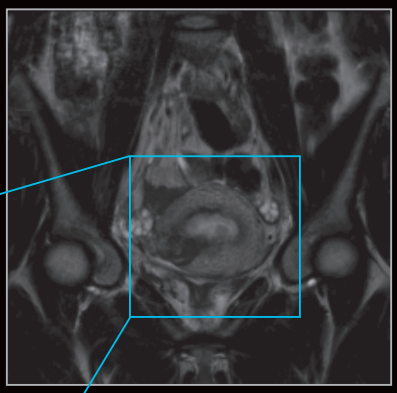

Coronal T2 FSE
0.6 x 0.8 x 5 mm
3:58 min.

Images courtesy of Osaka University Hospital, Osaka, Japan

Abdelhamid Derriche, MD
PRIISM, EHP Kara
Oran, Algeria

Orkia Ferdagha
PRIISM, EHP Kara
Oran, Algeria

Whole-body diffusion for evaluation of metastatic lesions

By Abdelhamid Derriche, MD, site radiologist, and Orkia Ferdagha, MR technologist, PRIISM, EHP Kara

Cancer patients are often referred for whole-body imaging to evaluate the presence of secondary or metastatic lesions, which can change the course of patient treatment. In our institution, whole-body diffusion MR is our preferred modality for this type of study.

Diffusion-weighted imaging (DWI) on MR has shown excellent sensitivity (82%) and specificity (97%) compared to PET/CT (sensitivity of 72% and specificity of 92%) in whole-body imaging in melanoma metastases.[1] Additionally, DWI MR has been shown to be the most accurate for detecting metastases in the bone, liver, subcutaneous and intra-peritoneal sites compared to PET/CT.[1]

However, non-optimal DWI MR acquisitions can produce scintigraphy-like images that may produce false positive results. Combining DWI MR with an inversion time technique can help overcome this issue by allowing for a better suppression of fat signal, which helps suppress background body signal. Further, utilizing an MR system that has strong magnet homogeneity allows for the acquisition of large field-of-view (FOV) images and helps reduce distortions in areas of off-center imaging, such as the extremities. DWI STIR with a "3-in-1" technique provides an excellent compromise between acquisition time and signal-to-noise ratio (SNR), allowing acquisition of thin slices that may help further enhance sensitivity of the DWI sequence.

Patient history

A 75-year-old female with known melanoma was referred for whole-body DWI MR for evaluation of suspected metastatic (secondary) lesions on her extremities. Post-contrast whole-body MR with LAVA Flex was also used to evaluate areas with suspicious contrast uptake.

MR findings

- Important effusion on the glenohumeral joint of the right shoulder, to be investigated
- Several bilateral swollen axillary lymph nodes, predominant in number and size at the right axillary region
- Lesion located on the proximal metaphysis of the ulna of the left arm and suspected to be metastatic, measuring 13 mm from its long axis, hyperintense in diffusion, hyperintense in STIR and gadolinium-enhanced on post-contrast T1 sequence
- Second suspicious lesion with similar aspect, measuring 9 mm and located on the distal diaphysis of the radius of the right arm
- Lesion on the left iliac joint, measuring 6 mm, hyperintense in diffusion, with no aspects on the other sequences
- Small nodule of 15 mm situated on the soft tissues of the right thigh, at the inferior part located within the posterior muscular compartment, hyperintense in diffusion.

SIGNA™ Explorer

PARAMETERS

	Coronal LAVA Flex	*Coronal STIR*	*Axial Diffusion STIR*	*Coronal LAVA Flex post contrast*
TR (ms):	5.8 (2nd station 5.7)	8000 (2nd station 2225)	6811	5.8
TE (ms):	3.1 (minimum TE)	33	60 (minimum TE)	3.1
FOV (cm):	48	48	48	48
Slice thickness (mm):	2.6	8	3	2.6
Frequency:	192	320	110	192 (170)
Phase:	160	224 (160)	110	160 (150)
NEX:	1	1	b0 = 3, b600 = 12	1
b-value:			0, 600	
Scan time (min):	0:42 (sec.)	2:00	1:49	0:42 (sec.)
Options / other:	2nd station 0:21 sec. for breath-hold	2nd station 1:30 min. with 0:18 sec. breath-hold	20 stations	2nd station 0:21 sec. for breath-hold

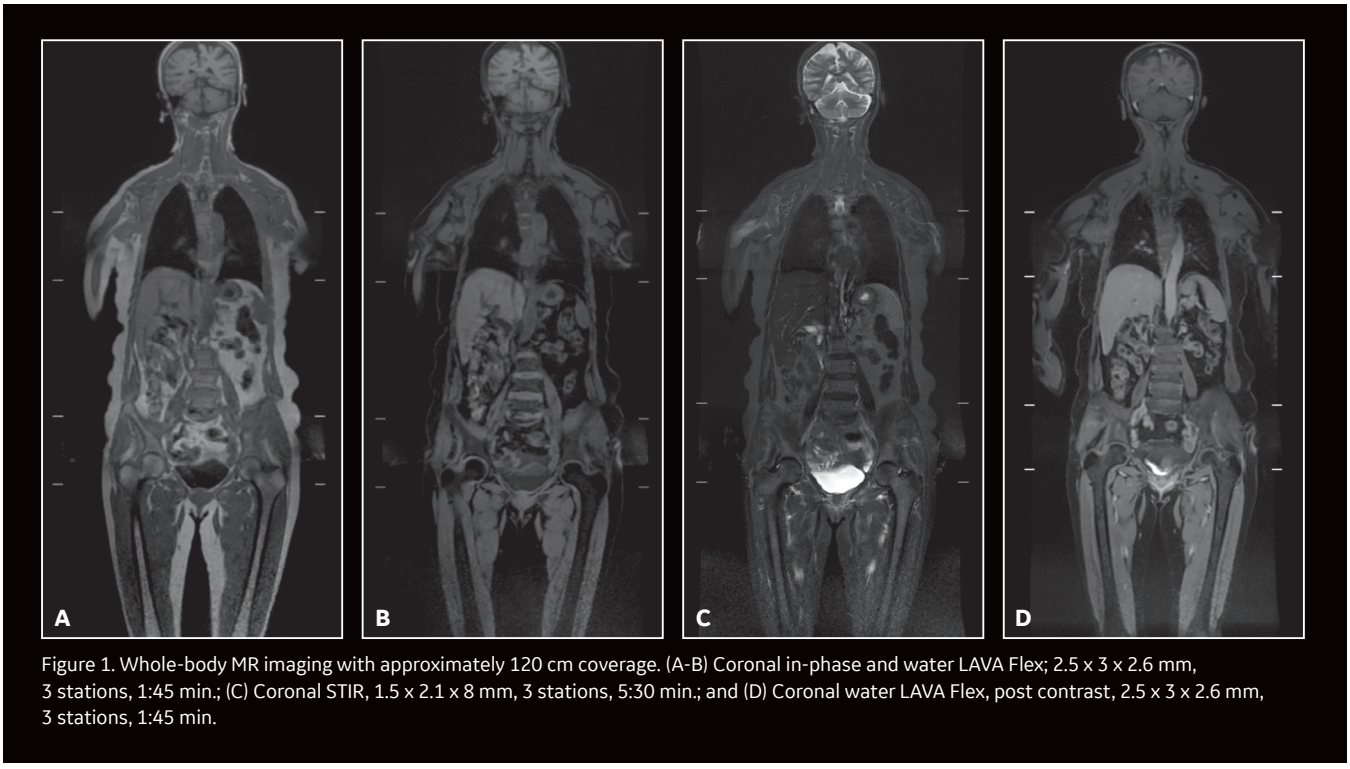

Figure 1. Whole-body MR imaging with approximately 120 cm coverage. (A-B) Coronal in-phase and water LAVA Flex; 2.5 x 3 x 2.6 mm, 3 stations, 1:45 min.; (C) Coronal STIR, 1.5 x 2.1 x 8 mm, 3 stations, 5:30 min.; and (D) Coronal water LAVA Flex, post contrast, 2.5 x 3 x 2.6 mm, 3 stations, 1:45 min.

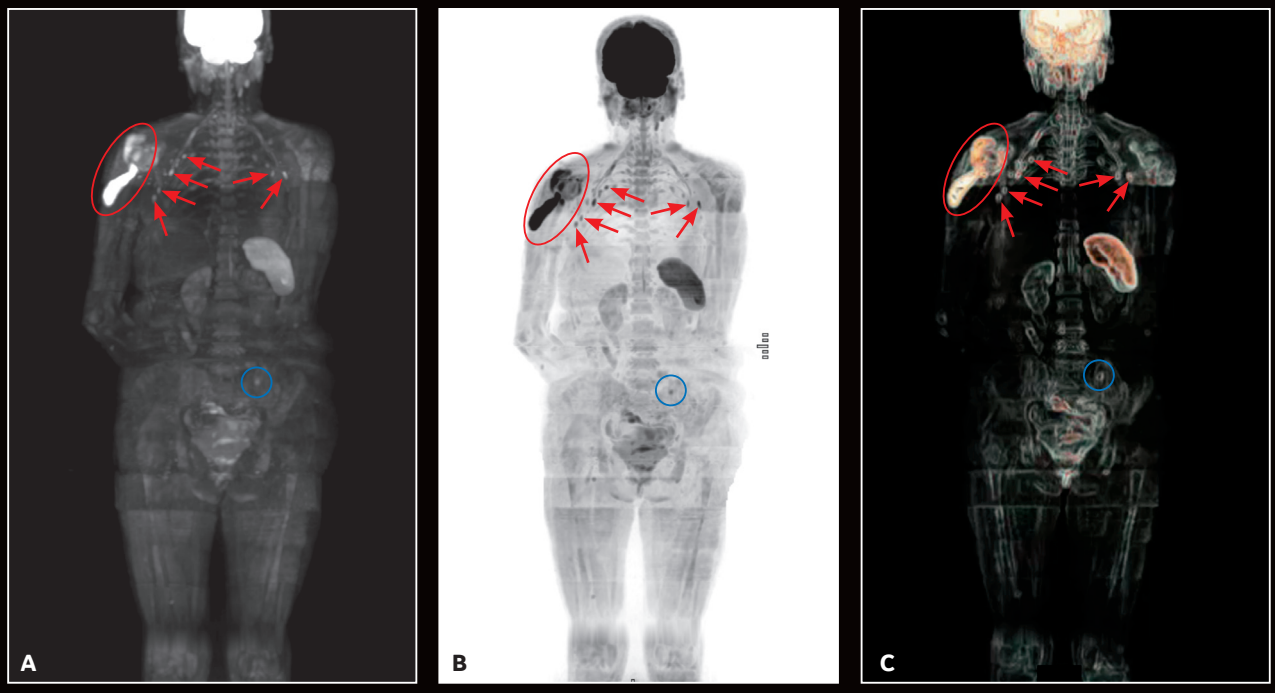

Figure 2. Whole-body MR imaging with approximately 120 cm coverage. Binded Axial diffusion STIR 3-in-1, b600, 4.4 x 4.4 x 3 mm, 20 stations, 36:20 min. (A-B) MIP projections; and (C) volume rendered image. Red circle depicts the effusion on the glenohumeral joint of the right shoulder. Red arrows show the bilateral swollen axillary lymph nodes. Blue circle denotes the lesion on the left iliac joint.

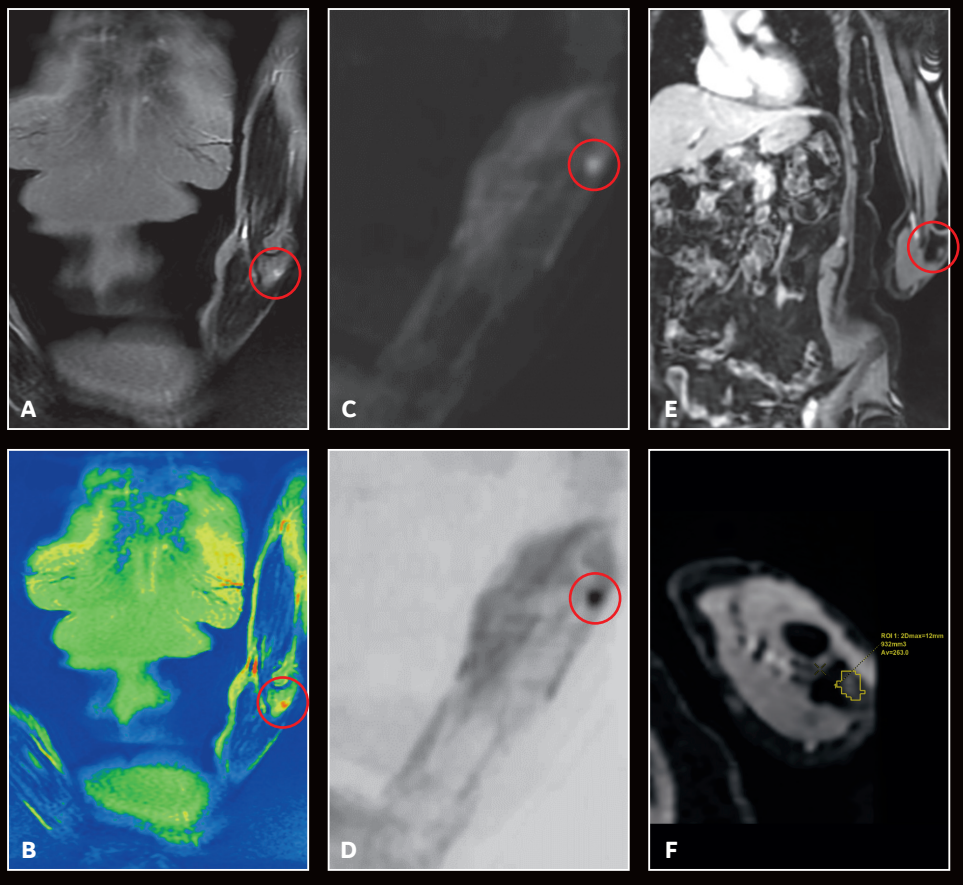

Figure 3. (A) Coronal STIR, 1.5 x 2.1 x 8 mm; (B) same image with color map; (C-D) diffusion STIR 3-in-1 b600, 4.4 x 4.4 x 3 mm; and (E-F) Coronal water LAVA Flex post contrast, 2.5 x 3 x 2.6 mm and Axial MPR. Lesion located on the proximal metaphysis of the ulna of the left arm (red circle), suspected to be metastatic.

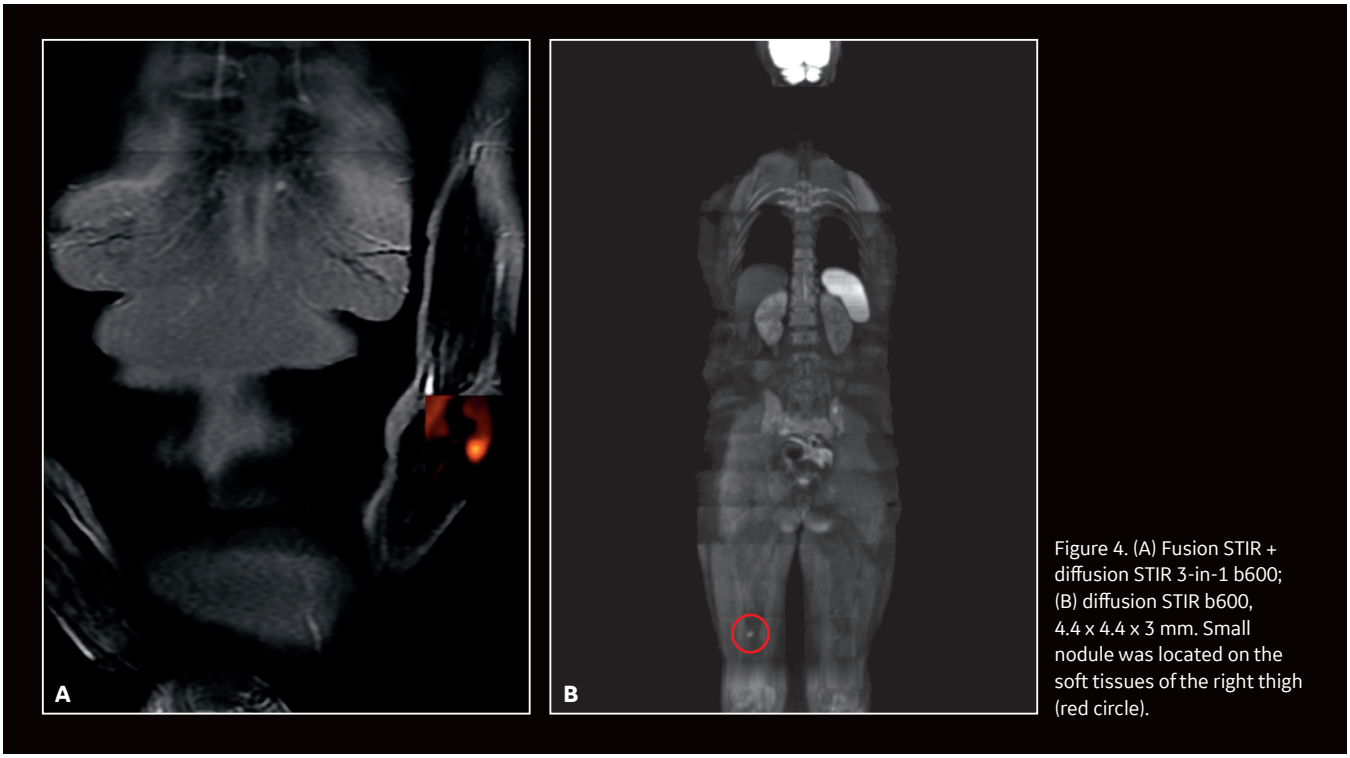

Figure 4. (A) Fusion STIR + diffusion STIR 3-in-1 b600; (B) diffusion STIR b600, 4.4 x 4.4 x 3 mm. Small nodule was located on the soft tissues of the right thigh (red circle).

Discussion

The patient has several small lesions suspected to be secondary bone lesions from her primary cancer, melanoma. Having the ability to detect these lesions on the patient's arms, iliac joint and thigh will enable the oncologist to re-stage the cancer and adapt therapy.

Whole-body DWI is an excellent option for evaluation of metastatic bone lesions compared to PET/CT and scintigraphy. It provides good image quality and provides the information clinicians need for patient management.

Even if PET/CT were recommended, this type of system is not available in all regions and is often more expensive than MR. Scintigraphy exposes the patient to additional radiation and MR has been found to provide similar sensitivity and specificity for patients with a small number of bone lesions, 58% sensitivity/33% specificity for whole-body DWI MR versus 67% sensitivity/58% specificity for scintigraphy; and patients with multiple bone lesions, 97% sensitivity/91% specificity for whole-body DWI MR versus 48% sensitivity/42% specificity for scintigraphy.[2]

With MR, we can avoid patient exposure to additional radiation dose and achieve a high sensitivity and specificity for detection of metastatic lesions. Additionally, the strong magnet homogeneity on the SIGNA™ Explorer helps to decrease distortion when imaging large FOVs and "3-in-1" diffusion STIR provides the thin-slice data needed for a confident diagnosis in shorter scan times.

References

1. Laurent V, Trausch G, Bruot O, Oliver P, Felblinger J, Regent D. Comparative study of two whole-body imaging techniques in the case of melanoma metastases: advantages of multi-contrast MRI examination including a diffusion-weighted sequence in comparison with PET-CT. Eur J Radiol. 2010 Sep;75(3):376-83.
2. Skeletal Radiol. 2010 Apr;39(4):333-43. doi: 10.1007/s00256-009-0789-4. Gutzeit A, Doert A, Froehlich JM, et al. Comparison of diffusion-weighted whole-body MRI and skeletal scintigraphy for the detection of bone metastases in patients with prostate or breast carcinoma. Skeletal Radiol. 2010 Apr;39(4):333-43.

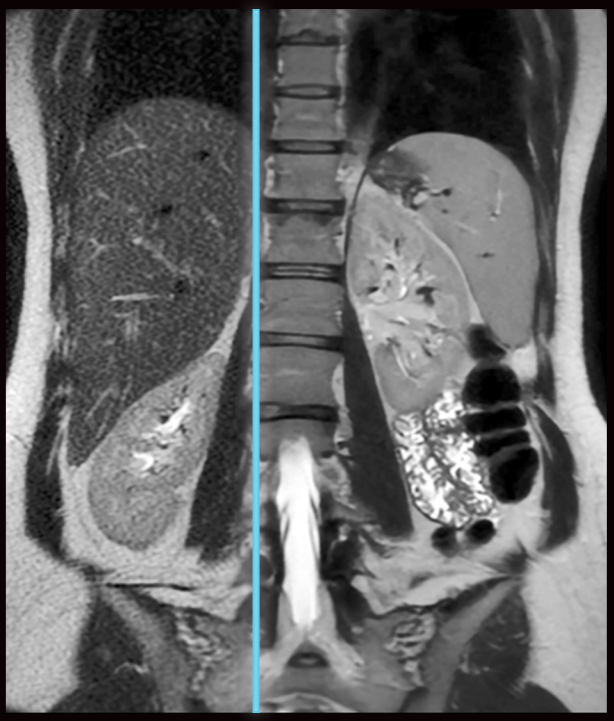

Level up your abdominal imaging quality with **AIR™ Recon DL**

AIR™ Recon DL, an innovative new reconstruction technology from GE Healthcare based on deep learning, offers a fundamental shift in the balance between image quality and scan time, resulting in TrueFidelity™ MR images that elevate the science of image reconstruction for clinical excellence without conventional compromises.

Use the QR code to learn more about how AIR™ Recon DL can revolutionize your clinical MR practice. Now available across the full 1.5T and 3T portfolio.